

**Performance Assessment of Satellite and
DACCIWA Optical Gauge Rainfall Products for the
Analysis of Trends and Drivers of Rainfall
Extremes in Ghana**

By
KNUST

ATIAH, WINIFRED AYINPOGBILLA

(MSc., Mathematical Sciences)

**A Thesis submitted to the Department of Physics, Kwame Nkrumah
University of Science and Technology in partial fulfilment of the
requirements for the degree of**

**DOCTOR OF PHILOSOPHY
(Meteorology and Climate Science)**

**College of Science
Faculty of Physical and Computational Sciences**

c Department of Physics

November, 2018

Declaration

I hereby declare that this submission is my own work towards the PhD and that, to the best of my knowledge, it contains no material previously published by another person nor material which has been accepted for the award of any other degree of the University, except where due acknowledgement has been in the text.

Winifred Ayinpogbilla Atiah (20410351)
Student Name & ID Signature Date

Certified by:

Prof. Leonard K. Amekudzi
Supervisor Name Signature Date

Certified by:

Prof Kwasi Preko
Co-supervisor Name Signature Date

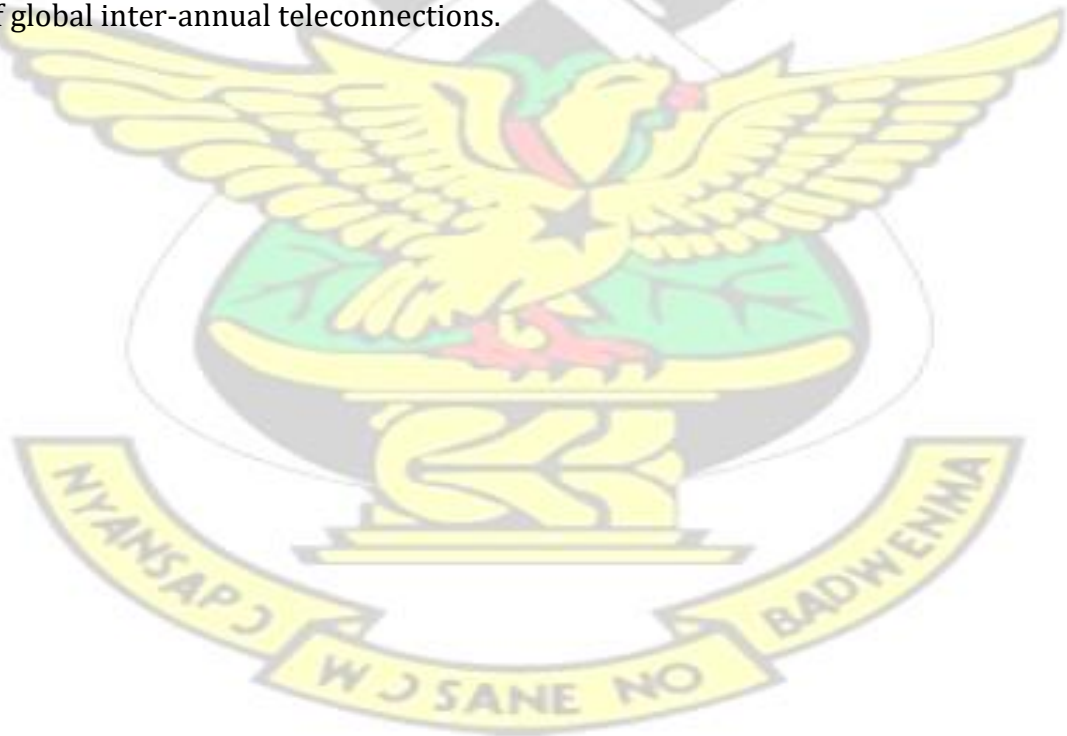
Certified by:

Prof. Leonard K. Amekudzi
Head of Dept.Name Signature Date

Abstract

Rainfall plays an important role in the socio-economic development of any nation. Below or above normal rainfall conditions have serious consequences on key socioeconomic sectors such as agriculture. This is particularly true for countries where rain-fed agriculture is a predominant practice as such, rainfall impact studies are important. In this thesis, rainfall impact studies in Ghana were examined in three different areas. The first part of the study evaluated the performance of satellites and merged rainfall products over Ghana in order to examine their reliability as surrogate ground-based gauge measurements for areas where gauge networks are sparse. Satellite products (TAMSAT, TRMM, ARC2, CMAP, GPCP and CHIRPs) and gauge-only products (CRU and GPCC) were validated with gridded rainfall data from the Ghana Meteorological Agency (GMet) on monthly to annual time scales using a suite of statistical analysis. The results showed that, the performance of the satellites and merged rainfall products is a function of the scales and locations used in the validation. While ARC2 showed large biases on both monthly and annual time scales, all other products, especially, TRMM and TAMSAT showed relatively good skills on the monthly scale ($r > 0.90$) than the annual. On the countrywide basis, CHIRPs and CRU markedly revealed better skills on both time scales. In all the four agro-ecological zones of the country, the products were able to capture the respective rainfall patterns, onset, cessation and spells (wet and dry) of each zone. Thus, TRMM and TAMSAT will serve as better surrogates at monthly time scale whereas CHIRPS and CRU would be better substitutes to ground-based gauge data for both time scales over the entire country and in the four ecological zones. In the second part of the study, the performance of the new Dynamic Aerosol Chemistry-Cloud Interactions in West Africa (DACCIIWA) optical rain gauge (DOG) measurements over the Ashanti region of Ghana were assessed. The study further examined the validities of subdaily rainfall data from IMERG and TRMM over the region for their exploits in the key socio-economic activities of the country such as agriculture, hydrology and water resource management. Daily rainfall data for nine co-located stations from the Ghana Meteorological agency (GMet) were used to assess the validity of the DOGs. A point-point assessment of IMERG and TRMM from 2016–2017 for the nine stations were then performed using the DOGs. The outcome of the assessment revealed that the DOGs were able to capture the diurnal and monthly rainfall patterns in the region. IMERG revealed a better skill in capturing the daily rainfall than TRMM although both products showed some similarities in the June–August (JJA) season. Both products slightly over-estimated gauge measurements (<2 mm/day) in all selected stations. The third part of the study examined the climatologies and trends of extreme rainfall events in Ghana. The

study further probed the links between the rainfall extremes and SST anomalies at the oceanic basin. The trend analysis revealed that CDD, CWD, R10mm and R20mm were in the range of 5–140, 5–14, 25–60 and 2–26 days per year respectively. Moreover, PRCPTOT, R95p, R99p, SDII, RX1day and RX5day were in the range of 800–1800 mm, 150–450 mm, 30–130 mm, 6–14 mm, 30–100 mm and 60–190 mm per year respectively. The maximum of temporally averaged intensity rainfall indices have shown to cover southwestern Ghana while the minimum of these indices covered northwestern and eastern coasts of Ghana. Significant decreasing trends in wet indices were observed over the Volta lake and central Ghana while low positive trends were dominant over the northern sectors of the country. In most cases, with the exception of the CDD and CWD indices, there were significant positive (negative) correlations with the Atlantic (Pacific and Indian) basins SSTs. IOD had a dipole effect on rainfall indices with the central and southern sectors generally covered by negative correlations while northern and coastal Ghana have shown positive correlations. The R95p index over central Ghana had negative correlations with AMO while positive correlations dominated some isolated parts of the country in the south and northeast. The impacts of AMO on PRCPTOT index were insignificant over most parts of the country with a few exceptions over southeastern and northern boarder regions. These results have implications on the improvement of monthly-annual forecasts of the Ghanaian rainfall and its extremes, and also provides prior knowledge for better understanding of multidecadal modulations of global inter-annual teleconnections.



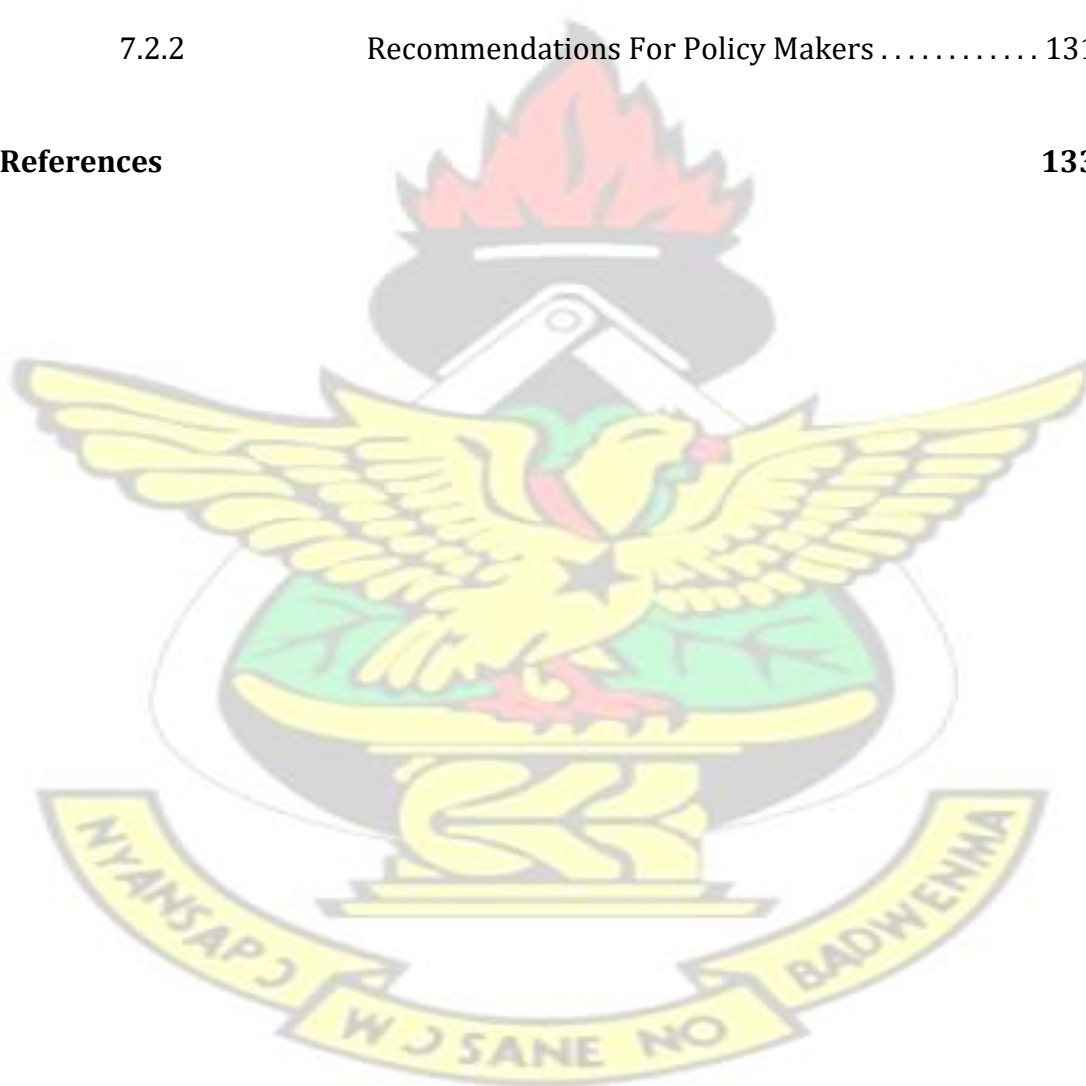
Contents

Declaration	ii
Abstract	iv
Table of Content	v
List of Tables	xii
List of Figures	xiii
1 Introduction	1
1.1 Background and Motivation	1
1.2 Problem Statement and Justification	3
1.3 Aim and Objectives	6
1.4 Research questions	7
1.5 Dissertation Outline	7
2 Literature Review	9
2.1 Drivers of Rainfall Variability in WA	9
2.2 Overview of Rainfall Extremes and Trends	14
2.3 Weather Systems in WA	16
2.4 Precipitation Measurement Techniques	20
2.4.1 Ground-Based Measurements	20
2.4.2 Existing Gauge Networks in WA	22
2.4.3 Satellite Rainfall Estimates Platforms	24
2.4.3.1 Geostationary (VIS/IR) method	24
2.4.3.2 Active Microwave Method (AMW)	25
2.4.3.3 Passive Microwave (PMW) Method	26
2.5 Satellite Rainfall Products Validation Studies	27

3.2.4.2	NINO3.4 Index	47
3.2.4.3	Atlantic Multidecadal Oscillation (AMO)	47
3.3	Research Methods	47
3.3.1	Validation of Satellite-based Rainfall products	47
3.3.1.1	Specific Objective One: Evaluate the accuracies and discrepancies of satellite and merged rainfall products over Ghana	48
3.3.1.2	Objective Two: Assess the performance of DOGs, IMERG and TRMM sub-daily rainfall products over the Ashanti region of Ghana	49
3.3.1.3	Statistical Metrics	51
3.3.1.4	Homogenization Method	54
3.3.2	Objective Three: Examine the climatologies, trends and drivers of extreme rainfall events in Ghana	56
3.3.2.1	Selected extreme rainfall indices	58
3.3.2.2	Mann Kendall (MK) trend test	58
3.3.2.3	Principal Components Analysis (PCA)	60
3.3.3	Summary	62
4 Evaluation the accuracies and discrepancies of satellite and merged rainfall products in Ghana		65
4.1	Introduction	66
4.2	Results and Discussions	68
4.2.1	Inter-annual Comparisons	68

4.2.2	Monthly comparisons	69
4.2.3	Taylor and error diagram evaluation	74
4.3	Summary	79
5	Assessment of the performance of DOGs, IMERG and TRMM sub-daily rainfall products over the Ashanti region of Ghana	81
5.1	Introduction	82
5.2	Results and Discussions	84
5.2.1	GMet gauge-DOGs Inter-comparisons	84
5.2.2	Gauge-satellite inter-comparisons	87
5.2.2.1	Diurnal inter-comparisons	87
5.2.2.2	Daily-seasonal inter-comparisons	90
5.2.2.3	Monthly-seasonal anomalies inter-comparisons ..	92
5.3	Summary	95
6	Examination of the climatologies, trends and drivers of extreme rainfall events in Ghana.	99
6.1	Introduction	100
6.2	Results and Discussions	102
6.2.1	Mean climatology of rainfall indices	102
6.2.2	Trends of rainfall indices	109
6.2.3	Correlations of SST anomalies and the rainfall indices over Ghana	113
6.2.3.1	Relation between sea surface temperature (SST) and rainfall indices	113
6.2.3.2	NINO3.4	117
6.2.3.3	Indian Ocean Dipole (IOD)	119

6.2.3.4	Atlantic Multidecadal Oscillation (AMO) 121
6.3	Summary 123
7	Conclusions and Recommendations	127
7.1	Conclusions 127
7.2	Recommendations 130
7.2.1	Recommendations For Further Studies 130
7.2.2	Recommendations For Policy Makers 131
References		133



List of Tables

3.1	Information on the seventeen DOG stations over the Ashanti region of Ghana, including the longitude, latitude, and elevation.	36
3.2	Summarized information on the nine validated rainfall products. .	42
3.3	Selected rainfall indices computed over Ghana adapted from the ETCCDI website.	59
4.1	Monthly performance of VRPs with respect to gauge in the four zones for the period of 1998–2012.	72
4.2	Monthly performance of VRPs with respect to gauge over the entire country for the period of 1998–2012.	72
5.1	Summary of statistics for the performance of DOGs with respect to Gmet in 2016.	84
5.2	Summary of statistics for the performance of DOGs with respect to Gmet in 2017.	86
5.3	Summary of statistics for the performance of IMERG with respect to DOG for the 2016 season.	88
5.4	Summary of statistics for the performance of TRMM with respect to DOG for the 2016 season.	89
5.5	Summary of statistics for the performance of IMERG with respect to DOG for the 2017 season.	89
5.6	Summary of statistics for the performance of TRMM with respect to DOG for the 2017 season.	90

List of Figures

2.1	Mean climatological annual rainfall change in WA. Adapted from; Earth Resources Observation and Science (EROS) Center-USGS.	17
2.2	An illustration of the swath coverage by GPM core satellite sensors (Image credits: NASA). Adapted from Kidd and Levizzani (2011).	26
2.3	A diagram of the multiple precipitation measurement satellites which comprise the GPM constellation (Image credits: NASA). Adapted from; Kidd and Levizzani (2011).....	26
3.1	Geographical location of the study area with locations of the seventeen DACCIWA optical rain gauge stations (in red) over the Ashanti region of Ghana.....	37
3.2	DOG rain gauge setup for inference of areal rainfall data; (a) data collector, (b) data logger+solar panel.....	38
3.3	Image showing a clogged DOG observed during field visit.	39
3.4	Image showing dust particles in the collector of DOG observed field visit.....	40
3.5	(a) Map of Ghana indicating the locations of all the 113 meteorological stations, (b) delineations of the four agro-ecological zones (b); Savannah (orange), Transition (yellow), Forest (cyan) and Coast (sky blue).....	41

3.6	A chart of the research design for the three specific objectives. . .	63
4.1		
	(a) countrywide and (b) Inter-zonal annual rainfall departures of rainfall products from gauge records for the of period 1998-2012; GPCP (black), ARC2 (cyan), TRMM (blue), TAMSAT (magenta), CRU (yellow) and CHIRPS (brown).....	69
4.2	Zonal monthly mean rainfall difference between VRPs and gauge for the period of 1998–2012.....	71
4.3		
	Colormaps showing the monthly to inter-annual rainfall difference between the VRPs and gauge in the entire country for the period of study.....	71
4.4		
	Scattergrams of monthly rainfall records for VRPs with respect to gauge over the entire country for a period of 1998–2012 ; GPCP (black), ARC2 (cyan), TRMM (blue), GPCP (green), CMAP (red), TAMSAT (magenta), CRU (yellow) and CHIRPS (brown).....	73
4.5		
	Inter-zonal annual rainfall cycle as captured by Gauge (red), TRMM (blue), TAMSAT (magenta), ARC2 (cyan), GPCP (black), CRU (yellow) and CHIRPS (brown) rainfall products.	74
4.6	Taylor (a) and error (b) diagrams showing the performance of the GPCP (black), ARC2 (cyan), TRMM (blue), GPCP (green), CMAP (red), TAMSAT (magenta), CRU (yellow) and CHIRPS (brown) on a monthly scale for the period of 1998–2012 in the	

entire country.....	75
4.7 Taylor diagrams showing the performance of the GPCC (black), ARC2 (cyan), TRMM (blue), GPCP (green), CMAP (red), TAM- SAT (magenta), CRU (yellow) and CHIRPS (brown) after removal of seasonality for the period of 1998–2012 in the entire country. .	76
4.8 Inter-zonal Taylor diagrams showing the performance of the GPCC (black), ARC2 (cyan), TRMM (blue), TAMSAT (magenta), CRU (yellow) and CHIRPS (brown) after removal of seasonality for the period of 1998–2012.....	76
4.9 Inter-zonal Taylor diagrams showing the performance of CRU (yellow), TAMSAT (magenta), TRMM (blue), GPCC (black), ARC2 (cyan) and CHIRPS (brown) with respect to Gauge.....	77
4.10 Inter-zonal error diagrams showing the performance of CRU (yellow), TAMSAT (magenta), TRMM (blue), GPCC (black), ARC2 (cyan) and CHIRPS (brown) with respect to Gauge.....	78
5.1 Monthly rainfall distribution for the GMet gauge (red) and DOG (green) during (a) 2016 and (b) 2017 period; Mampong (A), Agromet (B), Bekwai (C), Akrokeri (D), Bompata (E), Ejura (F), Jamasi (G), Mankranso (H), Nsuta (I).....	85
5.2 Duirnal patterns of rainfall from the DACCIWA gauge stations during 2016.....	85
5.3 Mean monthly rainfall as captured by DOG (green) with respect GMet (red) in the Ashanti region of Ghana (a) 2016 and (b) 2017.	87

5.4	Rainfall rate for IMERG (green) and TRMM (blue) rainfall products with respect to DOG (red) during March–November season of (a) 2016 and (b) 2017; Mampong (A), Agromet (B), Bekwai (C), Akrokeri (D), Bompata (E), Ejura (F), Jamasi (G), Mankranso (H) and Nsuta (I).	88
5.5	Rainfall distributions for IMERG (green) and TRMM (blue) rainfall products with respect to DOG (red) during March–May (MAM) season of (a) 2016 and (b) 2017 ; Mampong (A), Agromet (B), Bekwai (C), Akrokeri (D), Bompata (E), Ejura (F), Jamasi (G), Mankranso (H) and Nsuta (I).	90
5.6	Taylor plots showing the skill of IMERG (a) and TRMM (b) products in capturing the seasonal rainfall with respect to gauge during March–November period of 2016–2017.	93
5.7	Error plots showing the skill of IMERG (a) and TRMM (b) products in capturing the seasonal rainfall with respect to gauge during March–November period of 2016–2017.	94
5.8	Taylor plots showing the skill of IMERG (a) and TRMM (b) products in capturing the seasonal rainfall anomalies with respect to gauge during March–November period of 2016– 2017.	95
6.1	The study area (a) and the mean annual rainfall climatology over Ghana for the period of 1981–2015 (b).	103
6.2	Mean climatology of frequency indices for the period of 1981–2015 over Ghana. (a) CDD; (b) R10mm; (c) CWD; (d) R20mm.	105

6.3 Mean climatology of intensity indices for the period of 1981–2015 over Ghana. (a) PRCPTOT; (b) R95p; (c) SDII; (d) R99p; (e) RX1day; (f) RX5day.....	107
6.4 Trends of intensity indices for the period of 1981–2015 over Ghana. (a) CDD; (b) R10mm; (c) CWD; (d) R20mm.....	110
6.5 Trends of intensity indices for the period of 1981–2015 over Ghana. (a) PRCPTOT; (b) R95p; (c) SDII; (d) R99p; (e) RX1day; (f) RX5day.....	112
6.6 Spatial patterns of significant correlation between SST and rainfall indices; (a) CDD, (b) R10mm, (c) CWD, (d) R20mm for the period of 1981–2015.	114
6.7 Spatial patterns of significant correlation between SST and rainfall indices; (a) PRCPTOT, (b) R95p, (c) SDII, (d) R99p, (e) RX1day and (f) RX5day rainfall indices for the period of 1981–2015....	116
6.8 Correlation between NINO3.4 index and the PRCPTOT, R10mm and R20mm rainfall indices for the period of 1981–2015 over Ghana.	118
6.9 Correlation between IOD index and the PRCPTOT, R10mm and R20mm rainfall indices for the period of 1981–2015 over Ghana. .	121
6.10 Correlation between AMO index and the PRCPTOT and R95p rainfall indices for the period of 1981–2015 over Ghana.	122

List of Symbols and Acronyms

<i>AMO</i>	Atlantic Multidecadal Oscillation
<i>AMM</i>	Atlantic Meridional Mode
<i>CWD</i>	Consecutive wet days
<i>CDD</i>	Consecutive dry days
<i>DACCIWA</i>	Dynamic Aerosol Chemistry-Cloud Interaction in West Africa
<i>DOG</i>	DACCIWA Optical gauge
<i>GPM</i>	Global Precipitation Measurements
<i>GMet</i>	Ghana Meteorological Agency
<i>MCS</i>	Mesoscale Convective Systems
<i>PRCPTOT</i>	Annual rainfall total
<i>R95p</i>	Very wet day
<i>R99p</i>	Extremely wet day
<i>RX1day</i>	Daily maximum rainfall
<i>RX5day</i>	5-day maximum rainfall
<i>R20mm</i>	Very heavy rainfall day
<i>R10mm</i>	Heavy rainfall day
<i>SST</i>	Sea Surface Temperatures
<i>SRP</i>	Standard Rainfall Product
<i>SDII</i>	Simple daily rainfall index

Acknowledgement

My sincerest and foremost appreciation goes to the Almighty God for His love and protection throughout these years of study. My warmest gratitude goes to my supervisor, Prof Leonard K. Amekudzi for his guidance, constructive suggestions and discussion time spent with me without which this project would have been unsuccessful. I appreciate Prof. Andreas Fink, Prof. Gizaw Mengistu, Dr. Edmund Yamba, Prof. Kwasi Preko and Prof. Sylvester K. Danuor for their guidance, encouragement and the expertise they provided to make this research possible. I acknowledge Dr. Thompson Annor and Dr. Nana Ama Browne Klutse for their constructive criticisms and contributions.

I greatly appreciate the coordinator of the DACCIWA project, Prof. Peter Knippertz and all KIT team, Dr. Barbara J. Brooks and all the National Center for Atmospheric Science (NCAS) team, and the KNUST team for their immense contributions during the data gathering process of the June–July 2016 field campaign. Without them this research would not have been possible.

Many thanks to Elie Nuomon Allini, Maranan Marlon, Jeffrey Nii Armah Aryee and Benjamin Boadi for their availability and willingness to help anytime I called on them.

I acknowledge support from the Organisation of Women in Science for the Developing World (OWSD) sandwich programme and Botswana International University of Science and Technology (BIUST) for hosting and the teaching assis-

KNUST



tantship during my research stay in Botswana. I also acknowledge support from the African-German Network of Excellence in Science (AGNES) Intra-Africa Mobility grant for junior researchers from sub-Saharan Africa.

The research leading to these results has received funding from the European Union 7th Frame-work Programme (FP7/2007-2013) under Grant Agreement no. 603502 (EU project DACCIWA: Dynamics-aerosol-chemistry-cloud interactions in West Africa).



Dedication

My parents, Mr. and Mrs. John Atiah and all my family members.

KNUST



CHAPTER 1

Introduction

1.1 Background and Motivation

The African continent particularly, tropical West Africa (WA) is noted for its highly variable climatic patterns and trends. Studies have revealed the rainfall trends and variability over the tropics of WA to be far larger in recent years than other places on earth (Nicholson, 2000). However, variability of rainfall over these regions have received minimal attention as compared to the numerous studies carried over the Sahel thus accounting for the earthward rainfall trends in the region (Owusu and Waylen, 2009).

Rainfall has significant impact on the socio-economic development of any country, especially in areas where agriculture is predominantly rain-fed (Nicholson, 2000). In Africa, rainfall is reported to be one of the key determinants of the poor socio-economic state of the continent. For instance, Barrios et al. (2010) found that a decline in rainfall led to a reduction of about 30–40% in the Gross Domestic Product (GDP) in Africa. In Ghana, rainfall has a great impact on the general food production of the region as it determines the time and type of crops to grow (Yengoh et al., 2010). The Ghanaian agricultural sector contributes to 70% of employment to citizens and about 28% to the GDP of the country (Baidu et al., 2017; Ofori-Sarpong, 2001). The hydro-electric power generation, which is

the main energy source of the country solely relies on rainfall (Kunstmann and Jung, 2005a).

In WA, extreme rainfall events such as floods and droughts are reported (Owusu et al., 2008). A typical example is the six year severe drought in Sahel which claimed many lives, destroyed crops and properties (Nicholson, 1993). The trends of extreme rainfall are reported to increase in future especially in WA (Dashkhuu et al., 2015). Decreasing trends in the climatological rainfall amount over different locations in Africa have also been revealed. For example, in Ghana, Owusu and Waylen (2009) identified decreasing rainfall trends over all the four ecological zones in the country. Declining trends in the number of rainy days within the rainfall season were also identified in the entire Botswana (Batisani and Yarnal, 2010). Similarly, Tarhule and Woo (1998) reported significantly decreasing trends in the number of rainy days during the monsoon season in Nigeria. Seleshi and Zanke (2004) have also shown declining rainfall trends in Ethiopia.

Rainfall variability is accounted for by the irregular statistics of weather systems (e.g., Mesoscale convective systems), responsible for producing rainfall (Fink et al., 2006). Houze (2004) attributed most flooding cases to the presence of slowmoving, long-lived mesoscale convective systems (MCS). Moreover, other studies

(e.g., Lough (1986a); Opoku-Ankomah and Cordery (1994); Fontaine and Janicot (1996a); Losada et al. (n.d.)) have linked the rainfall variability in WA to sea surface temperature (SST) anomalies over oceanic basins. It is important then to understand the trends, intensity, distribution and drivers of extreme rainfall and

their impact on various key socio-economic sectors. These include water resource management such as the control of floods and droughts, irrigation for agriculture, hydrological studies and many others (Hou et al., 2014). Prior knowledge in the rainfall trends and variability is not only relevant in the water resource management sectors but also plays a key role in food and energy production. A better understanding of the rainfall variability is also key to the bio-geochemical cycles since rainfall has a direct impact on the atmospheric and oceanic circulations of any region (Trenberth, 2011; Hou et al., 2014).

Understanding the key characteristics of weather systems alongside an in-depth knowledge on the links of remote climate indices on the Ghanaian rainfall is very essential. This would serve as a benchmark to understanding the climatological rainfall variability in Ghana which would enhance better rainfall forecasts in the region.

1.2 Problem Statement and Justification

In recent times, rainfall extremes particularly, floods and droughts are becoming frequent phenomena in Ghana. For example, in June 2015, flash floods in parts of Accra resulted to an explosion of a gas station claiming more than 150 lives (Asumadu-Sarkodie et al., 2015). In northern Ghana, floods in 2007 affected many lives, crops and buildings (Armah et al., 2010). These happenings undoubtedly disrupt the socio-economic sectors of the country including, rain-fed agriculture, water resource management, hydro-power generations, fresh water accessibility

among others. Thus, rainfall variability have been reported to cause a reduction in the GDP by a margin of about 30% (Barrios et al., 2010).

Despite the high dependence of various socio-economic activities of the country on rainfall, the rain gauge networks are poor in terms of their numbers and distribution (Dinku et al., 2007). The limitation in ground-based gauge measurements has hampered the better understanding of various climate impact studies in the country. This has heightened the demand for use of satellite and merged rainfall products as substitutes to gauge measurements for climate impact studies (Dezfuli et al., 2017). Nonetheless, these satellite-based rainfall products have a number of associated uncertainties such as, sampling errors, algorithmic errors and instrumental errors (Gebremichael et al., 2005; Amekudzi et al., 2016). A number of studies (e.g., Dinku et al. (2007, 2008); Maggioni et al. (2016); Thiemig et al. (2012); Dinku et al. (2007); Pfeifroth et al. (2016); Nicholson et al. (2003)) have been carried out in various parts of Africa to assess the validity of satellite rainfall products. Such studies are regrettably limited in Ghana. Aside the limitation in validation studies in Ghana, the existing ones applied very few point stations data and satellite rainfall products (e.g., Amekudzi et al. (2016), Manzanas et al. (2014a)). In Amekudzi et al. (2016), the authors validated two satellite rainfall products thus, the Tropical rainfall measuring mission (TRMM) and Famine early warnings (FEWS) over parts of the Ashanti region of Ghana. As a contribution towards filling this gap, the present study makes use of gridded rainfall dataset obtained from a relatively dense gauge network in Ghana to validate nine rainfall products. With the aid of a suite of statistical and other evaluation tools, the abilities of the products to capture the

seasonal and annual rainfall patterns in the entire country and in the four agro-ecological zones are assessed.

High impact rainfall studies are not sufficiently documented in Ghana and this is because, such studies rely predominantly on high spatio-temporal rainfall datasets which are not readily available. High impact rainfall studies are however, very crucial for future planning and management of floods and droughts (Dezfuli et al.,

2017). High spatio-temporal satellite-based rainfall products are becoming increasingly available for such applications (e.g., the Integrated Multi-satellite Retrievals for Global Precipitation Measurements (IMERG) product) however, not well assessed. The recent DACCIIWA project have deployed seventeen optical rain gauges with a minute resolution over the Ashanti region of Ghana. The current study would for the first time assess the abilities of these gauges to effectively capture rainfall patterns in region. The study would further probe the potencies of high spatio-temporal satellite rainfall products to mimic the rainfall patterns as well as their abilities to capture high impact rainfall events in some locations of the Ashanti region of Ghana.

The contribution of MCS to extreme rainfall events in WA are scarcely known. Thus, a number of studies in WA have focused on understanding the drivers of rainfall variability in the region. Some studies have attributed rainfall variability in the region to the impact of MCS. Cetrone and Houze (2009) suggested that the latent heating in tropical Africa is linked to MCS which accounts for the bulk of the rainfall in the region. In the upper Ou'ém'e Valley of Benin, Fink et al. (2006) reported that about 50% of the rainfall in the region comes from Organised

Convective Systems (OCS). They also reported a contribution of approximately 26% of the annual rainfall to MCS. Related studies have linked the rainfall variability in WA to SST anomalies. Fontaine and Bigot (1993) attributed droughts in Sahel to warm SSTs over the oceanic basins and floods to cold SSTs at the north Atlantic and Pacific. Positive SSTs over the northern Atlantic were also associated with floods whereas negative SSTs over the eastern Pacific and Indian Oceans were linked to droughts in WA (Fontaine and Bigot, 1993; Fontaine and Janicot, 1996*b*; Janicot et al., 1998). Palmer (1986) revealed that, SSTs over the Indian ocean are accountable for rainfall deficits in eastern Sahel. However in Ghana, a handful of such studies exists and merely revealing the correlation between the SSTs over Oceanic basins and rainfall in the country. For instance, Opoku-Ankomah and Cordery (1994) showed positive correlations between the equatorial Atlantic SSTs and rainfall in Ghana. Nonetheless, these correlations are simply the average of the entire region and does not indicate which portions of the region are influenced and the extent to which these regions are controlled by SST anomalies. This knowledge is essential as rainfall patterns are not uniform throughout the country thus, may exhibit unique relationship with SST anomalies. It is therefore necessary to probe further in order to understand the sectoral impact of SST anomalies on the Ghanaian rainfall and its extremes.

1.3 Aim and Objectives

The main aim of this research is to investigate the climatologies, trends and drivers of extreme rainfall events using ground and satellite rainfall measurements in Ghana.

Specifically the study seeks to;

1. Evaluate the accuracies and discrepancies of satellite and merged rainfall products in Ghana.
2. Assess the performance of DOGs, IMERG and TRMM sub-daily rainfall products over the Ashanti region of Ghana.
3. Examine the climatologies, trends and drivers of extreme rainfall events in Ghana.

1.4 Research questions

In order to accomplish the objectives of this study, the following questions are asked.

1. How well do satellite rainfall products capture the daily, monthly and annual rainfall patterns in Ghana and can they serve as substitutes or complements to gauge in the country ?
2. How effective are the DOGs in capturing the diurnal rainfall patterns in the Ashanti region of Ghana?
3. Are the wet or dry rainfall indices over Ghana showing increasing or decreasing trends ?

4. Does SST anomalies over Oceanic basins have any impacts on rainfall in Ghana and which portions of the country are most impacted?

1.5 Dissertation Outline

This dissertation comprises of seven main chapters. Chapter one is made up of the background, problem statement and justification, study objectives and research questions. Chapter two presents a detailed review of literature. The review focuses on areas such as, drivers of rainfall variability in WA, overview of rainfall extremes and trends, weather systems in WA, precipitation measurement techniques and satellite rainfall products validation studies. The methodologies applied in order to achieve the aim of this research work are presented in Chapter three. Chapter four is based on the assessment of the performance of satellite and merged rainfall products. The validation of sub-daily and daily DOGs and satellite-based rainfall products in the Ashanti region of Ghana is carried out in Chapter five. In Chapter six, the trends of extreme rainfall and their drivers in Ghana are assessed. The conclusions and recommendations of this research are finally presented in Chapter seven.

CHAPTER 2

Literature Review

This Chapter presents the literature review on the topic and specifically focuses on areas such as, drivers of rainfall variability in WA, Overview of rainfall extremes and trends, weather systems in WA and precipitation types and measurement techniques.

2.1 Drivers of Rainfall Variability in WA

Various studies have highlighted a drastic deterioration in the African climate especially, rainfall in recent decades. For instance, a large amount of rainfall deficit of about 200 mm for the period of 1970s and 1980s with respect to 1950s and 1960s have been reported over eastern WA (Le Barb'e et al., 2002). These findings place more emphasis on the inhomogeneous nature of the spatial distribution of rainfall in the region. In addition, sub-Saharan Africa is well known for its extremely variable rainfall patterns which over the years have interrupted key socio-economic activities such as water resource management, agriculture, energy production among others (Le Barb'e et al., 2002). For instance, the six year severe drought in Sahel as reported in Nicholson (1993) rendered the agricultural sector, which serves as main source of livelihood of the region unproductive thus, bringing about loss of lives and property. This in effect, has

heightened the quest of many researches to better understand the drivers of the rainfall variability in the African continent.

Several research studies have linked the rainfall variability of parts of the African continent to sea surface temperature (SST) anomalies over Oceanic basins. A number of these studies have been carried out in the Sahel (Wolter, 1989; Hastenrath, 1990; Palmer, 1986; Nicholson and Webster, 2007; Lamb and Pepler, 1992*a*; Lough, 1986*a*; Janicot et al., 1996; Issa L'el'e and Lamb, 2010; Giannini et al., 2003; Bader and Latif, 2003*a*) whilst others were over sub-Saharan Africa (Lough, 1986*b*; Lamb and Pepler, 1992*b*; Lamb, 1978*a,b*), the entire West African region (Diatta and Fink, 2014; Balas et al., 2007; Janicot et al., 1998; Fontaine and Bigot, 1993; Fontaine and Janicot, 1996*b*; Opoku-Ankomah and Cordery, 1994) as well as Eastern Africa (Tsidu, 2017; Bahaga et al., 2015). Opoku-Ankomah and Cordery (1994) over Ghana also reported strong positive correlations between SSTs anomalies over eastern Atlantic Ocean and the rainfall in the country while also revealing contrasting relationship a few degrees north of Ghana, which lies in the Sahel. Anomalously low rainfall values in West African rainfall according to Fontaine and Bigot (1993) and Fontaine and Janicot (1996*b*) are associated with positive SSTs in the Indian and eastern Pacific Oceans as well as negative SST anomalies in the Gulf of Guinean and north Atlantic Oceans. Palmer (1986) on the other hand attributed reduced rainfall over Sahel to SST anomalies over the Atlantic and Pacific Oceans whereas, increased rainfall amount was associated with SSTs over the Indian Ocean.

Furthermore, Rowell et al. (1995) applied a blend of empirical and modelling approaches over Sahel, Sudanese and Guinean Coast in quest to extensively

understand the forcing of rainfall variability in Africa. The study revealed a strong correlation between the global sea surface temperatures (SSTs) and the rainfall variability over all three regions (Rowell et al., 1995). They further established an interconnection between the escaping land surface moisture and the rainfall variability over the regions nonetheless, the SSTs forcing on the rainfall variability was relatively appreciable than the surface moisture conditions. Clark et al. (2003) investigated the rainfall variability over coastal east Africa in relation to the Dipole mode index over the Indian ocean. Results revealed a strong correlation between SSTs in the Indian ocean and rainfall in the coasts of Kenya and Tanzania for the period of 1950–1999. The rainfall deficits over eastern Africa from October through November were also found to have relation with the reversal of SSTs and the phenomenon of the El nino southern oscillations (ENSO). Again, the impacts of SST anomalies over the ocean basins on the West African rainfall have been investigated by Losada et al. (n.d.) where an increased rainfall amount during summer in the region was revealed to have a good correspondence with the cooling phenomena of the Pacific Niña, Atlantic Niño and the western Indian Ocean. They further established contrasting correlations between the Sahelian rainfall variability and the SST anomalies in the Atlantic, Pacific and Indian oceans.

In addition, the northwestern Indian Ocean SST anomalies were investigated to have a casual link to rainfall variability in Ethiopia as well as the mean sea level pressure over the African continent, especially, during the spring (Tsidu, 2017). From the perspective of control simulation, the rainfall induced from the northwestern "secular" SST anomaly was also found to have some dry conditions

over the Eastern and equatorial Africa. The relationship between the monsoonal rainfall for three regions in tropical WA (West Sahel, Central Sahel and Guinea Coast) with different climate indices for eighty-nine years spanning the climatological period of 1921–2009 have been investigated (Diatta and Fink, 2014), where significantly positive correlations between the Sahelian rainfall and the Atlantic Multi-decadal Oscillation (AMO) and the Atlantic Meridional Mode (AMM) climate indices. The SST anomalies in the Eastern Mediterranean were also revealed to significantly correlate with the rainfall in the Central Sahel.

In order to understand the interconnection between SSTs and the West African rainfall variability, Fontaine and Janicot (1996a) applied the "composite analysis" technique and found four types of West African rainfall anomalies. These anomalies types were further correlated with the rainfall over the Guinean Coast and Sahel. Flooding cases experienced over WA according to their findings were associated with the positive SST anomalies in the northern Atlantic. In contrast, droughts over WA were associated with positive SST anomalies over the eastern Pacific and Indian oceans as well as negative SSTs over the north Atlantic and the Gulf of Guinea (Fontaine and Janicot, 1996a) which confirms other findings. Camberlin et al. (2001a) employed the Laboratoire de M'et'eorologie Dynamique atmospheric Global Circulation Model (GCM) in order to investigate the dynamics of the West African monsoon in relation to the SST anomalies over the eastern equatorial Atlantic and Pacific ocean basins. Their investigations revealed a positive SST anomaly over the eastern equatorial Pacific due to the zonal divergent circulations in the tropical Atlantic resulting to negative rainfall anomalies over WA. Fontaine and Janicot (1996a) concluded that the positive

SSTs over the eastern equatorial Atlantic were influenced by the southward migration of the ITCZ which is accompanied by rainfall deficits over the Sahel and heavy rainfall over the Guinea Coast.

Furthermore, some studies through model simulations (Polcher, 1995; Eltahir and Gong, 1996; Zheng and Eltahir, 1998) and observational data (Taylor and Lebel, 1998) have attributed the rainfall variability in WA to its surface conditions. Over south-western Niger, Taylor and Lebel (1998) investigated the feedback of surface conditions and the rainfall of the area using highly dense rain gauge data. They applied different surface conditions and found a positive feedback between the rainfall patterns of the area and its surface conditions suggesting strong interconnection between the convective-scale rainfall patterns and the surface conditions of the region. Polcher (1995) simulated the interconnection between tropical convection and surface conditions and revealed a direct relationship between the surface heat flux and the rate of convective activities. Thus, an increase in sensible heat flux amounts to a respective increase in the amount of convection whereas reduced evaporation rate resulted to decreased precipitation rate. Rawinsonde and ship observational datasets over tropical Atlantic were applied in order to investigate the impact of surface and airmass characteristics on the West African rainfall variability for the period of 1948–1998. These analyses revealed two main Sahelian droughts most often associated with the southward position of the ITCZ (Janicot, 1992), a further inference of the link between the position of the ITCZ and the rainfall variability over tropical Atlantic (Janicot, 1992).

Beer et al. (1977) related the southward migration of the subtropical jet to the rainfall amount during the rainy season which was subsequently tested using climatic data from Tamale (located in Northern Ghana) (Beer et al., 1977). This was further extended to two other regions (Niamey and Nigeria) within the West African continent. Their findings in all cases demonstrated a strong connection between the southward migration of the southern jet and the overall rainfall amount. Greenhut (1977) discovered the southward migration of the subtropical high over Sahel to be related to an increased rainfall amount over the region assuming the atmospheric particles are sufficiently available (Greenhut, 1977). Their findings further reiterated that atmospheric pollutants are perhaps not the cause of the severe droughts reported over Sahel which contradict an earlier finding by Bryson (1973) who applied the purported Z-criterion and found an appreciable correlation between the Sahelian drought and increased atmospheric pollutants. Again, Nicholson (1981) correlated the sub-Saharan West African rainfall amount to the relative position of the ITCZ and revealed a strong interconnection. Although, Nicholson (1981) found no correlation between the northward migration of the ITCZ and the West African rainfall, the southwards position of the ITCZ resulted to an increased rainfall amount in the region. Camberlin et al. (2001*b*) over Sahel and Gulf of Guinea have demonstrated an indirect relationship between the intensity of the African Easterly Jet (AEJ) and the rainfall variability of the regions. Drought cases were revealed over Gulf of Guinea in January–March and over Sahel in July–September when AEJ was in its intense phase (Camberlin et al., 2001*b*).

2.2 Overview of Rainfall Extremes and Trends

Climate variability in a region comes about as a result of climate change which induces extreme climatic conditions like droughts, floods, among others (Change, 2007). Climate variability have serious implications on sustainable livelihood especially in Africa, which is comparatively more vulnerable (Asante and Amuakwa-Mensah, 2014). As such, various studies have been carried out in different locations to investigate the impacts of climate change on rainfall trends and extremes. In WA, East Africa, Northern and Southern Kalahari, Nicholson (1980) has shown that the semi-arid regions of WA were marked to have experienced twenty years of below normal rainfall patterns for the period of 1970–1990. However, above-normal rainfall patterns were observed over the northernmost sectors of the Sahelo-Saharan zone. The rainfall trends of southern Africa from the model's perspective have revealed decreasing trends, especially, during summer (Shongwe et al., 2009). Shongwe et al. (2009) showed evidence of a shortened rainfall season during austral summer in southern Africa. Alexander et al. (2006) on the other hand, for a climatological period of 1951–2003 have shown some decreasing trends in precipitation over most continents in the globe, especially, Africa. Seleshi and Camberlin (2006) contradicts findings of Alexander et al. (2006) in Ethiopia during 1965–2002 and reported no trends in extreme rainfall events, especially, during the "Belg" and "Kiremt" dry seasons.

Rainfall trend analysis over Ghana are projected to significantly decrease in trends particularly in the years, 2020, 2050 and 2080 (Asante and Amuakwa-Mensah, 2014). These decreasing trends were further resolved to have short- and long-term negative impacts on the Ghanaian hydroelectric power generation and

sustainability of rooted plants (e.g cassava) and rice, which form part of the stable foods in the country. Lacombe et al. (2012) showed no significant observed changes in the annual rainfall nevertheless, over central Ghana, significantly decreasing trends in wet days were observed. Moreover, increasing trends in the number of dry days during the rainy season particularly over southern and central Ghana were also identified. In most parts of the country, a delayed rainfall onset was identified for the period of study.

Adu-Prah et al. (2017) revealed some decreasing rainfall trends in the four ecological zones of Ghana during 1981–2009. Baidu et al. (2017) confirms this with the aid of the wavelet approach whose results revealed downward trends in rainfall over most parts of the country whilst the Transition zones of the country showed almost steady trends. Similarly, significantly decreasing trends in monsoonal rainfall during the period of 1961–1985 were also revealed in Manzanas et al. (2014b) in most parts of the country. Drying trends in rainfall during the major (June–August) and minor (September–November) rainy seasons for the period of 1981–2000 were revealed in central Ghana (Owusu and Waylen, 2013a). Owusu and Waylen (2013a) also established in their study some shifts in the rainfall regime and significantly decreasing trends in the rainfall amount, especially, during the minor rainfall season of the region.

Furthermore, some conurbations of Africa which include, western central Africa, Guinea Conakry and Zimbabwe during the period of 1955–2006 showed increasing trends in the heavy rainfall index (Aguilar et al., 2009). However, decreasing rainfall trends were dominant over most parts of central Africa. No

significant trends in extreme rainfall were reported over the Guinean Conakry and Zimbabwe.

2.3 Weather Systems in WA

The rainfall in WA is highly variable in nature and recently decreasing in trend (Le Barb'e et al., 2002). For instance, Wigley et al. (1985) reported diminishing rainfall trends within the region. The annual decline in rainfall over WA is reported to migrate south–north with rainfall lapse of approximately 1 mm/km, from about 140 mm toward the coast at 5° N to nearly 110 mm along the boundary with the Saharan desert (Eltahir and Gong, 1996). The decline in rainfall of the region (see Figure 2.1) has serious implications on especially rain-fed agriculture, food security and livelihood.

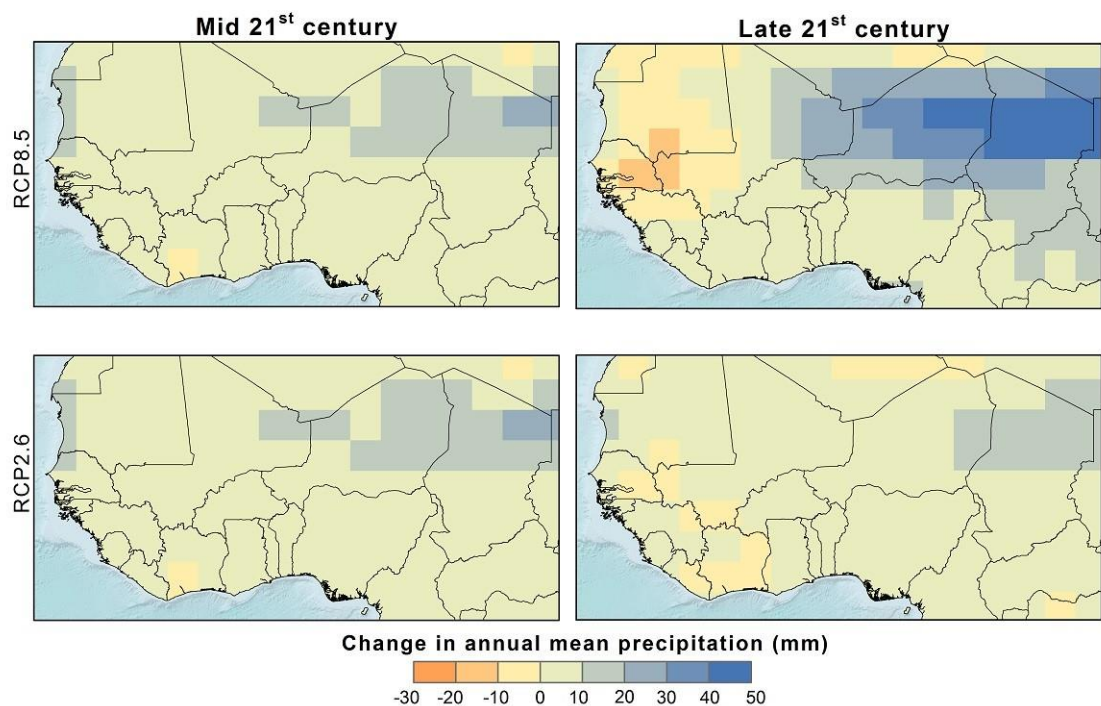


Figure 2.1: Mean climatological annual rainfall change in WA. Adapted from; Earth Resources Observation and Science (EROS) Center–USGS.

Tropical West African rainfall system is characterised by a "monsoon climate" mostly consisting of two seasons, the wet and dry seasons. During the rainfall season, the thermal heat low over the Saharan desert becomes intensified. As a result, moist south-westerlies are driven from the Gulf of Guinea into the region bringing appreciable amount of rainfall (Knippertz and Fink, 2008). In contrast, during Boreal winter, no rainfall is experienced in tropical WA as dry and dusty north-easterly trade winds are directed into to the region (Knippertz and Fink, 2008). Rainfall in the region begins in March from the west coast and intensifies through June, July, August and September but retreats in late October to almost the second dekad of November (Amekudzi et al., 2015).

Tropical convection has received a considerably great attention over the years owing to its relevance to the climate system of WA. This is because, there exists a strong interconnection between deep convection and the general atmospheric circulations. Specifically, moist convections are driven by two key atmospheric conditions including, instability and vertical motion which act to collectively supply the necessary energy needed to sustain convection (Mathon and Laurent, 2001). In WA, Mesoscale Convective Systems (MCSs), Mesoscale Convective Complexes (MCCs), squall lines (SL) among others have been reported through various studies to have great contributions to the rainfall and its variability.

MCSs are systems produced when individual convective cells come together to form a single organised cluster which is made up of two regions, the convective and stratiform (Mathon et al., 2002; Cetrone and Houze, 2009). MCSs are by far one of the largest convective systems which typically move in a westward direction and is strengthened by deep convection enabling it gain stronger speeds

and much longer life spans (Mathon and Laurent, 2001). These systems are the mainspring of global circulation and are accountable for majority of the latent heating in tropical WA (Cetrone and Houze, 2009; Houze, 1989). Hodges and Thorncroft (1997) have reported MCS contribution to rainfall not only in tropical Africa but also some portions of the mid-latitudes (Houze, 1989, 2004). MCSs have been identified as the dominant rainfall producing weather systems over most parts of

WA. As reported by Mathon et al. (2002) and Eldridge (1958) approximately 80–90 % of Sahelian and about half of Sudan Savannah annual rainfall is attributed to MCSs. Fink et al. (2006) over the upper Ou’em’è Valley of Benin also reported about 50% of rainfall contribution to Organised Convective systems (OCS) and approximately 26% of the annual rainfall of the region to MCSs. Slow-moving but long-lived MCS have also been revealed to be the dominant cause of flood cases within the region (Houze, 2004).

Furthermore, according to Frank (1978), squall lines (SL) are very much similar to a cluster of convective systems other than the fact that they have variations in their wind shear and speeds. SL are lines of organised thunderstorms which are oriented meridionally (north–south) with an average length reaching about 1000 km. SL contribute substantially to the annual rainfall totals in WA especially over the Sahel (Desbois et al., 1988; Rowell and Milford, 1993). Similar to the MCSs, SL are westward propagating with wind speeds mostly greater than winds at the various pressure levels and life spans of about several hours (Rowell and Milford, 1993). Pursuant to Fritsch and Forbes (2001); Cotton et al. (n.d.); Laing and Fritsch (1993), SLs are MCCs. According to Fritsch and Forbes (2001), SL have

four life cycles thus, the initiation stage, maturity stage, the development stage and the dissipation stage. According to Laing and Fritsch (1993), these MCCs are long-lived with life spans of about 12 hours and active in the night with the strongest influence over the Sahel.

Moreover, the interaction between AEWs and West African rainfall have also been extensively discussed in various research studies (Fink et al., 2006; Payne and McGarry, 1977; Duvel, 1990; Rowell and Milford, 1993; Diedhiou et al., 1999). African easterly waves (AEW) which come about as a result of the instability of African Easterly Jet (AEJ) and forms part of the key components of regional climate are responsible for regulating the West African rainfall. AEWs are well known as low-level, westward-propagating waves (Fink et al., 2006). They have three main life cycles which include, the initiation phase, the baroclinic growth and the west coast development phase (Berry and Thorncroft, 2005). According to findings in Berry and Thorncroft (2005), the AEWs are the most dominant synoptic scale convective systems over WA and tropical Atlantic during Boreal summer. Thorncroft and Hodges (2001) also highlighted that the mechanisms of Atlantic Tropical cyclone could be well modulated by the quantum of MCSs retreating the West African Coast.

2.4 Precipitation Measurement Techniques

Precipitation is formed when the necessary atmospheric conditions such as the availability of thick rain bearing clouds, sufficient amount of atmospheric water vapour and the presence of necessary cloud growth enhancing mechanisms are

in place. These cloud growth enhancing mechanisms include the warm and cold rain processes (Lensky and Rosenfeld, 2003). Warm rain processes are as result of the collision and coalescence of clouds in the atmosphere whereas cold rain processes are as a result of the aggregation of ice particles in the atmosphere (Rauber et al., 2000). There are various means through which precipitation could be inferred, among which are the in-situ measurement techniques and satellite estimates.

2.4.1 Ground-Based Measurements

Ground-based precipitation measurements are obtained via rain gauges, disdrometers and ground radars (Tapiador et al., 2012). Rain gauges and disdrometers provide direct point measurement of precipitation whereas ground radars have an indirect way of inferring precipitation over a comparably wider area (Joss et al., 1990; Wang and Lin, 2015). Rain gauges are globally the most appropriate and reliable means of precipitation measurements (Tapiador et al., 2012). These gauges are also known to present near truth records of rainfall over an area nonetheless, they have limitations in their coverage and are inapplicable over obscure locations. Wind could be another limiting factor to rain gauges measurements particularly when they are not wind-shielded. Gauges without wind-shields tend to underestimate areal rainfall amount. There are three main types of rain gauges thus, the standard, tipping bucket and weighing type rain gauges although other rain gauge types also exist (Strangeways, 2010). The standard rain gauge (SRG) is operated manually and is made of five

compartments which include, the lower layer, upper layer, the support, collecting jar and the measuring cylinder (Strangeways, 2006). Rainfall first goes into the collecting jar, then transferred unto the measuring cylinder where the amount of rainfall is recorded at the end of the rainfall event (Strangeways, 2010).

The measuring principle of the tipping bucket gauge (TBG) is quite robust compared to SRG. The TBG is made of a funnel, two calibrated buckets, and an electronic switch. Rainfall first enters one of its calibrated buckets through the funnel. When the bucket is full, it becomes unstable thus loses its balance then tips transferring the rainfall unto the outer compartment of the gauge (Strangeways, 2006). The electronic switch then counts the number of times the bucket tips. The rainfall amount is computed from the catchment area and the number of tips recorded by the electron switch (Strangeways, 2006).

Disdrometers are instruments used to measure the size and velocities of atmospheric droplets. Some disdrometers have a great skill of distinguishing between rain, graupel and hail (Bartholomew, 2016). Disdrometer measurements aid in quality checking droplet size distribution (DSD) retrievals from space-borne radar measurements (Tokay et al., 2013).

2.4.2 Existing Gauge Networks in WA

The sparse in-situ stations over the African continent is one challenge to climate impact studies over the region. This has thereby drawn our attention to satellite and other alternative products for various applications. Increasing the number and distribution of in-situ stations in the region would facilitate satellite and

model estimates evaluations. In recent times, initiatives have been taken to install in-situ stations all over Africa. Some among which are discussed in this section.

DACCIWA is an European Union 7th Framework programme that seeks to assess the effects of man-made and natural sources of atmospheric emissions on the sustainable livelihood of southwestern Africa (SWA) (Knippertz et al., 2015a). As part of the DACCIWA project, seventeen (17) optical rain gauges with minute temporal resolutions have been installed in the Ashanti region of Ghana. These gauges have been operational since June 2015–till date. The high temporal rainfall data from these optical rain gauges would facilitate the analysis of high impact rainfall events as well as aid with some validation studies in the region.

The Trans-African Hydro-Meteorological Observatory (TAHMO) project is a collaboration between the Delft University of Technology, Oregon State University, METER and IBM. TAHMO have installed approximately 20,000 ground-based sensing stations all over Africa (Van De Giesen et al., 2013). The TAHMO drip-counting rain gauges (TDRG) measure temperature, precipitation and other weather parameters. TDRG have high sensitivity and detectability such that, they detect precipitation as little as 0.02 mm. The TAHMO gauges have a high temporal resolution of 15–minute. This temporal resolutions of the sensors would facilitate the investigation of the diurnal rainfall patterns in the continent (e.g., Dezfuli et al. (2016)). Some researches have applied TDRG data for various studies all over Africa. Results from these studies reveal the skill of TDRG to mimic the diurnal-to-seasonal rainfall patterns within the WA region (Dezfuli et al., 2016, 2017).

The NASA African Monsoon Multidisciplinary Analyses (NAMMA) project is another rain gauge network project sponsored by the National Aeronautics and Space Administration (NASA). The project has deployed a total of about forty (40) rain gauge stations in Senegal. The purpose of this initiative is to facilitate detailed investigation of the mechanisms of the African Easterly Waves (AEWs). This initiative also intends to fill the gap of the less documented MCS and their impacts in WA (DeLonge et al., 2010; Snyder et al., 2010). The NAMMA rain gauge has a minute temporal resolution which effectively captures the amount and rate of rainfall as reported in a number of studies (e.g., Wu (2009); Turk et al. (2008); Snyder et al. (2010); Wu (2009)).

Quantifying Weather and Climate Impacts on Health in Developing Countries

(QWECI) project was funded by the European Commission within the Seventh Framework Programme (Ermert et al., 2012). The aim of QWECI is to investigate the interactions between atmospheric parameters as well as the causes of certain diseases in developing countries (Morse et al., 2012; Ermert et al., 2012).

Within this framework, three QWECI weighing rain gauges were installed in Kumasi-Ghana together with an Automated Weather Stations (AWS) in Owabi (Ashanti region of Ghana). The AWS provide information on the rainfall amount (with high temporal resolutions), relative humidity, temperature, heat flux, 3D wind, pressure, short and long-wave radiations. Recent studies within Ghana (e.g., Amekudzi et al. (2016) and Aryee et al. (2018)) and the entire Africa (e.g., Ermert et al. (2012)) have reported the reliability of the use of QWECI rainfall data for various hydro-climatic impact studies.

2.4.3 Satellite Rainfall Estimates Platforms

The advent of meteorological satellites in recent times has improved the spatiotemporal coverage of precipitation worldwide. Precipitation estimates from satellites are produced from various input datasets and from different sensors. Satellite retrieval techniques have been grouped into three thus, VIS/IR, microwave and multi-sensor (Kidd et al., 2003).

2.4.3.1 Geostationary (VIS/IR) method

The VIS/IR satellite retrieval provides near real and good spatio-temporal measurement of precipitation. VIS/IR algorithm relates cloud properties to surface rainfall (Tapiador et al., 2010). In VIS, rainfall is inferred based on the brightness temperature of the clouds. Brighter clouds, which are thicker would imply heavy downpour and vice versa. In IR, surface rainfall amount is linked to the cloud top temperatures (CTT). Colder CTTs means heavy rainfall whereas warm clouds signifies no or little surface rainfall (Ebert and Manton, 1998a). This indirect relationship between rainfall and cloud properties could raise issues as far as this retrieval method is concerned. For instance, cold clouds may not necessarily sometimes infer rainfall likelihood. Also, cirrus clouds could be mistaken as rain bearing with this method (Tapiador et al., 2010).

2.4.3.2 Active Microwave Method (AMW)

AMW algorithm uses a relatively direct precipitation retrieval method. This radar operates like any weather radar such that, backscatter radiations from the

precipitation are used to determine the intensity and number of precipitation particles (Tapiador et al., 2010). Backscatter radiations are proportional to the number of precipitation particles and intensity of the precipitation (Kidd and Levizzani, 2011). The disadvantage of AWM is that, the indirect link between back scatter radiations and precipitation particles is not always true (Kidd and Levizzani, 2011). The Global Precipitation Measurement (GPM) mission launched by NASA and JAXA serves to build upon the success of TRMM (Tapiador et al., 2010). The GPM operates on some core satellites (see figures 2.2 and 2.3) with non-synchronous orbit and a dual-wavelength precipitation radar (13.6 and 35.5 GHz). The dual wavelength improves the sensitivity of the algorithm.



Figure 2.2: An illustration of the swath coverage by GPM core satellite sensors (Image credits: NASA). Adapted from Kidd and Levizzani (2011).

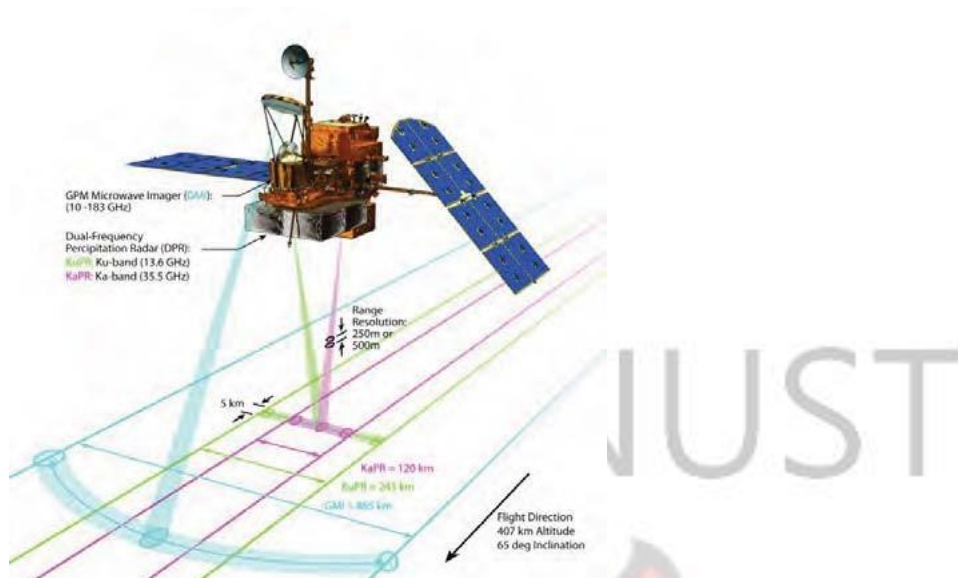


Figure 2.3: A diagram of the multiple precipitation measurement satellites which comprise the GPM constellation (Image credits: NASA). Adapted from; Kidd and Levizzani (2011).

2.4.3.3 Passive Microwave (PMW) Method

The PWM method includes two main techniques in its operation thus, the emission-based and scattering-based techniques. Emission-based techniques are most suitable over the oceans whereas scattering-based techniques can be applied in both ocean and land. A disadvantage of the PWM technique is that, it has limited spatial resolution in both land and ocean. Again, the PWM is currently only accessible to low-orbiting satellites (Kidd and Levizzani, 2011).

2.5 Satellite Rainfall Products Validation

Studies

Satellite rainfall estimates in recent times have gained so much attention in the world of applications partly because of their ability to represent high spatiotemporal resolution of rainfall data and largely because of the sparse and poorly distributed rain gauge networks worldwide. These rainfall estimation alternatives are mostly used as substitutes and or complement to in-situ rain gauge measurements especially over the African continent where their network is fast deteriorating in an unprecedented scale. It should, however, be noted that these alternatives come along with certain discrepancies. There is therefore the necessity to thoroughly assess their strengths and weaknesses especially over geographical locations in which they are frequently applied to gain some level of confidence in their use for various applications.

A number of validation studies have been carried out on different satellite rainfall products (SRPs) with various spatio-temporal resolutions worldwide. Some of these validation studies were carried out with the prime motive of investigating the impact of topography, seasonality and the intensity of rainfall event on the performance of the satellite rainfall products (e.g., Maggioni et al. (2016);Thiemig et al. (2012),Pfeifroth et al. (2016)). The performance assessment of high-resolution satellite rainfall products (SRP) including, the TMPA 3B42, CPC morphing technique (CMORPH), Global Satellite Mapping of Precipitation (GSMaP), Precipitation Estimation from Remotely Sensed Information using Artificial Neural Networks (PERSIANN), and PERSIANN-Cloud Classification System (PERSIANN-CCS) demonstrated the impact of seasonality, topography and climatology on the functionality of the selected rainfall products (Maggioni

et al., 2016). It was specifically discovered that satellite rainfall products performed quite poorly over semiarid and areas over complex terrains. Again, light rains especially during the winter seasons were poorly represented by these satellite rainfall products.

In a similar study, Dinku et al. (2007) applied various statistical measures including, the linear correlation, mean error, root mean squared error, efficiency and bias to check the validity of various satellite rainfall estimates thus, the Global Precipitation Climatology Project (GPCP), the National Oceanographic and Atmospheric Administration Climate Prediction Center (NOAA-CPC) merged analysis (CMAP), the Tropical Rainfall Measuring Mission (TRMM-3B43), NOAA-CPC African rainfall estimation algorithm, GPCP one-degree-daily(1DD), TRMM-3B42, Tropical Applications of Meteorology using Satellite and other data (TAMSAT) estimates, and the CPC morphing technique (CMORPH). Their results highlighted the dynamic nature of the satellite-rainfall products over the East African complex topography. Their findings to some extent agreed with Maggioni et al. (2016) as they also demonstrated the poor performance of SRPs over complex terrains however, the CMORPH, TAMSAT and TRMM-3B42 were observed to prove better skill compared to the other products in the region.

As a follow up study, Dinku et al. (2008) validated six high-resolution SRPs including, TRMM-3B42, CMORPH, PERSIANN, NOAA-CPC African rainfall estimation algorithm (RFE) and the Naval Research Laboratory's blended product in the Ethiopian complex topography and Zimbabwe. Their results revealed all six SRPs to averagely perform quite good over the Ethiopian complex topography and Zimbabwe. They again revealed here that the CMORPH and TRMM-3B42

products proved better skill in capturing the seasonal-annual rainfall over the two regions. The RFE was also found to perform poorly over the complex topography of Ethiopia and very well in Zimbabwe.

Furthermore, Thiemig et al. (2012) investigated the accuracies of the CMORPH, the Rainfall Estimate (RFE2.0), TRMM 3B42, GPROF 6.0, PERSIANN and GSMaP MVK. They applied standard statistical methods and visual inspection for a period four years to assess their performance over sparsely gauged African river basins. Regarding their detectability and estimation strength, it was found that the selected SRPs showed an underestimation of heavy rainfall and the number of rainy days especially over the Tropics. Nonetheless, these satellite rainfall estimates showed good skill during the driest seasons and were able to capture the diurnal and bimodal precipitation patterns effectively.

In addition, over the West African continent Pfeifroth et al. (2016) in agreement with the finding of Thiemig et al. (2012) demonstrated the potency of four selected SRPs to replicate the diurnal rainfall patterns as well as their variabilities over the region reasonably well. Their study considered SRPs with sub-daily temporal resolutions including, TRMM Multi-satellite Precipitation Analysis (TMPA), TRMM 3G68, CMORPH and PERSIANN rainfall products. They revealed generally that the selected SRPs underestimated the time of occurrence of nocturnal peak precipitation organised as a result of "locally induced" convective systems for nearly two (2) hours. CMORPH and TMPA similar to Dinku et al. (2007), were shown to have proven better skill averagely compared to the other estimates. The performance of the TRMM and FEWS SRPs were also assessed over the Ashanti region of Ghana by Amekudzi et al. (2016). Their study brought

to light the general good skill of both satellite rainfall nonetheless, TRMM outperformed FEWS in the region.

On the other hand, Nicholson et al. (2003) revealed the strengths and weaknesses of four (4) other satellite and blended rainfall products which included the Global Precipitation Climatology Center (GPCC), Global Precipitation Climatology Project (GPCP), GOES Precipitation Index (GPI) and the Special Sensor Microwave/Imager (SSM/I) rainfall products over Africa for the period of 1988–94 and 1998. Their study revealed a similarity in the performance of the GPCC and GPCP rainfall products over the region which were both relatively good in capturing monthly-seasonal rainfall patterns. However, they found the GPI and SSMI to exhibit a rather relatively high bias and root mean square errors demonstrating their deficiencies especially over Africa.

Again, Ali et al. (2005) inter-compared the Global Precipitation Climatology Project (GPCP), Global Precipitation Climatology Center (GPCC), Geostationary Operational Environmental Satellite (GOES) precipitation index (GPI) together with the Climate Prediction Center (CPC) merged analysis of precipitation (CMAP) using various statistical techniques over the Sahel region. They reported that the CMAP rainfall products relatively performed well on the average followed by GPCC, GPCP, and GPI. From their results, the conclusion for the GPI product was in agreement with Nicholson et al. (2003) however, the bias and rmse values as reported by the former were seen to be a little overestimated.

These findings thereby give a clear indication that regional validation studies seem to present the true performance of the SRPs rainfall products compared to larger scale and global validation studies.

Attempts to validate SRPs in other parts of the world aside Africa have revealed various results with a couple of them confirming and others contradicting findings in Africa. Gridded gauge data from highly dense gauge network over Greece was applied to assess the performance of widely used SRPs including, the TRMM Microwave Imager (TMI) precipitation product (3A12), TRMM 3B42 and TRMM 3B43, the Global Precipitation Climatology Project one-degree daily (GPCP-1DD) analysis, GPCP Satellite and Gauge (GPCP-SG) product, and the National Oceanographic and Atmospheric Administration Climate Prediction Center (NOAA-CPC) Merged Analysis (CMAP) for a period spanning 1998–2006 (Feidas, 2010). This exercise demonstrated the efficacy of the TRMM and CMAP SRPs over Greece thus, similar to the findings of Dinku et al. (2007, 2008); Thiemig et al. (2012); Amekudzi et al. (2016) over various sectors and spatio-temporal resolutions in Africa.

Over the Southern Korean Peninsula, the performance of four highly-resolved satellite rainfall estimates namely, HRPPs, the TRMM Multi-satellite Precipitation Analysis (TMPA), CMORPH, PERSIANN and the National Research Laboratory (NRL) blended precipitation dataset (NRL-blended) were thoroughly investigated for a period of four years (Sohn et al., 2010). This was done applying minutely resolved gauge network consisting of a total of 520 sites from the Automated Weather Stations (AWS) network which were obtained from the Korean Meteorological Administration (KMA). Their results revealed the TMPA product to agree well with rain gauge records compared to the other selected SRPs they assessed. Sohn et al. (2010) found the diurnal rainfall cycles as

represented by the AWS over the Korean Peninsula to be generally underestimated by the PERSIANN, CMORPH and the NRL-blended products.

Again, for a period of three years, McCollum et al. (2002) investigated the performance of two satellite algorithms thus, the multi-spectra and micro-wave algorithms over the continental United States. Their results showed that the microwave algorithm overestimates rainfall in summer and underestimates during winter. The multi-spectral algorithm on the other hand greatly overestimated daytime overpasses in the region. Similarly, Ebert et al. (1996) intercompared three Global Precipitation Climatology Project (GPCP) algorithms. Geostationary-based satellite algorithms were found to relatively capture the monthly rainfall well. Polar algorithms on the other hand were able to capture monthly rainfall appreciable well however, this only happened when data from the satellite products were readily accessible.

Xie et al. (1996) validated various spatio-temporal satellite rainfall products on monthly scales and found that the precipitation distribution of both infra-red (IR) and microwave (MW) based satellite rainfall products possess some similarities. They also revealed the poor performance of IR-based satellite rainfall products over land especially during the cold seasons. Their findings proves that no one satellite rainfall product can be used as a representative of a global monthly rainfall product as they all seem to have various strengths and weaknesses over specific locations of the globe.

In the Washita watershed region in Oklahoma, Zeweldi and Gebremichael (2009a) applied various statistical techniques to inter-compare the performance of the CMORPH and the gauge-adjusted Next Generation Weather radar

(NEXRAD) rainfall observations for a period of three years. From their results, it was shown that the CMORPH SRP had a strong tendency to overestimate (underestimate) rainfall records in summer (winter) season which is consistent with the findings of McCollum et al. (2002). They again brought to light the dynamical nature of the SRPs and thus recommended that rainfall data from these products to be accompanied by their various error information so as to make the data more feasible and meaningful for applications.

Jamandre and Narisma (2013) over the Philippines assessed the performance of two SRPs CMORPH and TRMM using eight ground-based station data and gridded data for a period of three years. From their results, it was shown that TRMM and CMORPH notably showed good skill however, TRMM was found to out-perform the CMORPH product in most cases. Again, TRMM and CMORPH were able to capture strong rainfall events ranging from 50–200 mm/day. They again highlighted that the two products were quite good over the north-eastern sectors of the Philippines but poor over the southern sectors indicating the performance of the SRPs is mainly dependent the nature of geographical location and the intensity of the rainfall estimated.

Joyce et al. (2004) applied high quality rain gauge datasets from the Climate Prediction Center real-time daily gauge analysis to validate the CMORPH data in the United States. Their findings revealed that, the morphing technique used for the CMORPH rainfall estimates proved to be much better than a combination of the Infra-red and passive microwave (IR-PMW) rainfall estimates thus, the great performance of CMORPH product in the region.

Gebremichael et al. (2005) applied the "conditional" and "unconditional" continuous technique alongside the categorical statistical evaluation techniques to assess the performance of the GPCP 1DD SRP over the Mississippi river basin on seasonal-annual temporal resolutions for a period of four (4) years. The GPCP 1DD product was revealed to effectively detect the number of rainy days as well as the spatio-temporal rainfall variability in the region.



CHAPTER 3

General Methodology

3.1 Study Area

This study was carried out in Ghana which is located at the West African Guinea Coast and its climate is determined by the West African monsoon. Rainfall is bi-modal in the sub-humid south and uni-modal in the semi-arid north. The first rainy season at the coast peaks in May-June and is stronger than the second rainy season in October-early November (Fink et al., 2017). In between, the little dry season culminates in August, with the major dry season occurring in boreal winter. Farther inland, the rainy season is still bi-modal, but the second rainy season is now stronger and occurs already in September. The northern part is characterized by a uni-modal rainy season peaking in August, thus resembling the situation in the Sahel zone (e.g., Fink et al. (2017)). Ghana has been sub-divided into four agro-ecological zones based on the climate and natural vegetation which are, coastal, forest, transition, and savannah zones (Aryee et al., 2017; Amekudzi et al., 2016). Recently, Maranan et al. (2018) have shown that while the bulk of rainfall is provided by Mesoscale Convective Systems (MCSs), less-organized and more isolated systems become more important at the coast. In a 100-km wide strip paralleling the coast, land-sea breeze convection is relevant.

On average, the annual rainfall total over the entire country ranges between 800–1800 mm/year with relatively high rainfall values in the southern part and low

values in northern part. Specifically, southwestern and eastern parts of the Volta lake have the highest annual rainfall total approximately 1200–1800 mm/year whereas an annual total of about 800–1200 mm/year covers the eastern coasts and most parts of Northern Ghana (Baidu et al., 2017; Aryee et al., 2017).

The Ashanti region of Ghana serves as the Dynamics-Aerosol-Chemistry-Cloud Interactions in West Africa (DACCIWA) project rain gauge site. This initiative has installed seventeen optical rain gauges over various locations in this region for high temporal rainfall measurements (see Table 3.1).

Table 3.1: Information on the seventeen DOG stations over the Ashanti region of Ghana, including the longitude, latitude, and elevation.

Station Name	Gauge number	Longitude [W]	Latitude[N]	Elevation [m]
Mampong	RG01	1.24	7.03	439
Agromet	RG02	1.34	6.41	282
Anwomaso	RG04	1.31	6.41	288
Ejura	RG06	1.23	7.22	228
Jamasi	RG07	1.28	6.58	316
Effiduase	RG08	1.24	6.51	368
Akrokeri	RG09	1.39	6.18	259
Bekwai	RG10	1.34	6.27	241
Nyinahin	RG11	2.07	6.35	196
Owabi	RG13	1.42	6.45	237
Kuntenase	RG14	1.29	6.32	301
Nsuta	RG15	1.24	7.00	465
Bompata	RG16	1.03	6.38	236
Konongo	RG17	1.14	6.37	255
Kubease	RG18	1.22	6.40	239
Agogo	RG19	1.04	6.48	417
Mankranso	RG20	1.52	6.80	243

The region lies between latitudes, 5.50° N–7.46° N and longitudes, 2.25° W–

0.15° W and occupies a total area of about 25,000 Km² (see Figure 3.1).

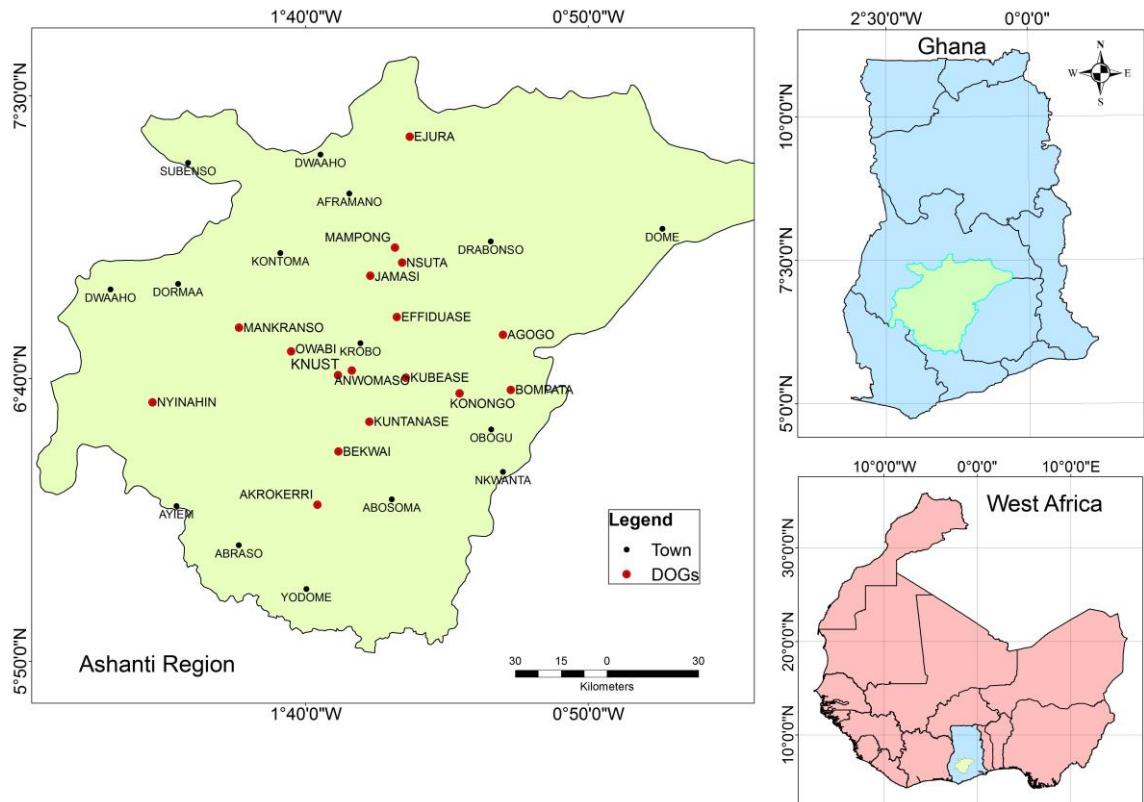


Figure 3.1: Geographical location of the study area with locations of the seventeen DACCWA optical rain gauge stations (in red) over the Ashanti region of Ghana.

3.2 Data Sources and Climate Indices

3.2.1 Gauge Datasets

The in-situ datasets used to carry out this research study were obtained from the Ghana Meteorological Agency (GMET) and DACCWA project measurements.

3.2.1.1 DACCWA Optical Rain Gauge (DOG) Data

DACCWA is an European funded project with a prime mandate of examining the health and agricultural impacts of human and natural emissions on the general atmospheric compositions of the south West African region (Knippertz et al.,

2015b, 2017).

Within the scope of this project, seventeen optical rain gauges (see Figure 3.1 and Table 3.1) with minute temporal resolutions have been deployed over the Ashanti region of Ghana. Some of the rain gauges have been operational since June 2015–till date. However, for the purpose of the performance assessment carried in this study, DOG data for the co-located GMet gauge stations were used for the period of 2016–2017.

The measuring technique of the DOG is such that, rainfall collected into the DOG collector (Figure 3.2a) is detected and counted by a sensor in the DOG logger (Figure 3.2b). The DOG works with the principle that, any raindrop through its collector assumes the size of its orifice. The rainfall amount for any rainfall event can therefore be inferred as follows;

$$R_a = r * R_{Nd}. \quad (3.1)$$

Where R_a is the rainfall amount, r is the constant radius of the orifice (0.01 mm) and R_{Nd} represents the number of raindrops.



(a)



(b)

Figure 3.2: DOG rain gauge setup for inference of areal rainfall data; (a) data collector, (b) data logger+solar panel.

The DOGs like any ground-based measurement technique are associated with some discrepancies which are mainly as a result of environmental impacts or their measurement procedure. One common error source of the gauges arise from the clogging of the gauge collector. Since the DOGs have a very tiny orifice (0.01 mm), it makes it highly susceptible to clogs (see Figure 3.3). This is mostly serious especially in cases of a high wind shear. The winds carry particles like fine sand, dust, dry weeds and many others unto the collector which thereby causes a blockage of the orifice and at the long run underestimating the actual rainfall amount (see Figure 3.4). Again, the DOGs are less wind-shielded thus, in an event of strong winds, rain drops are deviated from the orifice of the gauges.



Figure 3.3: Image showing a clogged DOG observed during field visit.

Owing to the number of errors these gauges are exposed to, frequent maintenance are thereby crucial. These gauges are maintained by cleaning the data collector to get rid of clogs that must have occurred as well as clearing long weeds that could block the data collector. DOGs are also tested during the visits

to make sure that the sensor of the data collector is able to effectively detect and record rainfall drops.



Figure 3.4: Image showing dust particles in the collector of DOG observed field visit.

3.2.1.2 GMet Standard Rain Gauge (SRG) Data

Monthly rainfall fields were derived from a relatively dense network of 113 rain gauge stations over Ghana (see Figure 3.5a) from GMet for a period of fifteen years (1998–2012). These datasets were gridded and later applied as reference data for assessing the performance of satellite and merged rainfall datasets over the entire country. This data was used in the gauge–satellite validation which is the focus of specific objective one of the thesis.

Daily rainfall datasets for nine synoptic stations (Mampong, Agromet, Bekwai, Akrokeri, Bompata, Ejura, Jamasi, Mankranso and Nsuta) over the Ashanti region of Ghana were also obtained from GMet for the period 2016–2017. The rainfall data for the nine synoptic stations were used to assess the potencies of DOG data in co-located stations, which is the focus specific objective two of this thesis.

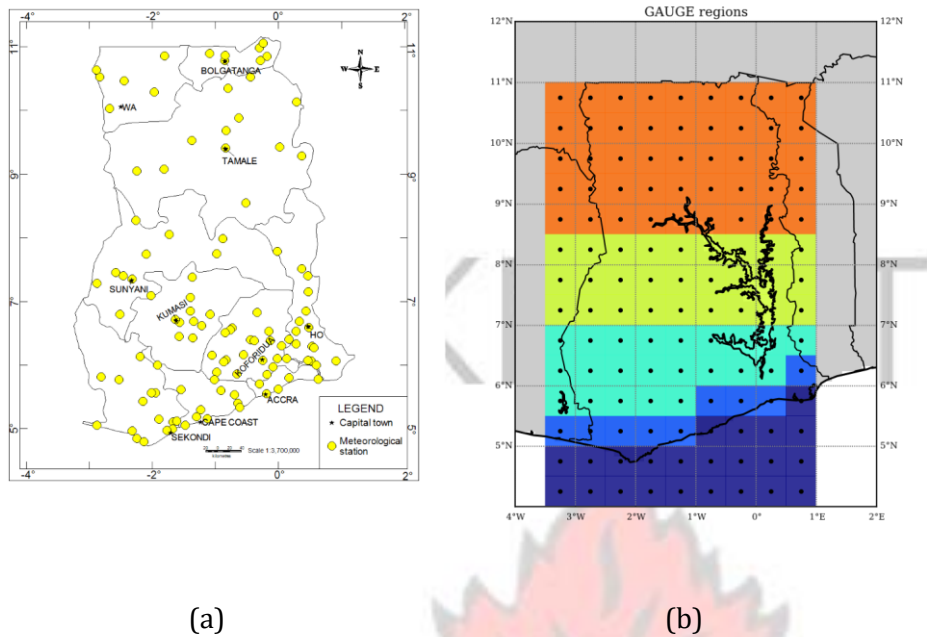


Figure 3.5: (a) Map of Ghana indicating the locations of all the 113 meteorological stations, (b) delineations of the four agro-ecological zones (b); Savannah (orange), Transition (yellow), Forest (cyan) and Coast (sky blue).

3.2.2 Satellite Datasets

The validation studies carried out in this thesis used a total of seven satellite-based and two gauge-only rainfall products. These satellite rainfall products have been selected on basis on their long time series availability, near real-time and public domain availability as well their frequent usage for hydrological applications in the region. Summarised information on the products are given in Table 3.2 whereas a brief description of each product is presented in the following sections.

3.2.2.1 Integrated Multi-satellite Retrievals for Global Precipitation Measurements

(IMERG)

IMERG rainfall product is an initiative of the National Aeronautics and Space Administration (NASA) and the Japan Aerospace Exploration Agency (JAXA). IMERG is produced to build upon the success of the Tropical Rainfall Measuring Mission (TRMM) rainfall product (Adler et al., 2017). The product provides global observations of rainfall at temporal resolutions of 30 minutes, 3 hour and 1 day and spatial resolution of $0.1^\circ \times 0.1^\circ$. IMERG product has been operational since 2014. For the purpose of the objective two of this study, daily rainfall data for the period of 2016–2017 was used.

3.2.2.2 Tropical Rainfall Measuring Mission (TRMM)

TRMM like IMERG is also a collaboration between JAXA and NASA. TRMM was produced to facilitate the monitoring of tropical and sub-tropical precipitation systems (Huffman et al., 2007). The product uses two main instruments thus, the Precipitation Radar (PR) and TRMM Microwave Imager (TMI) for its precipitation estimation (Huffman et al., 2007). TRMM has a high spatial resolution of $0.25^\circ \times 0.25^\circ$ and produces rainfall data in timestamps of 3 hour, 1 day and 1 month intervals over the Tropics. More information on the product can be found in Table 3.2.

Table 3.2: Summarized information on the nine validated rainfall products.

Dataset	Spatial Resolution [°]		Temporal Resolution		Product type	Coverage	References
	Original	Used	Original	Used			
CMAP	2.50	2.50	Monthly	Monthly	Satellites+gauge	Global	Xie and Arkin (1997)
GPCP V2.2	2.50	2.50	Monthly	Monthly	Satellites+gauge	Global	Adler et al. (2003)
GPCC V6	0.50	0.50	Monthly	Monthly	Gauge-only	Global	Schneider et al. (2014)
ARC2 2	0.10	0.50	Daily	Monthly	Satellites+gauge	Africa	Fensholt and Rasmussen (2011)
CRU TS3.21	0.50	0.50	Monthly	Monthly	Gauge-only	Global	Trenberth et al. (2014)
TAMSAT V3	0.0375	0.50	Daily	Monthly	Satellites+gauge	Africa	Maidment et al. (2017)
TRMM 3B43	0.25	0.50	Monthly	Monthly	Satellites+gauge	Tropics	Huffman et al. (2007)
TRMM 3B42RT	0.25	0.25	3 hour	3 hour	Satellites+gauge	Tropics	Huffman et al. (2007)

CHIRPS V2	0.25	0.50	Daily	Monthly	Satellites+gauge	Africa	Funk et al. (2015)
IMERG V2	0.10	0.10	30 minutes	3 hour & daily	Satellites	Global	Adler et al. (2017)

3.2.2.3 Global Precipitation Climatology Centre (GPCC) V6

The GPCC rainfall product was established by the World Meteorological Organisation (WMO) in 1989 and currently operated by the Deutscher Wetterdienst (National Meteorological Service of Germany). This is to serve as the German contribution to the World Climate Research Programme (WCRP) (Schneider et al., 2008). The product provides global monthly precipitation measurements using in-situ rain gauge datasets at a spatial resolution of $0.5^\circ \times 0.5^\circ$. Schneider et al. (2014) provides further details on the GPCC rainfall product.

3.2.2.4 Climate Rainfall Unit (CRU)

The CRU rainfall product produces precipitation measurements based on the reanalysis of nearly 4000 gauge stations at spatial resolution of $0.5^\circ \times 0.5^\circ$. Besides precipitation, the product includes measurements of other climate variables such as mean temperature, vapour pressure, cloud cover among others (Trenberth et al., 2014). More information on the product is found in Trenberth et al. (2014) and Harris et al. (2014).

3.2.2.5 Tropical Applications of Meteorology using Satellite data and ground-based observations (TAMSAT)

TAMSAT was established by the University of Reading the year, 1977 however, over the past years TAMSAT have collaborated with the Climate Division of the National Centre for Atmospheric Science (NCAS) and the National Centre for

Earth Observation (NCEO) (Tarnavsky et al., 2014). The purpose of this collaboration was to broaden the range of climate variables TAMSAT provides. The algorithm for the TAMSAT rainfall product is based on the assumption that cold cloud-top temperatures of tropical storms identify clouds that are rain bearing (Thorne et al., 2001). The cold cloud-top temperatures are obtained from the Meteosat Infra-red imagery and Cold Cloud Duration (CCD) imagery. The TAMSAT algorithm assumes that CCD is directly proportional to the rainfall amount (Thorne et al., 2001). The relationship between rainfall and CDD is expressed as:

$$\text{Rainfall} = b_0 + b_1(\text{CDD}), \quad (3.2)$$

where b_0 and b_1 are constants with each parameter in Equation 3.2 obtained by using rain gauge data.

3.2.2.6 African Rainfall Climatology (ARC2)

ARC2 serves as the United States Agency for International Development (US-AID) contribution to the drought monitoring initiative in Africa (Love et al., 2004). The rainfall measurement algorithm for this product includes estimates of IR data as well as daily rainfall data from GTS reports (Fensholt and Rasmussen, 2011). ARC2 has a spatial resolution of $0.1^\circ \times 0.1^\circ$ and a daily temporal resolution.

3.2.2.7 Climate Hazards Group Infra-red Precipitation with Station data (CHIRPS V2)

The CHIRPS rainfall data was obtained from the International Research Institute for Climate and Society (IRI) data website. The product is as a result of the joint collaboration between scientists in the U.S. Geological Survey (USGS) and the Earth Resources Observation and Science (EROS) Center with the aim of providing rainfall data suitable for climate-impact studies such as, floods and droughts monitoring, trend analysis among others (Funk et al., 2015). CHIRPS is a quasi-global product which provides data with a daily temporal resolution and a spatial resolution of $0.25^\circ \times 0.25^\circ$. This rainfall product is a combination of satellite imageries at resolution of 0.05° and ground-based station datasets. The CHIRPS algorithm also incorporates various temporal resolutions of Cold Cloud Duration (CCD) based precipitation.

3.2.2.8 CPC Merged Analysis of Precipitation (CMAP)

The CMAP is a global rainfall product which has been operational since 1979–present. The rainfall data produced by CMAP has a temporal resolution of pentad and monthly aggregations and a spatial resolution of $2.5^\circ \times 2.5^\circ$ (Xie and Arkin, 1997). The CMAP rainfall measuring algorithm as described by Xie and Arkin (1997) applies the merging technique by combining gauge data with satellite estimates.

3.2.2.9 Global Precipitation Climatology Project (GPCP) V2.2

GPCP is established by the World Climate Research Program (WCRP) which was later joined by the Global Energy and Water Exchange program (GEWEX). This product was produced to contribute in solving the problem of biased quantification of global precipitation (Huffman et al., 2011). GPCP is a monthly rainfall product with a spatial resolution of $2.5^\circ \times 2.5^\circ$. Its algorithm combines precipitation data from rain gauge stations, satellites and sounding observations to estimate precipitation globally. Further information on this rainfall product is found in Huffman et al. (1997); Adler et al. (2003).

3.2.3 Global sea surface temperature (SST) Data

The SST data employed in this study is the National Oceanic and Atmospheric Administration extended reconstructed SST data called, ERSST V5. ERSST V5 is the current version of SST data which has monthly temporal resolution and a spatial resolution of $2^\circ \times 2^\circ$. This product includes the newly released SST from the International Comprehensive Ocean-Atmosphere Dataset (ICOADS) (Huang et al., 2017). To achieve the objective three of this study, annual averages for the period of 1981–2015 were computed and applied. Further details on the product could be obtained in Huang et al. (2017).

3.2.4 Remote Climate Indices

3.2.4.1 Dipole Mode Index (DMI)

The DMI also known as the Indian Ocean Dipole (IOD) is a coupled ocean-atmosphere phenomenon occurring in Indian Ocean (Diatta and Fink, 2014). It describes the SST anomalous difference between the western parts of the equatorial Indian Ocean (50°E - 70°E and 10°S - 10°N) and the south eastern equatorial Indian Ocean (90°E - 110°E and 10°S - 0°N) (Vinayachandran et al., 2002). Monthly fields of DMI were obtained from the National Oceanic and Atmospheric Administration (NOAA), Global Climate Observing system (GCOS) for a period of 1870–2017. The data was averaged to have annual means covering the period of 1981–2015 to match the rainfall indices along time axis for further analysis in objective three of this thesis.

3.2.4.2 NINO3.4 Index

The NINO3.4 is the average SST anomalies in the NINO3.4 region (5°N to 5°S , from 170°W to 120°W) (Barnston and Tippet, 2013). Monthly fields of the NINO3.4 were obtained from the National Oceanic and Atmospheric Administration (NOAA) Global Climate Observing system (GCOS) for the period of 1948–2018. Annual means for 1981–2015 were computed from the monthly fields and applied for this study. More details on NINO3.4 can be found in Trenberth and Stepaniak (2001) and Trenberth et al. (2001).

3.2.4.3 Atlantic Multidecadal Oscillation (AMO)

The AMO index is a basin-scale mode of observed multi-decadal climate variability which describes the average SSTs in the north of Atlantic (0° – 70° N) (Enfield et al., 2001, and references therein). It is based on the Kaplan SST data with spatial resolution $5^{\circ} \times 5^{\circ}$ spanning the period from 1856 to 2018. More information on the AMO index is found in Enfield et al. (2001).

3.3 Research Methods

3.3.1 Validation of Satellite-based Rainfall products

West Africa is known for its sparse rain gauge networks as a result, satellite and merged rainfall products are most often than not applied for various climate impact studies in the region. However, satellite products come along with some discrepancies as such, this study serves as a foremost step to assessing the potencies of satellite and merged rainfall products in Ghana. This would help increase our confidence in their applications for various key activities in the country.

3.3.1.1 Specific Objective One: Evaluate the accuracies and discrepancies of satellite and merged rainfall products over Ghana

The reference monthly rainfall datasets for this validation were obtained from the Ghana Meteorological agency (GMet) for a total of 113 synoptic stations during the period of 1998–2012 as earlier discussed in Section 3.2.1. The satellite and merged rainfall products validated in this first half of the validation exercise are the TRMM 3B43, GPCP, TAMSAT, FEWS ARC2, CRU, GPCP, CMAP and CHIRPS (see Section 3.2.2 and Table 3.2).

Procedurally, the monthly rainfall data for all the 113 stations over Ghana were first subjected to a homogenization process with the aid of the RHtestsV4 software package (see section 3.3.1.4 for details) for a thorough quality check of the data. Thereafter, the minimum surface curvature (MSC) technique was applied to grid the resultant homogenised rainfall datasets over the country. The MSC technique is a widely used gridding method applied especially in the field of earth and physical sciences (Aryee et al., 2017; Smith and Wessel, 1990). This method applies continuous second order derivatives and minimal total squared curvature to interpolate the reference rainfall datasets to be gridded (Smith and Wessel, 1990). MSC gridding approach is extensively described in Aryee et al. (2017, and references therein). The GMet gridded rainfall data was then aggregated into the respective spatial resolutions of the rainfall products (see Table 3.2) for an unbiased assessment.

In order to assess the performance of these rainfall products in Ghana, two strategies were employed thus, a country-wide validation and assessments based

on the four ecological zones (see Figure 3.5b). Rainfall data was extracted for the four ecological zones based on the delineation in Figure 3.5b for the gridded gauge data and all satellite rainfall products. The inter-zonal assessment was not carried out on the CMAP and GPCP rainfall products because they have relatively coarse spatial resolutions of $2.5^\circ \times 2.5^\circ$ hence, difficult to be sub-sectioned into zones. Monthly averages were computed for all satellite rainfall products in daily timescales over the entire country and in the four ecological zones. Furthermore, for both strategies, the assessments were carried out based on four inter-comparison techniques thus, inter-seasonal, inter-seasonal anomalies, inter-annual and interannual bias assessments. Lastly, the quality of the rainfall products with respect to gauge were investigated with a suite of statistical techniques discussed in Section 3.3.1.3. Results and discussions for this objective are presented in the Chapter four.

3.3.1.2 Objective Two: Assess the performance of DOGs, IMERG and TRMM sub-daily rainfall products over the Ashanti region of Ghana

The second phase of validation study is aimed at assessing the performance of high spatio-temporal satellite-based rainfall products during the DACCIWA project over the Ashanti region of Ghana. Satellite-based rainfall products validated in this phase are the IMERG and TRMM sub-daily rainfall products (see Section 3.2.2).

Daily rainfall fields for nine co-located GMET and DACCIIWA Optical rain gauges (DOG) synoptic stations were obtained for a period of 2016–2017 (Section 3.2.1.2). As a foremost step, the rainfall data from the gauge measurements (GMet and DOG) for the nine co-located stations were first quality checked (see Section 3.3.1.4) thereafter, stations with missing data were subjected to the proximal interpolation technique for data gap filling. The proximal interpolation estimates missing values of a station with the nearest neighbouring station known values. This data gap filling approach has been successfully applied in several studies including Desmet (1997); Chen et al. (2003); Olivier and Hanqiang (2012). The DOG rainfall data were then averaged to daily time steps and later time synchronised to GMet observation hours (09–09 GMT) for an unbiased inter-comparison with the GMet daily rainfall fields.

This assessment took a two-phase strategy, the first was aimed at the daily and seasonal assessments of DOGs over the nine co-located stations with respect to GMet rainfall measurements. The purpose of this initiative was to first assess the validities of the new DOGs datasets over the region before applying them as reference in the second phase. The second strategy was dedicated to understanding the performance of high temporally resolved IMERG and TRMM rainfall products over the region. Rainfall datasets for IMERG and TRMM were extracted for all selected stations during the monsoonal season of 2016 and 2017. Thereafter, DOGs with minute temporal resolution were averaged to daily time steps for a point-point validation of the pre-averaged daily IMERG and TRMM rainfall data.

The daily, monthly and seasonal assessments of the two satellite rainfall products with respect to DOGs were then performed for all nine stations. The quality of the DOG, IMERG and TRMM for all stations were assessed statistically with metrics described in Section 3.3.1.3.

KNUST

3.3.1.3 Statistical Metrics

The Pearson correlation coefficient (r) is a non-dimensional measure of the linear relationship between two parameters thus, the observations and estimates. The Pearson r clearly measures the strength as well as the direction of relatedness between the gauge and the estimates. Pearson correlation coefficient has range between -1 and +1 where, -1 denotes an inverse relationship, 0 denotes no relationship and 1 is a perfect relationship between measures.

$$r = \frac{N \sum_{i=0}^N G_i V_i - \sum(G_i) \sum(V_i)}{\sqrt{(N \sum G_i^2 - \sum(G_i)^2)(N \sum V_i^2 - \sum(V_i)^2)}} \quad (3.3)$$

Bias is a measure of how much an estimator underestimates or overestimates observations. The bias value quantifies the level or amount of systematic errors that could be present using the estimates. The accuracy of the estimates is mostly affected by the systematic errors thus by the bias value, one can tell how accurate the estimates are with respect to the observations. A bias value of 1 is a perfect score, bias value > 1 is an overestimation whereas bias < 1 is an underestimation.

$$Bias = \frac{\sum_{i=0}^n V_i}{\sum_{i=0}^n G_i} \quad (3.4)$$

The root mean square error (RMSE) is a measure of the mean deviation of the estimates from the observations thus, measuring the RMSE estimates the margin of random errors present. Random errors affects the reliability of the data estimated thus, RMSE can be used to infer the reliability of the data. RMSE value of 0 is a perfect skill.

$$RMSE = \frac{\sqrt{\frac{1}{n} \sum_{i=0}^N (G_i - V_i)^2}}{\bar{G}_i} \quad (3.5)$$

The Nash-Sutcliffe efficiency coefficient (eff) gives a measure of how well the estimate predicted the observations. Eff also quantifies the quality of an estimator. Eff ranges from $-\infty$ to 1. Eff value of 0 means the gauge mean is as good as the estimates. Negative values of eff means gauge mean is better than the estimates. Eff value of 1 means there is a perfect match between the means of the gauge and the estimates.

$$eff = 1 - \frac{\sum_{i=0}^N (G_i - V_i)^2}{\sum_{i=0}^N (G_i - \bar{G}_i)^2} \quad (3.6)$$

The Probability Of Detection (POD) measures the fraction of the gauge records correctly detected by the satellite estimates.

$$POD = \frac{h}{h + m} \quad (3.7)$$

The False Alarm Ratio (FAR) is the fraction of rainfall observed by satellite however, not confirmed by gauge.

$$FAR = \frac{f}{f + h} \quad (3.8)$$

The Critical Success Index (CSI) is a relative measure of accuracy which depends on the false alarms and missed events. CSI ranges from 0 (no skill) to 1 (perfect skill).

$$CSI = \frac{h}{h + f + m} \quad (3.9)$$

The Volumetric Hit Index (VHI) is a measure of the volume of gauge rainfall data that is correctly detected by the satellite estimates.

$$VHI = \frac{\sum_{i=1}^n (V_i | (V_i > t \& G_i > t))}{\sum_{i=1}^n (V_i | (V_i > t \& G_i > t)) + \sum_{i=1}^n (G_i | (V_i \leq t \& G_i > t))} \quad (3.10)$$

The Volumetric False Alarm Ratio (VFAR) represents the volume of falsely detected satellite records above a predefined threshold normalised by the sum of the gauge observations. It has range from 0 (perfect skill) to 1 (no skill).

$$VFAR = \frac{\sum_{i=1}^n (V_i | (V_i > t \& G_i \leq t))}{\sum_{i=1}^n (V_i | (V_i > t \& G_i > t)) + \sum_{i=1}^n (V_i | (V_i > t \& G_i \leq t))} \quad (3.11)$$

The Volumetric Miss Index (VMI) is the ratio of the volume of missed satellite estimates relative to gauge observations.

$$VMI = \frac{\sum_{i=1}^n (G_i | (V_i \leq t \& G_i > t))}{\sum_{i=1}^n (V_i | (V_i > t \& G_i > t)) + \sum_{i=1}^n (G_i | (V_i \leq t \& G_i > t))} \quad (3.12)$$

The Volumetric Critical Success Index (VCSI) measures the volume of performance of the estimator. VCSI has range between 0 (no skill) to 1 (perfect score).

$$VCSI = \frac{\sum_{i=1}^n (V_i | (V_i > t \& G_i > t))}{\sum_{i=1}^n ((V_i | (V_i > t \& G_i > t)) + (G_i | (V_i \leq t \& G_i > t)) + (V_i | (V_i > t \& G_i \leq t)))}. \quad (3.13)$$

Where Hit (h) is the correct detection of rainfall, Miss (m) depicts the rainfall that is observed yet not detected, False (f) is the rainfall detected yet not observed, V_i is the validated estimate, G_i is the gauge records and t is the threshold value set as 0. These metrics were adapted from AghaKouchak et al. (2011); Amekudzi et al. (2016, and references therein).

3.3.1.4 Homogenization Method

The homogenization of the rainfall datasets used in this study was carried out with the aid of the RHtestsV4 software package. This method serves to quality check and remove all non-climate features from the datasets. RHtestsV4 is a successor of RHtestsV3 software which has a new feature of Quantile Matching (QM) adjustment (Wang and Feng, 2010). The QM aids in the adjustment of the

input data so that distributions of all parts of the de-trended base series are in conformity with each other (Wang and Feng, 2010). RHtestsV4 uses the twophase regression model to detect change-points in the input data. It also has the ability to detect multiple change-points where available in the data (Wang and Feng, 2010; Lund and Reeves, 2002).

The two-phase regression model is represented as follows;

$$X_t = \begin{cases} \mu_1 + \alpha_1 t + \epsilon_t, & 1 \leq t \leq c \\ \mu_2 + \alpha_2 t + \epsilon_t, & 1 \leq c \leq n \end{cases} \quad (3.14)$$

Where, $\{\epsilon_t\}$ is the zero-mean independent random error (with constant variance, σ^2), c is known as the change-point when $\mu_1 = \mu_2$ for a step-type analysis and when $\alpha_1 = \alpha_2$ for a trend-type analysis.

RHtestsV4 is based on the penalized maximal t test described in Wang et al. (2007) and the penalized maximal F test (Wang, 2008b) which is embedded in a recursive testing algorithm (Wang, 2008a).

For instance, at time $T \in 2, \dots, m - 1$ the F-statistic for a change-point in the reference series is given as;

$$F_T = \frac{(Mod_{red} - Mod_{full})/2}{Mod_{full}/m - 4} \quad (3.15)$$

where, Mod_{full} depicts the full-model which is the sum of square errors given as;

$$Mod_{full} = \sum_{t=1}^T (X_t - \hat{\mu}_1 - \hat{\alpha}_1 t) + \sum_{t=T+1}^m (X_t - \hat{\mu}_2 - \hat{\alpha}_2 t) \quad (3.16)$$

Mod_{red} represents the reduced model given as;

$$Mod_{red} = \sum_{t=1}^T (X_t - \hat{\mu}_{red} - \hat{\alpha}_{red} t). \quad (3.17)$$

Where $\hat{\mu}_{red}$ and $\hat{\alpha}_{red}$ are estimated under the constraints, $\mu_1 = \mu_2 = \mu_{red}$ and $\alpha_1 = \alpha_2 = \alpha_{red}$ respectively.

Further details on the RHtestsV4 algorithm could be obtained from Wang and Feng (2010); Lund and Reeves (2002); Wang et al. (2007); Wang (2008b,a).

3.3.2 Objective Three: Examine the climatologies, trends and drivers of extreme rainfall events in Ghana

Rainfall extremes have serious implications on rain-fed agriculture, water resource management and other key socio-economic activities in the African continent including Ghana. This objective of the research investigates the spatio-temporal trends of rainfall extremes and their links to SST anomalies over oceanic basins.

The rainfall data used for this analysis is the CHIRPS daily rainfall data (Section 3.2.2). CHIRPS rainfall data was first validated as described in Section 3.3.1.1. Thereafter, rainfall fields for a total of 560 grids over Ghana were extracted. The

rainfall data for all grids were then subjected to a homogenization process using the RHtestsV4 software package described in section 3.3.1.4. The FClimDex package, a Fortran based software was then amended with a python script to compute the selected rainfall indices (see Section 3.3.2.1) for all 560 grids homogenised rainfall data. The Mann Kendall trend test technique (see section 3.3.2.3) was applied to detect trends in all extreme rainfall indices for all grids. The significance of trends were tested at a confidence interval of 95%.

In order to investigate the possible SST forcing on the rainfall extremes in Ghana, annual averages (equation 3.18) of the monthly SST anomalies were computed and correlated with a combined first three principal components of the extreme rainfall indices. The principal components were obtained from principal component analysis technique described in Section 3.3.2.2. The significance of the correlation coefficients obtained were tested at a confidence interval of 95%.

$$sst_y = \frac{1}{12} \sum_{i=1}^{12} sst_i, \quad (3.18)$$

$$P_c = \frac{\sum_{y=1}^n (sst_y - \overline{sst_y})(I_y - \bar{I}_y)}{\sqrt{\sum_{y=1}^n (sst_y - \overline{sst_y})^2} \sqrt{\sum_{y=1}^n (I_y - \bar{I}_y)^2}}, \quad (3.19)$$

where sst_y is SST data for a particular year, sst_i represents the monthly SST data

points, $\overline{sst_y}$ is the mean of SSTs for all years, I_y is the annual rainfall indices and \bar{I}_y is the mean of rainfall indices for all years and P_c is the Pearson correlation coefficient.

The correlation coefficients between SSTs and the extreme rainfall indices revealed significant correlations over oceanic basins however, there were no indications as to which portions of the country were influenced. Therefore further probing was required to investigate this. Annual averages of monthly NINO3.4,

AMO and IOD indices were first computed and correlated with the extreme rainfall indices at all grids (see equation 3.19). The significance of these grid-wise correlations were further investigated by computing the respective p-values for all grids which was later compared to a significance value of 0.05 (confidence interval of 95%). Grids with p-values greater than the significance value are considered insignificant whereas those less than the significance value are considered significant.

3.3.2.1 Selected extreme rainfall indices

The extreme rainfall indices explored in this study include, the Consecutive Dry Days (CDD), Consecutive Wet Days (CWD), Number of heavy rainfall days (R10mm), Number of heavy rainfall days (R10mm), Annual wet-day rainfall total (PRCPTOT), Very wet day (R95p), Extremely wet day (R99p), Simple daily intensity index (SDII), Daily maximum rainfall (RX1day) and 5-day maximum rainfall (RX5day). These indices analysed in this study are recommended by the World Meteorological Organization-Commission for Climatology (WMO-CCI) and the research program on Climate Variability and Predictability (CLIVAR) and JCOMM and have been extensively used in several studies (e.g., Sanogo et al.

(2015); Manzanas et al. (2014b); dos Santos et al. (2012); Zhang et al. (2001)).

Table 3.3 presents details of the selected extreme rainfall indices analysed in this study.

3.3.2.2 Mann Kendall (MK) trend test

This is a non-parametric trend test technique which is employed to detect trends in meteorological and hydrological time series among others (Blain, 2015). The Table 3.3: Selected rainfall indices computed over Ghana adapted from the ETCCDI website.

Indices	Name	Computation	Definition	Units
CDD	Consecutive Dry Days	$RR_{ij} < 1mm$	Maximum number of Days consecutive days with RR < 1 mm	Days
CWD	Consecutive Wet Days	$RR_{ij} > 1mm$	Maximum number of Days consecutive days with RR \geq 1 mm	Days
R10mm	Number of heavy rainfall days	$RR_{ij} > 10mm$	Annual count of days when RR >10 mm	Days
R20mm	Number of very heavy rainfall days	$RR_{ij} > 20mm$	Annual count of days when RR >20 mm	Days
PRCPTOT	Annual wet-day rainfall total	$\sum_{i=1}^n RR_{ij}$	Annual total rainfall in wet day (RR >1 mm)	mm
R95p	Very wet day	$R95p_j = \sum_{i=1}^N RR_{ij}$	Annual total rainfall when RR >95 percentile	mm
R99p	Extremely wet day	$R99p_j = \sum_{i=1}^N RR_{ij}$	Annual total rainfall when RR >99 percentile	mm
SDII	Simple daily intensity index	$SDII_i = \frac{\sum_{i=1}^N RR_i}{N}$	Annual mean rainfall with (RR \geq mm)	mm
RX1day	Daily maximum rainfall	$Rx1day = \max(RR_{ij})$	Annual maximum day rainfall	1- mm
RX5day	5-day maximum rainfall	$Rx5day = \max(RR_{ij})$	Annual maximum 5-day rainfall	5- mm

null hypothesis (H_0) of the Mann Kendall trend test assumes that the data comes from a population with independent variables which are identically distributed. The alternative hypothesis (H_A) on the other hand suggests that the data follows a monotonic trend (Pohlert, 2016).

Supposing the input data is X which consists of x values with a sample size of n , the MK is computed by first estimating the S statistic, given as;

$$S = \sum_{k=1}^{n-1} \sum_{j=k+1}^n \text{sgn}(X_j - X_k), \quad (3.20)$$

where sgn is given as,

$$\text{sgn} = \begin{cases} 1 & \text{if, } x > 0 \\ 0 & \text{if, } x = 0 \\ -1 & \text{if, } x < 0 \end{cases} \quad (3.21)$$

As the S statistic approaches a normal distribution with a mean $E[S] = 0$, the variance, σ^2 , it can be depicted as;

$$\sigma^2 = \frac{n(n-1)(2n+5) - \sum_{i=1}^n t_i(t_i-1)(2t_i+5)}{18}, \quad (3.22)$$

where n is the number of tied groups in the input data and t_j is the number of data points in the j th tied group.

The MK is then given as,

$$MK = \begin{cases} \frac{s-1}{\alpha} & \text{if, } s > 0 \\ 0 & \text{if, } s = 0 \\ \frac{s+1}{\alpha} & \text{if, } s < 0 \end{cases} \quad (3.23)$$

3.3.2.3 Principal Components Analysis (PCA)

PCA is a mathematical tool used to reduce the dimension of multivariate dataset which possibly has some patterns and structures within it (Jolliffe, 1986). PCA reduces the multivariate data into a set of uncorrelated mutually orthogonal variables also known as principal components without interfering with the variability of the original data (Jolliffe, 1986). The principal components (PCs) are ordered based on the order of the decreasing variance thus, the first principal component has the most variance whereas the last principal component has least variance. Since these PCs are ordered, they can thereby be truncated by simply chopping off PCs with least variance (noise) and retaining the PCs with the most variance. The PCs with the most variance explains most of the variability in the data (Richardson, 2009).

Mathematically, PCA is defined as the eigen decomposition of a covariance matrix (Jolliffe, 1986). Suppose the covariance matrix is denoted by X, then the convolution of the Covariance matrix and its transpose gives us a resultant of the eigenvectors (loadings) and eigenvalues (variances). This is expressed as,

$$X^T X \rightarrow \begin{cases} W \\ \lambda \end{cases}, \quad (3.24)$$

where, X^T is the transpose of the covariance matrix, W are the eigenvectors and λ the eigenvalues. W is first arranged in a decreasing order of the λ values. This implies that, each column of W represents the principal components (pcs) from the highest to the least variance of the data. Thereafter, W is truncated based on the number of pcs that explains most of the variance of the data. Suppose r number of pcs explains most of the variance of the data then,

$$W \rightarrow W_r \quad (3.25)$$

Therefore a product of the truncated W and X gives the scores depicted by $T_r X W_r = T_r$ (3.26)

3.3.3 Summary

This research study serves to increase our limited knowledge on the performance of SRPs as well as the climatologies and trends of rainfall extremes in Ghana. The study further enhances our understanding on the interrelationship between SST anomalies over Oceanic basins and rainfall extremes in Ghana. Towards achieving this main objective, three specific objectives were carried out. The first objective evaluates the inter-seasonal and inter-annual performance of two gauge-only and six satellite-based rainfall products using gridded GMet gauge data over Ghana. The second objective serves as a follow up study to the first objective. Objective two assessed the performance of the new DACCIWA optical rain gauge (DOGs) data over the Ashanti region of Ghana. This objective further evaluates

the ability of high spatio-temporal satellite rainfall products to capture the rainfall patterns at various time scales with respect to the DOGs. The objective three of this study applied the pre-validated CHIRPS rainfall data to analyse the mean climatologies, trends and drivers of extreme rainfall in Ghana. A summarized research design for the entire study is shown in Figure 3.6.

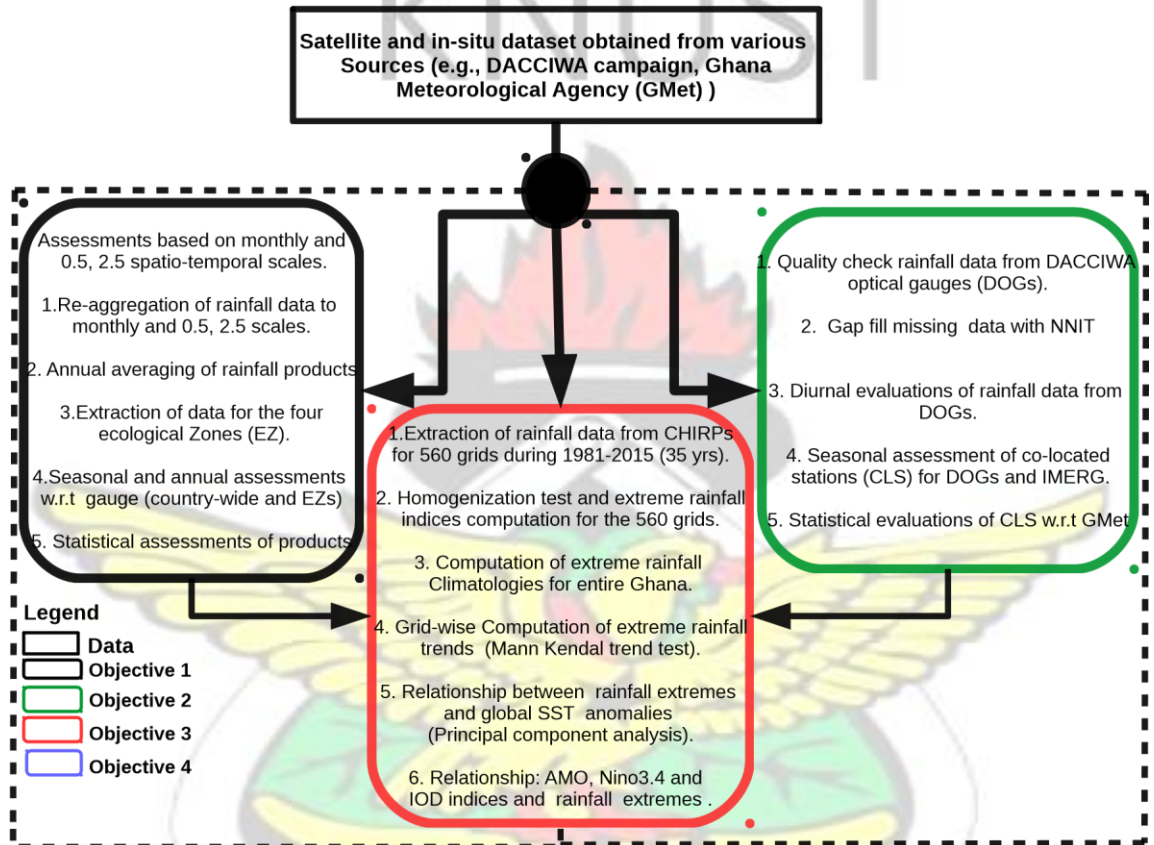


Figure 3.6: A chart of the research design for the three specific objectives.

CHAPTER 4

Evaluation the accuracies and discrepancies of satellite and merged rainfall products in Ghana

This chapter assesses the performance of various satellite and gauge rainfall products in the entire Ghana and over the four ecological zones of the country. The accuracies and discrepancies of the products were evaluated on monthly to annual time scales using a suite of statistical techniques.



4.1 Introduction

Rainfall plays an essential role in the effective management of key socio-economic activities including, rain-fed agriculture, land use, hydro-electrical power generation, water resource management and risk reduction of floods and droughts among others (Aryee et al., 2017; Amekudzi et al., 2015). In Ghana, agriculture which is the dominant source of livelihood for citizens depends mainly on rainfall. For instance, seasonal rainfall onset determines the time and type of crops to grow at any point in time within the season (Manzanas et al., 2014b).

Rain gauges are the most accessible means through which rainfall can be measured and have long been known to provide relatively precise point rainfall measurements. However, within the African region, gauge networks are sparse and fast deteriorating (Dinku et al., 2007; Asadullah et al., 2008). Pursuant to Dinku et al. (2007), rainfall data accessibility is a primary constrain to the effectiveness of water resource model applications such that, rainfall inputs into the model matters more than the choice of the model itself.

In recent times, rainfall estimates derived from meteorological satellites have gained considerable attention worldwide following their attractive complements to ground-based rainfall measurements (Dinku et al., 2007). Nonetheless, these alternatives from various studies are revealed to be associated with a number of biases and stochastic errors. It is therefore imperative to validate these products with ground measurements in order to obtain some level of certainty in their exploit for various applications.

There exists a number of validation works to assess the performance of satellite rainfall products on various spatio-temporal scales within Africa. For example, Asadullah et al. (2008) assessed the performance of five satellite-based rainfall estimates (CRU, CMORPH, TAMSAT, RFE 2.0 and PERSIANN) over the entire Uganda and showed good performance of the products. Dinku et al. (2007) assessed the potencies of ten satellite rainfall products over the East African Complex topography. Their results showed reasonable abilities of the rainfall products to capture the rainfall patterns in the region. Thiemig et al. (2012) on the other hand, validated six satellite-based rainfall estimates (CMORPH, RFE2.0, TRMM 3B42, GPROF 6.0, PERSIANN, GsMap MVK and ECMWF Re-Analysis (ERA-Interim)) over the African river basins. They revealed TRMM 3B42 and RFE2.0 as the best performed satellite products in the region which is similar to findings in Amekudzi et al. (2016) over the Ashanti of Ghana . Furthermore, Maggioni et al. (2016) analysed the accuracies of merged highly resolved satellite rainfall products during the TRMM era and showed good skill of the products. Similarly, the diurnal cycles of rainfall in Africa were accessed using TRMM, TMPA, TRMM 3G68, PERSIANN and CMORPH products in Pfeifroth et al. (2016) which revealed the capabilities of all satellite products in capturing the diurnal rainfall cycle with respect to ground observations. They also concluded that the CMORPH and TMPA rainfall products showed overall good performance than the others.

Satellite-based validation studies are however limited in Ghana. Moreover, the existing studies are based on few point stations in the country and a handful of satellite rainfall products (e.g., Amekudzi et al. (2016), Manzanos et al. (2014a)).

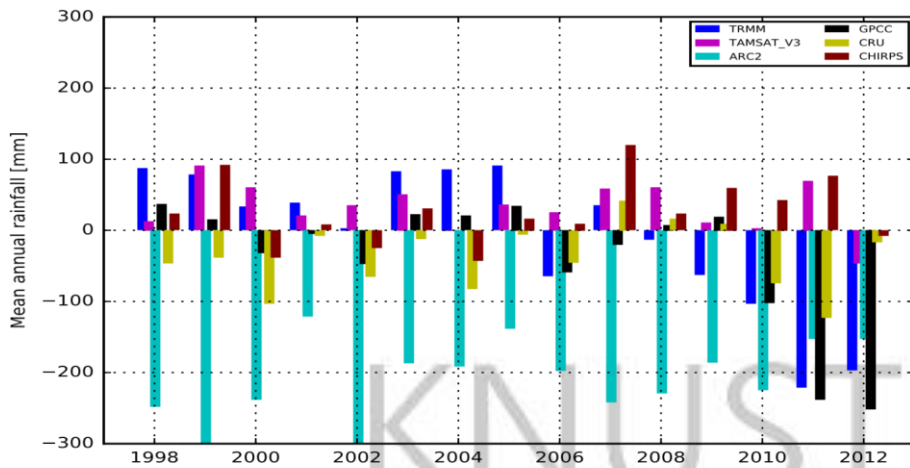
In Amekudzi et al. (2016), the authors validated two satellite rainfall products thus, TRMM and FEWS over parts of the Ashanti region of Ghana.

The present study extensively validates the performance of two gauge-only and six satellite and merged rainfall products referred to as validated rainfall products (VRPs) over the entire country and in the four ecological zones during the TRMM era.

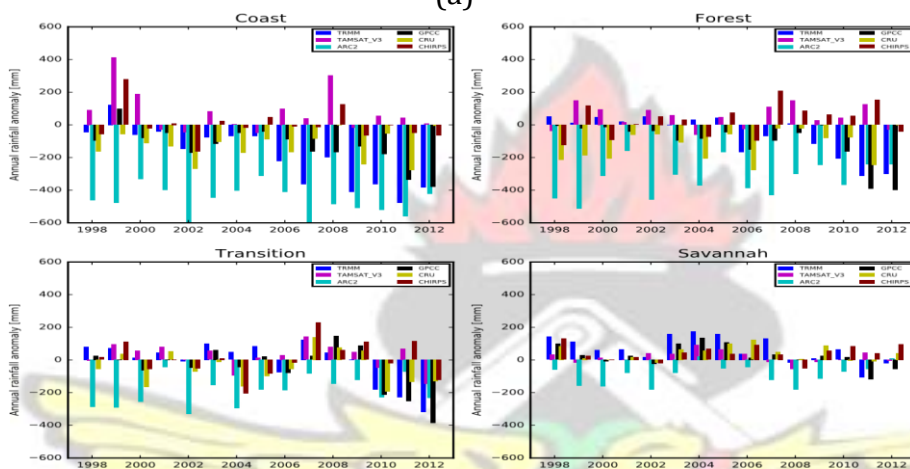
4.2 Results and Discussions

4.2.1 Inter-annual Comparisons

Figure 4.1 shows the annual rainfall departures between VRPs and gauge countrywide (Figure 4.1a) and in the four zones (Figure 4.1b). It is observed that, all VRPs but TAMSAT and CHIRPS generally underestimated gauge. ARC2 was observed to be very dry with respect to gauge with bias > 250 mm/year throughout the entire county. In the Savannah zone, ARC2 was observed to underestimate gauge whilst the other VRPs overestimated approximately less than 200 mm/year. Overall, all except TAMSAT and CHIRPS were observed to underestimate gauge in the Transition, Forest and Coastal zones of the country.



(a)



(b)

Figure 4.1: (a) countrywide and (b) Inter-zonal annual rainfall departures of rainfall products from gauge records for the of period 1998-2012; GPCP (black), ARC2 (cyan), TRMM (blue), TAMSAT (magenta), CRU (yellow) and CHIRPS (brown).

4.2.2 Monthly comparisons

The results for the monthly performance of the VRPs over the entire country and in the four zones are presented in this section. Figure 4.2 shows the zonal monthly mean rainfall difference between VRPs and gauge over the entire country for the study period. Figure 4.2 is aimed at assessing the abilities of the VRPs to capture the wet and dry spells in the rainfall.

In general, the rainfall patterns over the entire country were captured by the VRPs, although there were instances of under/over estimations similar to the case over tropical Africa in Pfeifroth et al. (2016). CMAP and GPCP were wetter than gauge in some parts of southern Ghana during the January–May period. TRMM, TAMSAT, GPCC, CHIRPS and CRU showed dry anomalies during the July–September period far north. TAMSAT and CHIRPS throughout the entire country were observed to be comparatively wetter than gauge. ARC2 performed poorly throughout the entire country as it showed dry bias most of the time in the region. All VRPs generally showed some wet bias in the northern sectors of the country. Figure 4.3 represents the monthly to inter-annual rainfall amounts captured by gauge and VRPs over the entire country. On the average, rainfall onsets were in March and cessations in November (Figure 4.3). All VRPs were able to capture the onsets, cessations and the spells (wet and dry) with respect to gauge however, sometimes under/over estimated gauge. ARC2 was generally drier than gauge throughout the entire country particularly during May–October. In contrast, CHIRPS was wetter than gauge during July–September of the period of study. CMAP and GPCP were observed to be drier than gauge during October–November. Slight overestimations were observed in July–September during 2003–2007 for TRMM, CRU and GPCC. During May–September, TRMM and GPCC were generally drier than gauge in 2010–2012.

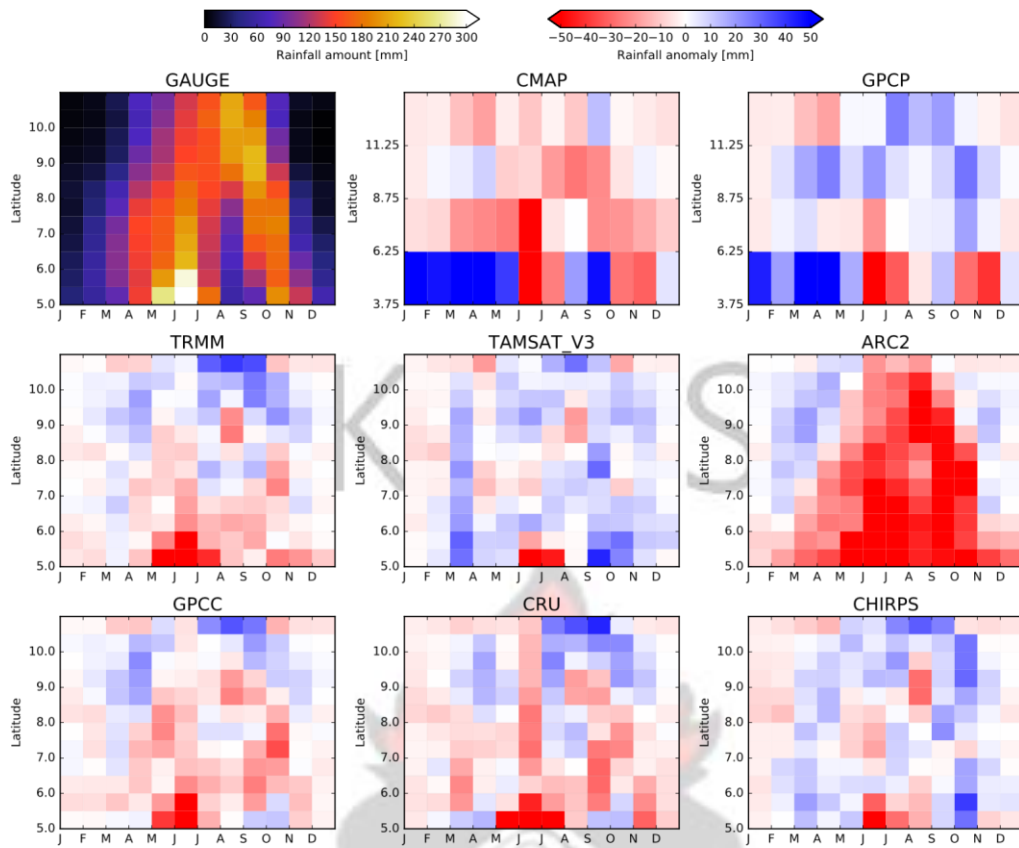


Figure 4.2: Zonal monthly mean rainfall difference between VRPs and gauge for the period of 1998–2012.

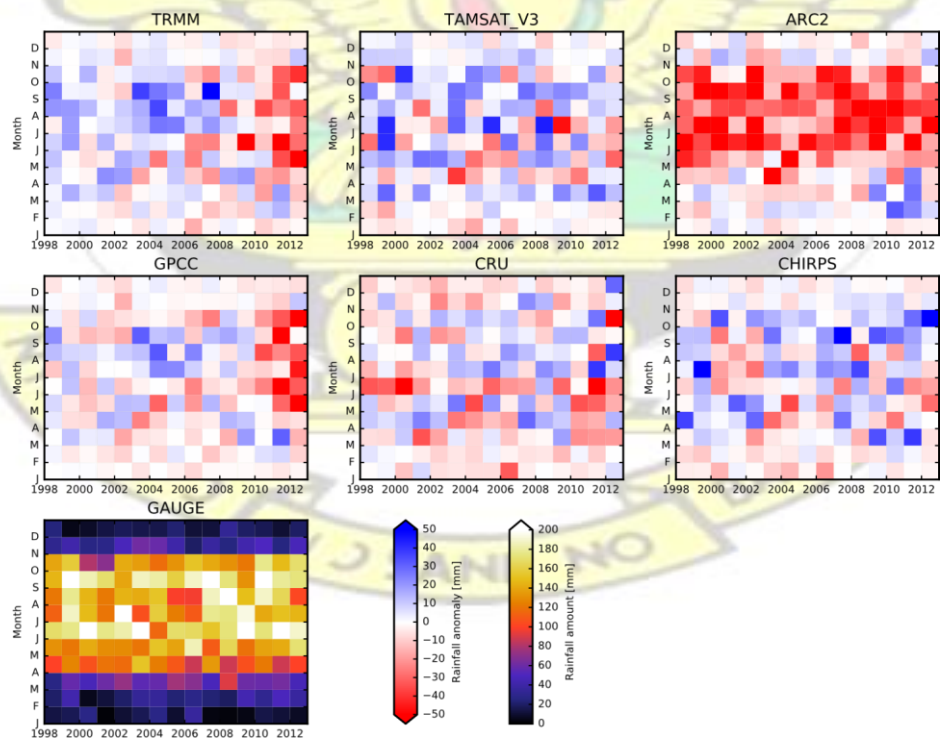


Figure 4.3: Colormaps showing the monthly to inter-annual rainfall difference between the VRPs and gauge in the entire country for the period of study.

Figure 4.4 represents scatter plots of the VRPs with respect to gauge for the period of study. The figure assesses the consistency between the monthly rainfall recorded by VRPs with respect to gauge. Generally, all VRPs performed very well with $r > 0.90$ however, CHIRPS and TAMSAT were observed to slightly overestimate gauge whereas the remaining VRPs underestimated (see Table 4.1). CHIRPS was observed to be the most efficient followed by CRU, TRMM and TAMSAT with eff values 0.95, 0.94, 0.93 and 0.92 respectively. ARC2, CMAP and GPCP were the least performed VRPs which is evident from the large RMSE and low eff values (see Table 4.2).

Table 4.1: Monthly performance of VRPs with respect to gauge in the four zones for the period of 1998–2012.

Dataset	Savannah				Transition				Forest				Coast			
	r	RMSE	bias	eff	r	RMSE	bias	eff	r	RMSE	bias	eff	r	RMSE	bias	eff
GPCC	0.98	0.21	1.02	0.95	0.92	0.29	0.96	0.83	0.95	0.23	0.92	0.86	0.94	0.26	0.90	0.85
ARC2	0.96	0.31	0.91	0.86	0.90	0.42	0.84	0.55	0.88	0.49	0.76	0.32	0.88	0.74	0.65	0.1
CRU	0.97	0.22	1.04	0.94	0.93	0.26	0.96	0.86	0.92	0.28	0.91	0.81	0.92	0.31	0.91	0.80
TAMSAT	0.96	0.24	1.04	0.93	0.94	0.23	1.04	0.88	0.93	0.22	1.06	0.85	0.90	0.29	1.09	0.79
TRMM	0.97	0.23	1.06	0.94	0.94	0.25	0.99	0.88	0.93	0.23	0.96	0.85	0.91	0.35	0.86	0.71
CHIRPS	0.98	0.20	1.04	0.95	0.93	0.26	1.00	0.87	0.94	0.21	1.02	0.89	0.94	0.23	1.00	0.89

Table 4.2: Monthly performance of VRPs with respect to gauge over the entire country for the period of 1998–2012.

Satellite Product	RMSE	Eff	r	Bias
CMAP	0.276	0.769	0.928	0.938
GPCP	0.217	0.865	0.953	0.960
GPCC V5	0.167	0.936	0.970	0.967
ARC2	0.359	0.643	0.949	0.824
CRU	0.169	0.938	0.970	0.969
TAMSAT	0.179	0.922	0.963	1.053
TRMM	0.171	0.933	0.966	0.992
CHIRPS	0.152	0.948	0.975	1.021

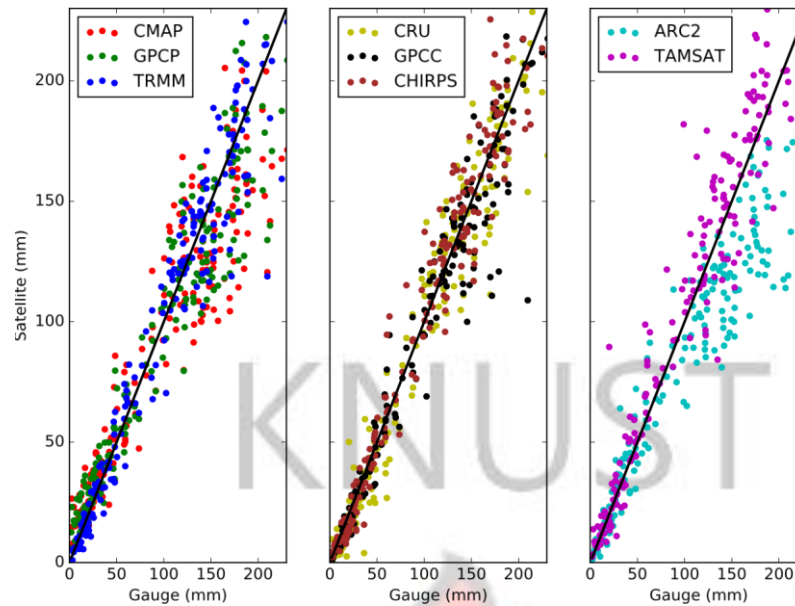


Figure 4.4: Scattergrams of monthly rainfall records for VRPs with respect to gauge over the entire country for a period of 1998–2012 ; GPCP (black), ARC2 (cyan), TRMM (blue), GPCP (green), CMAP (red), TAMSAT (magenta), CRU (yellow) and CHIRPS (brown).

Figure 4.5 represents the mean monthly rainfall patterns captured by VRPs with respect to gauge in the four zones. All VRPs were observed to capture the unimodal rainfall pattern in the Savannah zone considerably well. The peak rainfall amount (approximately 200 mm) in August was slightly overestimated by all VRPs except ARC2 which underestimated. The bimodal rainfall patterns in the transition, forest and coastal zones (with peak rainfall in June and September/October) were well captured and consistent with findings of Aryee et al. (2017). Peak rainfall amount in September was slightly overestimated by TRMM, CHIRPS and TAMSAT and underestimated by CRU, GPCP and ARC2 in the transition zone. The Peak rainfall in October is slightly underestimated by ARC2, TRMM, CRU and GPCP and overestimated by TAMSAT and CHIRPS in the Forest zone.

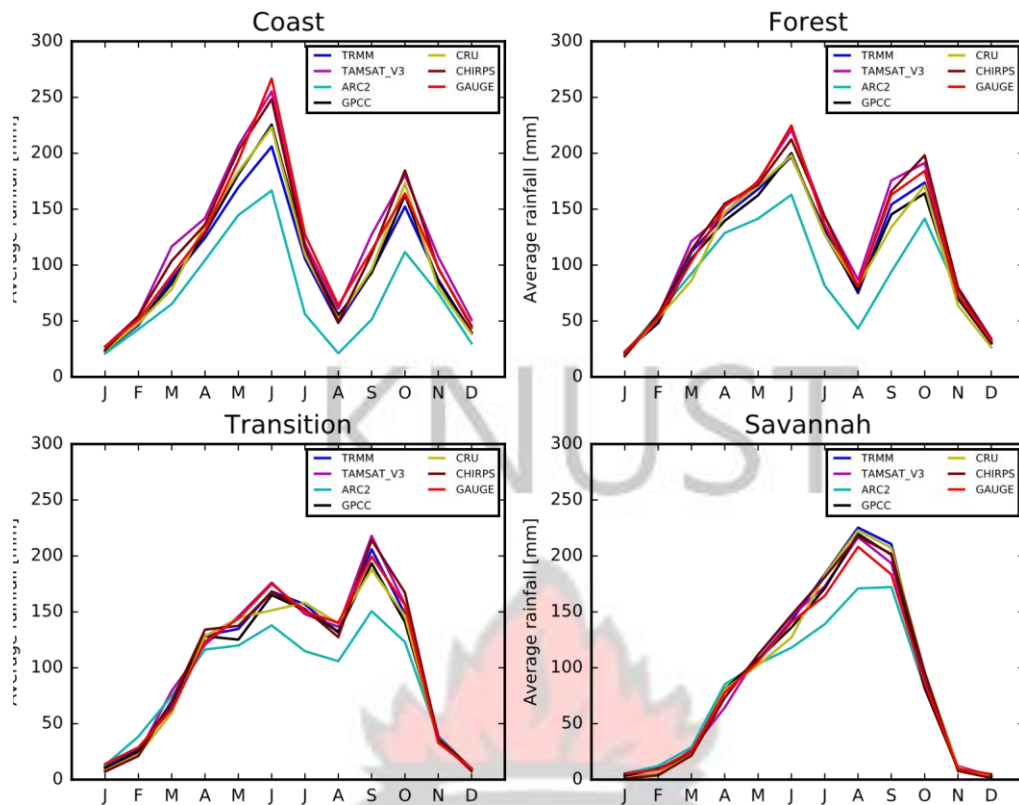


Figure 4.5: Inter-zonal annual rainfall cycle as captured by Gauge (red), TRMM (blue), TAMSAT (magenta), ARC2 (cyan), GPCC (black), CRU (yellow) and CHIRPS (brown) rainfall products.

4.2.3 Taylor and error diagram evaluation

Figure 4.6 shows the monthly performance of the VRPs over the entire country. It was observed that, all satellite rainfall products showed good agreement with gauge over the entire country with r values > 0.90 . CHIRPS was the best among the VRPs in the entire country with the least RMSEe value of approximately 15 mm/month and relatively high r values. CRU and GPCC showed similar strength of agreement with gauge with $r > 0.93$ and $RMSE < 20$ mm/month over the entire country. All rainfall products except TAMSAT and CHIRPS slightly underestimate gauge throughout the entire country. ARC2 was the least performed with

relatively large RMSE and high bias values of 24 mm/month and 18 mm/month respectively.

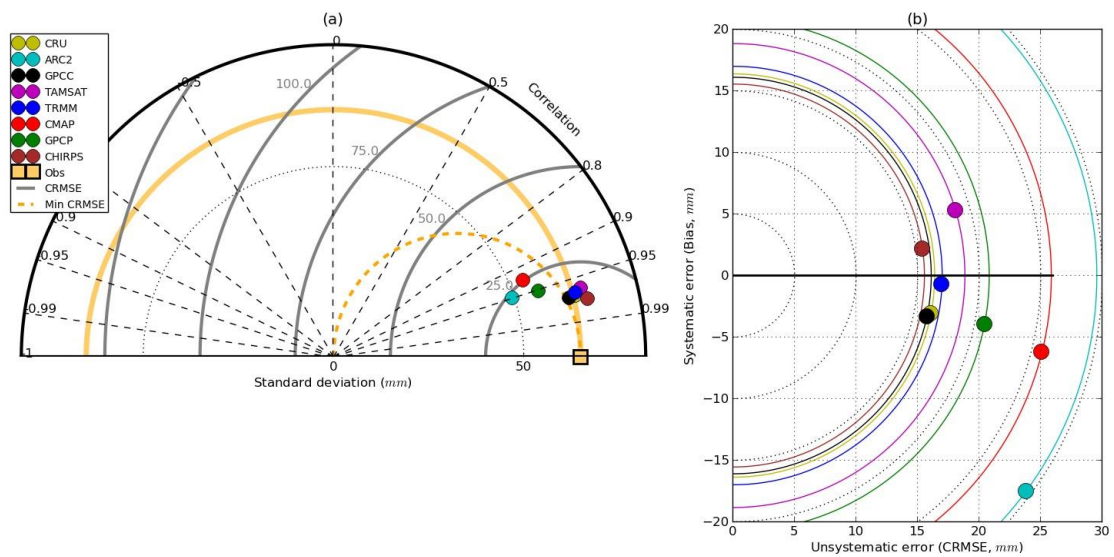


Figure 4.6: Taylor (a) and error (b) diagrams showing the performance of the GPCC (black), ARC2 (cyan), TRMM (blue), GPCP (green), CMAP (red), TAMSAT (magenta), CRU (yellow) and CHIRPS (brown) on a monthly scale for the period of 1998–2012 in the entire country.

Figure 4.7 shows the performance of the various products after removal of seasonality from their respective rainfall data with respect to gauge in the entire country. It is observed that, the monthly performance of the VRPs were relatively better than their performance after removal of seasonality as $r \leq 0.80$. CHIRPS was observed to be the best followed by CRU, GPCC then TRMM whilst the remaining VRPs had r values < 0.65 . This thereby suggests the VRPs sometimes averagely captured rainfall relative to gauge however, the amount recorded by gauge was either overestimated or underestimated.

On average, all VRPs were observed to perform relatively poor in all four ecological zones after removal of seasonality from their respective datasets (see Figure 4.7). Specifically in the Savannah zone, CHIRPS showed a relatively better skill followed by CRU, GPCC and TRMM however, correlation coefficients were

< 0.80 for all products. In the transition zone, the correlation coefficients for all products were less than 0.60. Comparatively, CHIRPS and GPCP showed a relatively similar and better skill in the forest and coastal zones with $r \geq 0.80$ whereas the remaining VRPs had r values < 0.80.

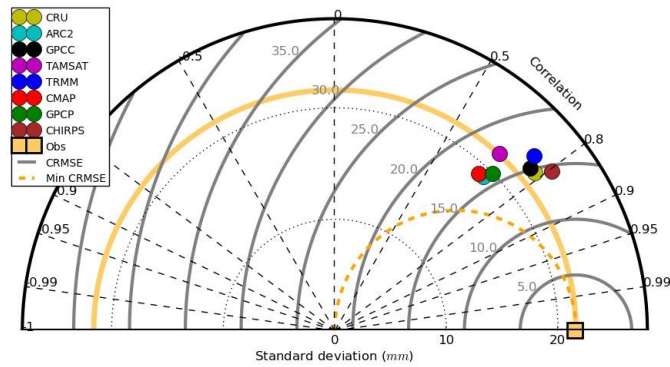


Figure 4.7: Taylor diagrams showing the performance of the GPCP (black), ARC2 (cyan), TRMM (blue), GPCP (green), CMAP (red), TAMSAT (magenta), CRU (yellow) and CHIRPS (brown) after removal of seasonality for the period of 1998–2012 in the entire country.

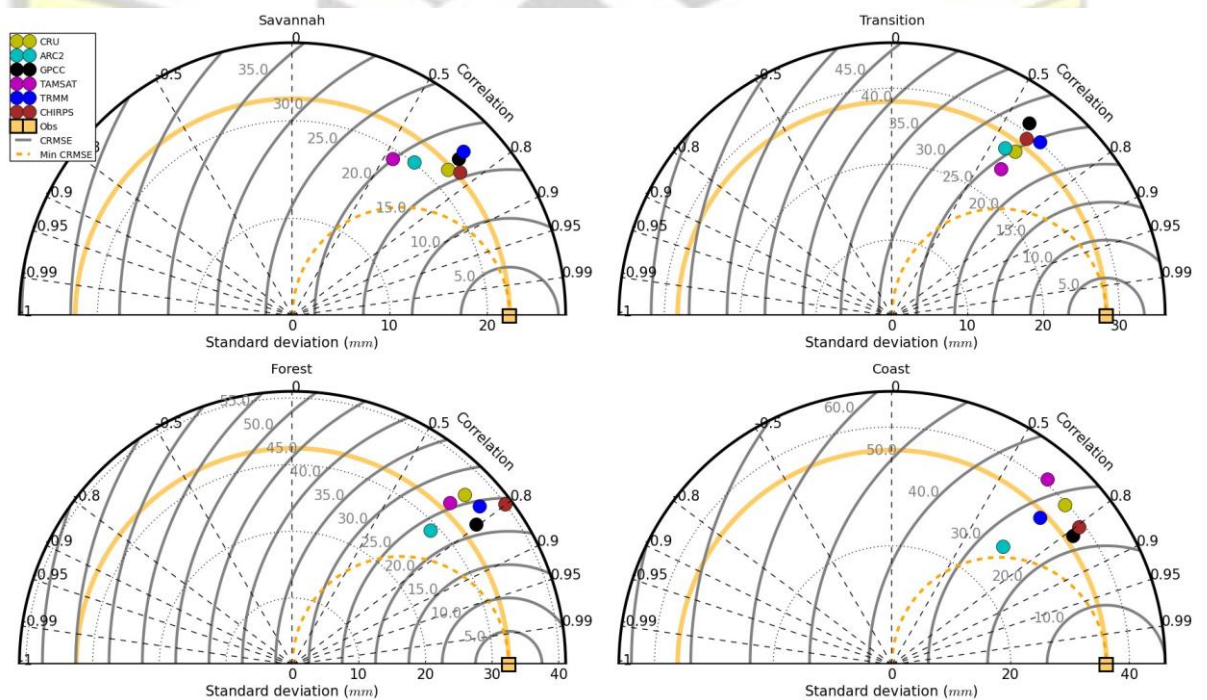


Figure 4.8: Inter-zonal Taylor diagrams showing the performance of the GPCP (black), ARC2 (cyan), TRMM (blue), TAMSAT (magenta), CRU (yellow) and CHIRPS (brown) after removal of seasonality for the period of 1998–2012.

Figure 4.9 depicts the inter-zonal Taylor diagrams while Figure 4.10 is the interzonal error diagrams showing the monthly performance of the rainfall products with respect to gauge. All VRPs except ARC2 were observed to have similar strength of performance with gauge with good correlation coefficients ($r > 0.95$) in the Savannah zone nonetheless, CHIRPS showed a relatively better skill. Rainfall was overestimated (< 6 mm) by all VRPs but ARC2 which underestimated (> 6 mm)) in the Savannah zone. All products were observed to perform well in the Transition zone with $r > 0.80$ however, ARC2 underestimated gauge.

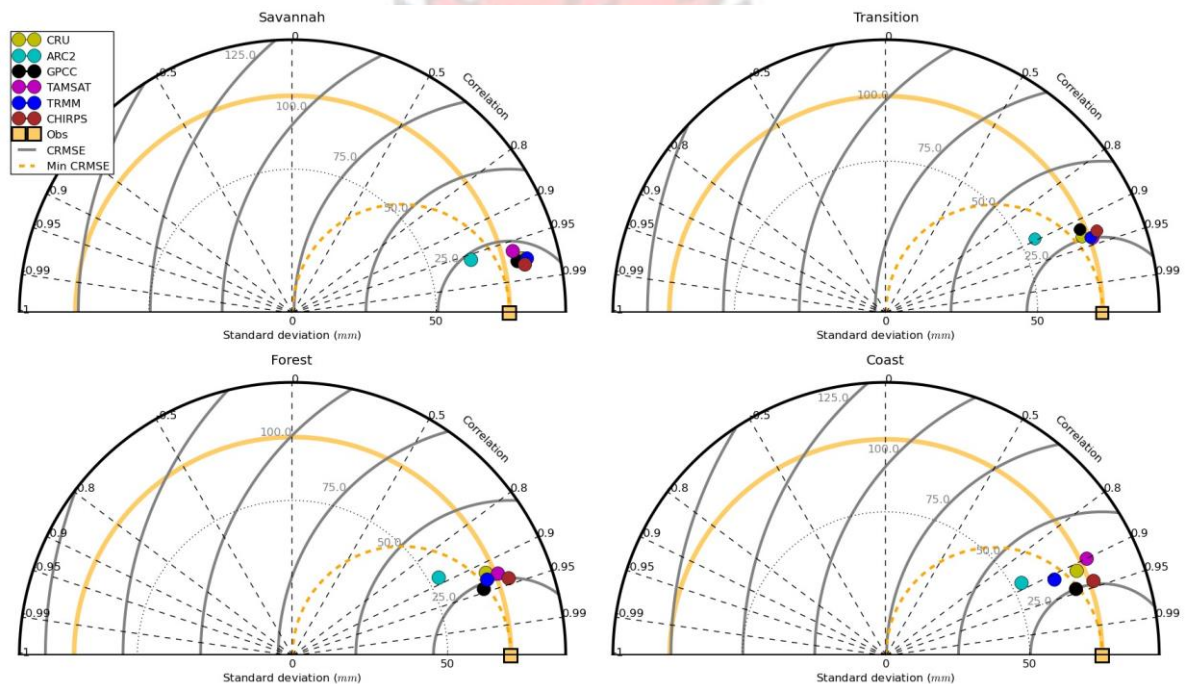


Figure 4.9: Inter-zonal Taylor diagrams showing the performance of CRU (yellow), TAMSAT (magenta), TRMM (blue), GPCC (black), ARC2 (cyan) and CHIRPS (brown) with respect to Gauge.

Again, all VRPs were observed to have good agreement with gauge ($r > 0.80$) however, CHIRPS was found to have the least bias and RMSE values whereas ARC2 recorded relatively large RMSE value. In general, rainfall was underestimated by all except CHIRPS and TAMSAT in the forest zone. All except

TAMSAT and CHIRPS underestimate gauge in the coastal zone (bias < 40 mm/month) whereas CHIRPS was observed to have minimal bias and RMSE values. The GPCC, CRU and CHIRPS were observed to have relatively small bias and RMSE values whereas ARC2 had the largest RMSE and bias values. The general performance of all satellite rainfall products in all zones were much closer except for ARC2 in the Savannah, Transition and Forest zones than their performance in the coastal zone.

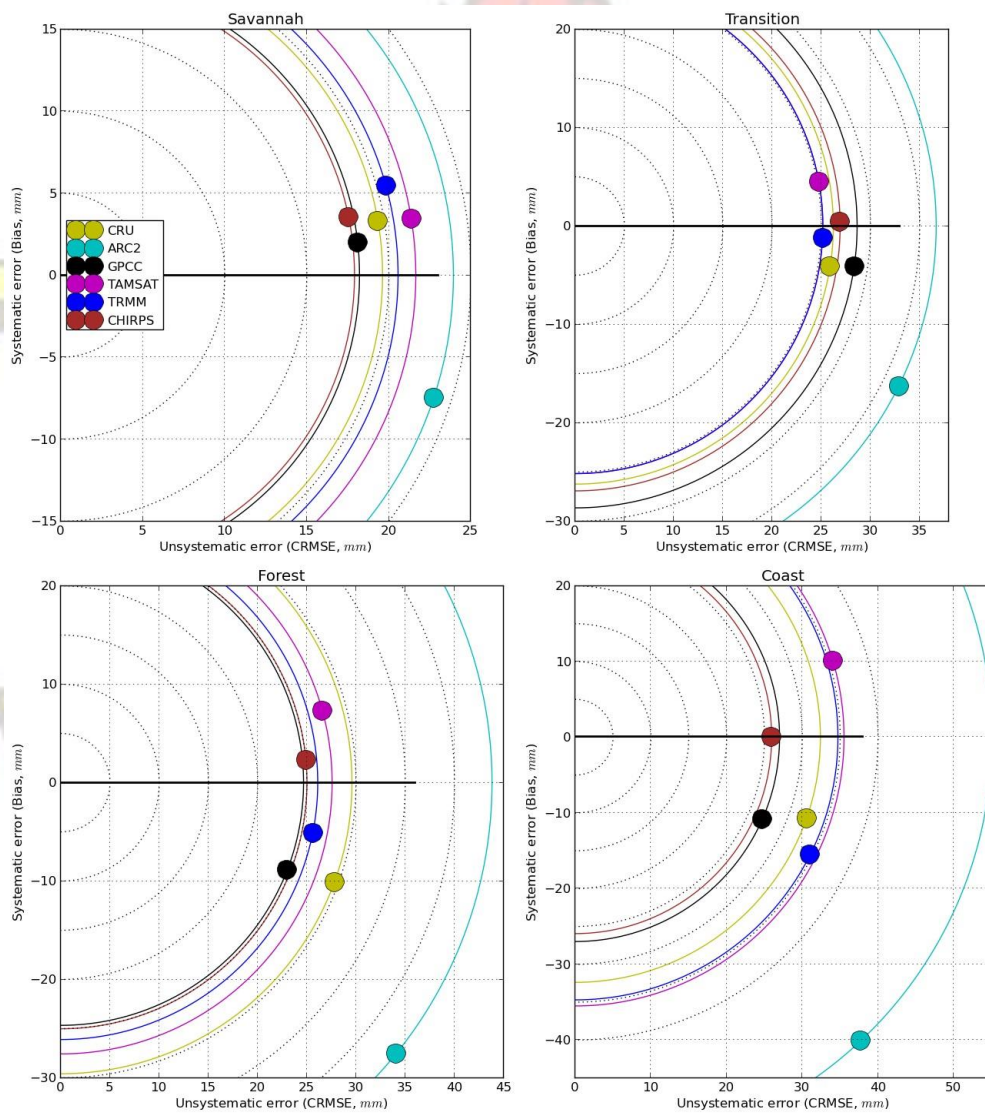


Figure 4.10: Inter-zonal error diagrams showing the performance of CRU (yellow), TAMSAT (magenta), TRMM (blue), GPCC (black), ARC2 (cyan) and CHIRPS (brown) with respect to Gauge.

4.3 Summary

Satellite-based rainfall products are revealed through various studies (e.g., Pfeifroth et al. (2016); Roca et al. (2010)) to present crucial information on the rainfall variability in data-sparse West Africa. However, satellite products are associated with a number of in-variate errors therefore, assessing their performance in our region is very essential to boost our confidence in their exploits for various applications.

In this study, an extensive validation of two gauge-only and six satellite-based rainfall products have been carried out in Ghana. The current study forms part of the Dynamic Aerosol Chemistry-Cloud-Interaction in West Africa (DACCIWA) project, Work Package (WP6) aim to quantify the uncertainties and accuracies associated with satellite rainfall estimates over West Africa. Also, the study contributes to sub-regional validation studies that are limited in literature and provides a comprehensive assessment of the quality of the GMet gridded gauge data.

The performance of validated rainfall products (VRPs) with respect to gauge were assessed on two strategies thus, countrywide and based on the four ecological zones on monthly and annual scales using a suite of statistical techniques. Our results revealed the abilities of the VRPs to capture the rainfall patterns in the ecological zones (forest, transition, coastal and savannah) similar to observations in the African river basins in Thiemig et al. (2012). The onsets, cessations and spells (wet and dry) over the entire country were also captured however, sometimes over/under estimated. Similar to Pfeifroth et al. (2016) and Ebert and

Manton (1998b), our results reveal the performance of the satellite-based rainfall products to be dependent on the scale and location. The monthly performance of all VRPs were relatively better than their performance annually. All VRPs except TAMSAT and CHIRPS were observed to underestimate gauge records in the entire country. The products showed relatively good skills on the monthly scale ($r > 0.90$) than the annual and after removal of seasonality from their respective datasets however, CHIRPS showed a better skill in all cases. ARC2 was the least performed product evident from the relatively large bias and RMSE values it recorded. The performance of the rainfall products except ARC2 with respect to gauge were observed to have little variations from each other except in the coastal zones. CHIRPs markedly revealed a better skill on both monthly and annual scales countrywide.

For climate impact studies based on fine temporal resolution rainfall products, CHIRPS, TRMM and TAMSAT would be great substitutes in the absence of gauge records. CHIRPS, CRU and possibly TAMSAT also serve as complements to gauge for annual rainfall studies. GPCP could complement gauge records for studies involving coarse spatial rainfall resolution.

Within the DACCIWA project, seventeen portable optical rain gauges with a minute temporal resolution has been deployed over the Ashanti Region of Ghana. These would provide a high quality dense network of rainfall data for the analysis of high impact rainfall events and further validation studies in the region.

CHAPTER 5

Assessment of the performance of DOGs, IMERG and TRMM sub-daily rainfall products over the Ashanti region of Ghana

This chapter evaluates the performance of the new DOGs installed in the Ashanti region of Ghana. The study further applies DOG data to assess the performance of sub-daily satellite rainfall products using various statistical techniques.



5.1 Introduction

Our understanding of hydro-climatic processes and other key climate-impact studies, especially within the African continent has been hindered by the lack of dense gauge networks. Various alternatives have been sorted to either serve as complements or substitutes to the existing gauge measurements (Dezfuli et al., 2017). However, satellite-based rainfall products are becoming increasingly available for such applications on a regional to global scale. Most of these products are based on monthly aggregations of rainfall data (Gebremichael et al., 2005). As a result, water resources and other hydrological models within West Africa have been rendered less effective due to unavailability of high spatio-temporal rainfall datasets and the fact that these models most often than not are based on sub-daily time scales (Dinku et al., 2007). More so, one prime obstacle of rainfall measurements in West Africa lies on the great discrepancies in spatio-temporal scales between gauge rainfall and satellite estimates (Zeweldi and Gebremichael, 2009b).

In recent times, efforts are being made to increase the number of high temporal rain gauge networks while extending the satellite-based rainfall products to much higher spatio-temporal scales within the continent. The Dynamic Aerosol Chemistry-Cloud Interactions in West Africa (DACCIWA) rain gauge network is a typical example of such projects. In this initiative, seventeen high temporal resolved optical rain gauges have been deployed over the Ashanti region of Ghana.

(IMERG) satellite rainfall product, a successor of the Tropical rainfall Measuring Mission (TRMM), produces rainfall estimates over the entire globe with temporal resolutions of 30 minutes, 3 hourly at a spatial resolution of, 0.1°. However, satellite-based rainfall products are associated with a number of discrepancies including, sampling errors, algorithmic errors, instrumental errors (Gebremichael et al., 2005; Amekudzi et al., 2016). It is therefore imperative to validate these rainfall estimates with gauge rainfall measurements in order to ascertain their validities within our region for their exploitation in key socio-economic sectors such as rain-fed agriculture, hydrology, water resource managements. This current work is therefore a major contribution towards filling this gap.

Existing validations studies of high spatio-temporal rainfall products within West Africa are limited although recent efforts are undertaken to assess the accuracies of IMERG and TRMM sub-daily rainfall products over varied locations (e.g., Amekudzi et al. (2016); Dezfuli et al. (2017)). In a recent work, Amekudzi et al. (2016) highlighted the potency of the TRMM rainfall product to capture the diurnal rainfall patterns as well as onsets, cessions, wet and dry spells in the rainfall fields in the Ashanti region of Ghana. Moreover, Dezfuli et al. (2017) evaluated the validities of the IMERG and TRMM within East and West Africa and reported better skill of IMERG to TRMM.

The current paper validates sub-daily TRMM and IMERG satellite-based rainfall products in selected locations within the Forest zones of Ghana. Specifically, the diurnal and seasonal distribution of rain events during the monsoonal season of 2016 and 2017 as captured by the two products with respect to DOG records is

assessed. The abilities of the products to capture the wet and dry spells in the rainfall data with respect to DOGs has also been investigated.

5.2 Results and Discussions

5.2.1 GMet gauge–DOGs Inter-comparisons

Figure 5.1 represent the monthly rainfall distribution as captured by the DOGs with respect to GMet gauge for 2016 and 2017 respectively over the nine collocated stations. DOGs were observed to mimic GMet gauge records considerably well during the 2016 season with correlation coefficients > 0.95 and $rmse < 0.35$ except for the Mampong station where $r < 0.80$ (see Table 5.1). Figure 5.2 assesses the abilities of the DOGs to capture the diurnal rainfall patterns over selected stations in the Ashanti region of Ghana. It is observed from the figure that, bulk of the rainfall amount in all stations are recorded during the afternoon hours of the day, mid-night and early mornings (15-03 GMT). Relatively low rainfall amount are experienced between 04-12 GMT. This pattern somewhat, though not conclusive (given the short data range) mimics a more diurnal rainfall pattern which is consistent with earlier findings. Thus, the DOGs are able to capture the diurnal rainfall patterns in the region reliably well.

Table 5.1: Summary of statistics for the performance of DOGs with respect to Gmet in 2016.

Station	r	rmse	bias	eff
Mampong	0.7695	0.5134	1.0471	0.3815
Agromet	0.9965	0.1201	0.9214	0.9816
Bekwai	0.9940	0.0859	0.9825	0.9876
Akrokeri	0.9871	0.1731	0.9357	0.9529
Bompata	0.9961	0.0795	0.9976	0.9917
Ejura	0.9687	0.3303	0.8513	0.8024
Jamasi	0.9577	0.1974	0.9899	0.9167

Mankranso	0.9924	0.1303	0.9564	0.9789
Nsuta	0.9971	0.1315	0.9566	0.9836

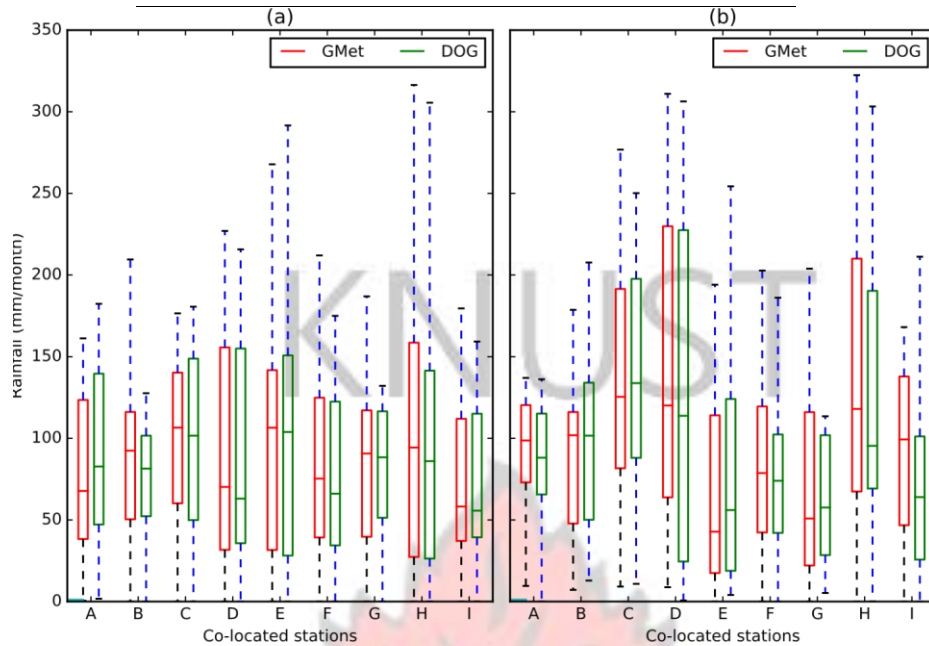


Figure 5.1: Monthly rainfall distribution for the GMet gauge (red) and DOG (green) during (a) 2016 and (b) 2017 period; Mampong (A), Agromet (B), Bekwai (C), Akrokeri (D), Bompata (E), Ejura (F), Jamasi (G), Mankranso (H), Nsuta (I).

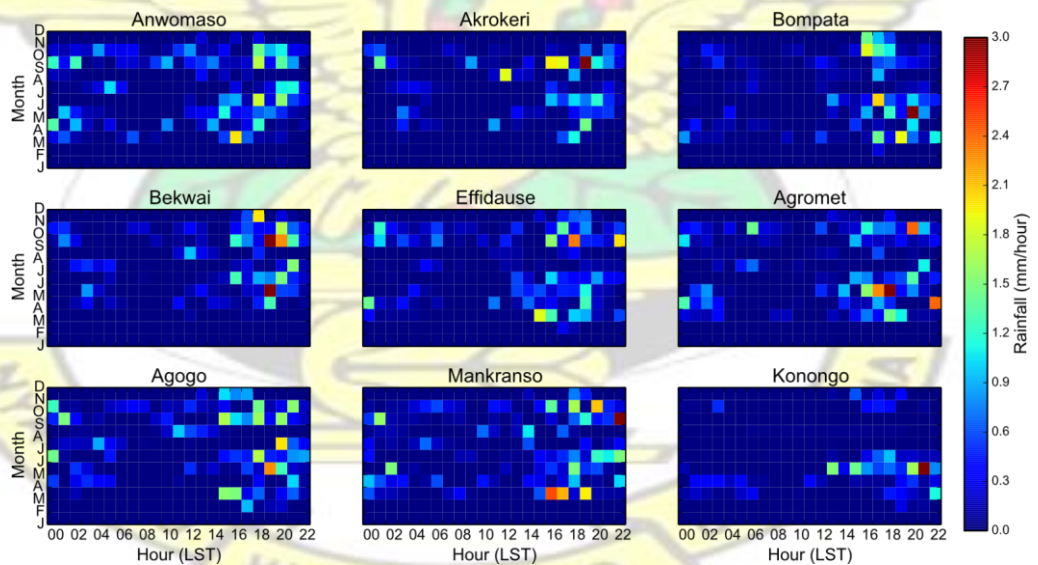


Figure 5.2: Diurnal patterns of rainfall from the DACCWA gauge stations during 2016.

Rainfall values as recorded by GMet gauge were slightly underestimated in all except the Mampong station where overestimations were observed. This

relatively poor performance of DOG in the Mampong station is possibly attributable to its missing data during the short rainfall period of 2016 thus, the gap filling with neighbouring stations data may have introduced some errors coupled with the fact that there are instances of rain gauge clogging as a result of high winds introducing dust particles into the tiny orifice.

It is observed in 2017 that, DOGs like in 2016 performed well in capturing the rainfall with respect to gauge with high r and eff values in the range of 0.91–0.98 and 0.83–0.99 respectively and low $rmse$ values < 0.35 for all except in Akrokeri and Nsuta stations with relatively high $rmse > 0.50$ (see Table 5.2). Rainfall was observed to be slightly overestimated in the Mampong, Akrokeri, Nsuta, Mankranso and Ejura stations and underestimated in the remaining stations.

Figure 5.3 shows the mean monthly rainfall as captured by the DOGs in the Ashanti region of Ghana with respect to GMet. DOG showed good skill in capturing the monthly rainfall patterns in the region with little over/under estimations in some cases. For instance in 2016, DOG slightly underestimated (< 10 mm) GMET in May, June September and October. DOG was observed to underestimate GMet during June–July and overestimate during April–May.

Table 5.2: Summary of statistics for the performance of DOGs with respect to Gmet in 2017.

Station	r	$rmse$	bias	eff
Mampong	0.9957	0.0883	1.0516	0.9865
Agromet	0.9880	0.1192	0.9465	0.9700
Bekwai	0.9238	0.2397	0.9866	0.8311
Akrokeri	0.7868	0.5190	1.0784	0.5845
Bompata	0.9814	0.2080	0.9413	0.9484
Ejura	0.9771	0.2997	1.1405	0.8507
Jamasi	0.9866	0.2147	0.8909	0.9551
Mankranso	0.9120	0.3448	1.1155	0.7704

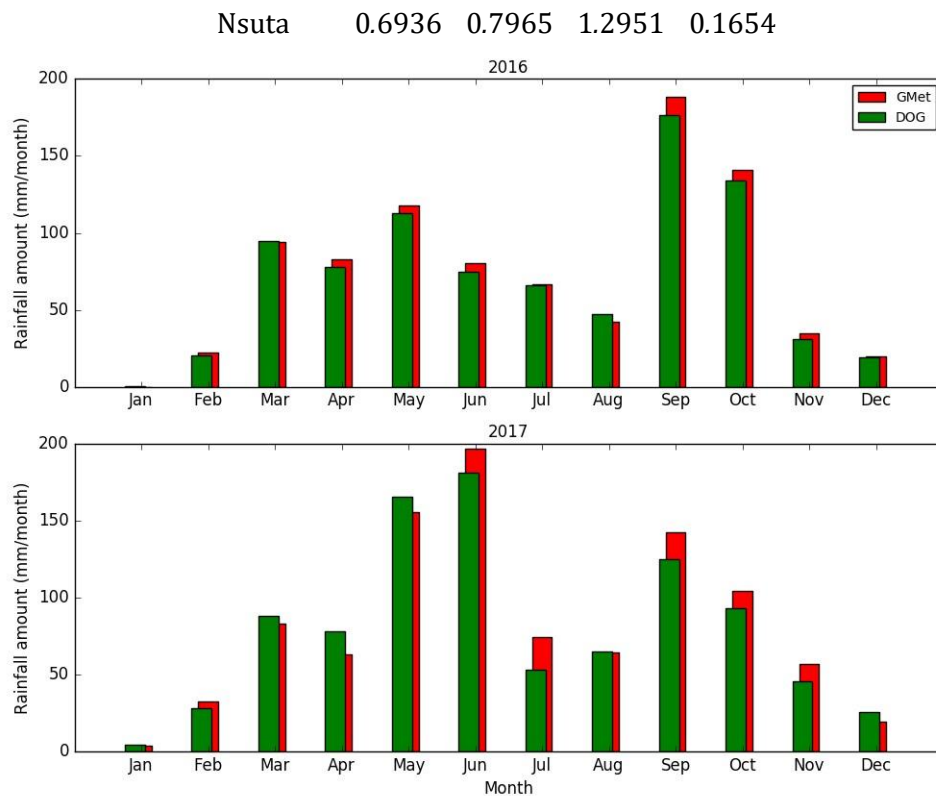


Figure 5.3: Mean monthly rainfall as captured by DOG (green) with respect GMet (red) in the Ashanti region of Ghana (a) 2016 and (b) 2017.

5.2.2 Gauge-satellite inter-comparisons

5.2.2.1 Diurnal inter-comparisons

Figure 5.4 shows the evaluation results for the inter-comparison between IMERG and TRMM satellite-based rainfall products with respect to the DOGs for the nine stations during 2016 and 2017, respectively. Tables 5.3 and 5.4 present results from the various statistical measures between the two products and DOG in the selected stations during March–November season of 2016 for IMERG and TRMM respectively, whereas Tables 5.5 and 5.6 display same measures however, during March–November season of 2017.

From Figure 5.4, it is observed that IMERG markedly represents the diurnal rainfall patterns in 2016 better than TRMM with VHI and POD values in the range of 0.9231–0.9968 and 0.8333–0.9107, respectively, for the former and 0.4128–0.9228 and 0.5922–0.7411 for the latter. However, the mean diurnal rainfall intensities were observed to be slightly underestimated by IMERG in Bompata, Mankranso and Nsuta stations and overestimated in the remaining stations. Similarly, TRMM underestimates rainfall in Bompata and Mankranso and overestimates in the remaining stations (see Tables 5.3 and 5.4).

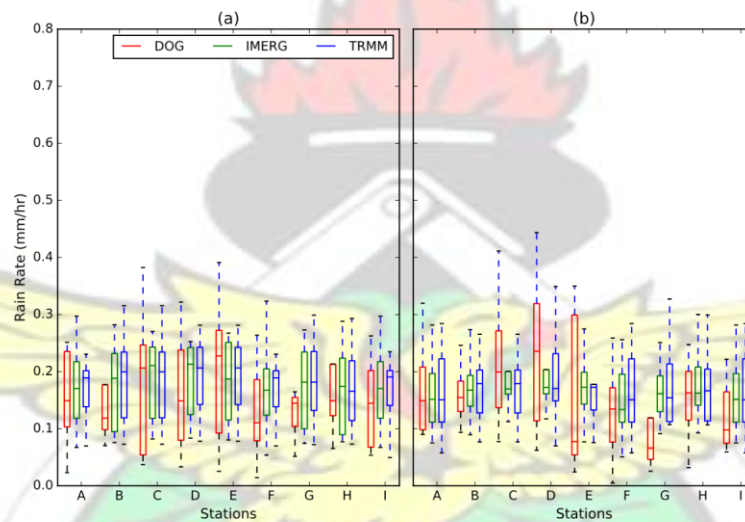


Figure 5.4: Rainfall rate for IMERG (green) and TRMM (blue) rainfall products with respect to DOG (red) during March–November season of (a) 2016 and (b) 2017; Mampong (A), Agromet (B), Bekwai (C), Akrokeri (D), Bompata (E), Ejura (F), Jamasi (G), Mankranso (H) and Nsuta (I).

Table 5.3: Summary of statistics for the performance of IMERG with respect to DOG for the 2016 season.

Station	Bias	POD	VHI	FAR	VFAR	CM	VMI	CSI	VCSI
Mampong	1.0688	0.9107	0.9864	0.4186	0.1300	0.0893	0.0136	0.5231	0.8589
Agromet	1.0569	0.8898	0.9766	0.4952	0.2491	0.1102	0.0234	0.4751	0.7376
Bekwai	1.0327	0.9130	0.9933	0.4952	0.1979	0.0870	0.0067	0.4817	0.7978
Akrokeri	1.1026	0.9417	0.9968	0.4619	0.1687	0.0583	0.0032	0.5207	0.8291
Bompata	0.8788	0.9016	0.9852	0.4737	0.1930	0.0934	0.0148	0.4971	0.7974
Ejura	1.2313	0.9604	0.9935	0.4868	0.1216	0.0396	0.0065	0.5026	0.8734

Jamasi	1.1319	0.9320	0.9951	0.5317	0.3079	0.0680	0.0049	0.4528	0.6901
Mankranso	0.8640	0.9186	0.9056	0.6220	0.3269	0.0814	0.0944	0.3657	0.6290
Nsuta	0.9784	0.8333	0.9231	0.6210	0.3245	0.1667	0.0769	0.3518	0.6395

Table 5.4: Summary of statistics for the performance of TRMM with respect to DOG for the 2016 season.

Station	bias	pod	vhi	far	vfar	cm	vmi	csi	vcsi
Mampong	1.1171	0.7411	0.9228	0.3413	0.1434	0.2589	0.0772	0.5355	0.7994
Agromet	1.0875	0.5424	0.8135	0.4530	0.1132	0.4576	0.1865	0.3743	0.5933
Bekwai	1.0478	0.6609	0.8204	0.3504	0.2275	0.3391	0.1796	0.4872	0.6608
Akrokeri	1.1230	0.6333	0.8426	0.3770	0.2408	0.3667	0.1574	0.4578	0.6649
Bompata	0.8879	0.6148	0.7430	0.3852	0.2831	0.3852	0.2570	0.4438	0.5744
Ejura	1.3166	0.7327	0.8724	0.4127	0.2101	0.2673	0.1276	0.4831	0.7081
Jamasi	1.3345	0.5922	0.8547	0.4741	0.3103	0.4078	0.1453	0.3861	0.6173
Mankranso	0.8894	0.6977	0.7216	0.4828	0.2624	0.3023	0.2784	0.3861	0.5742
Nsuta	1.0329	0.5119	0.4128	0.6614	0.6934	0.4881	0.5872	0.4223	0.2135

The diurnal rainfall during the rainy season of 2017 was considerably well represented by both products although IMERG again showed a better skill than TRMM. This was demonstrated in the high POD and VHI values which are > 0.80 and 0.75 respectively, and relatively low VFAR in the range, 0.0669–0.4992 for IMERG. However, POD values were > 0.65 whereas VHI > 0.66 for all stations with VFAR values in the range, 0.1066–0.5207 for TRMM (see Tables 5.5 and 5.6).

Table 5.5: Summary of statistics for the performance of IMERG with respect to DOG for the 2017 season.

Station	Bias	POD	VHI	FAR	VFAR	CM	VMI	CSI	VCSI
Mampong	0.8581	0.9411	0.9919	0.4378	0.0669	0.0583	0.0081	0.5433	0.9261
Agromet	1.0586	0.8286	0.8853	0.5792	0.3287	0.1714	0.1147	0.3867	0.6176
Bekwai	0.8606	0.8053	0.8679	0.5517	0.3532	0.1947	0.1321	0.4044	0.5889
Akrokeri	0.7790	0.9406	0.9988	0.5433	0.2007	0.0594	0.0012	0.4439	0.7985
Bompata	1.1521	0.8440	0.9738	0.5598	0.2972	0.1560	0.0262	0.4071	0.6897
Ejura	1.0157	0.9783	0.9932	0.5522	0.1443	0.0217	0.0068	0.4433	0.8507
Jamasi	1.4500	0.8235	0.9681	0.6774	0.4740	0.1765	0.0315	0.3017	0.5170
Mankranso	1.1048	0.9304	0.9968	0.4880	0.1928	0.0696	0.0032	0.4935	0.8051
Nsuta	1.1144	0.8333	0.7668	0.7264	0.4992	0.1667	0.1667	0.2594	0.4346

Table 5.6: Summary of statistics for the performance of TRMM with respect to DOG for the 2017 season.

Station	bias	pod	vhi	far	vfar	cm	vmi	csi	vcsi
Mampong	0.8907	0.7167	0.8931	0.2951	0.1066	0.2833	0.1069	0.5313	0.8071
Agromet	1.0554	0.5810	0.6850	0.5159	0.4336	0.4190	0.3150	0.3588	0.4493

Bekwai	0.8261	0.6018	0.6603	0.4603	0.3465	0.3982	0.3397	0.3977	0.4897
Akrokeri	0.8064	0.7426	0.8434	0.4681	0.2339	0.2514	0.1566	0.4491	0.6707
Bompata	1.1549	0.6606	0.8132	0.4820	0.3304	0.3394	0.1868	0.4091	0.5804
Ejura	1.1240	0.7609	0.9051	0.4262	0.2873	0.2391	0.0949	0.4861	0.6632
Jamasi	1.4571	0.5765	0.8047	0.6475	0.4837	0.4235	0.1953	0.2800	0.4588
Mankranso	1.0088	0.7130	0.8315	0.3492	0.1438	0.2870	0.1685	0.5157	0.7296
Nsuta	1.1567	0.6515	0.6618	0.6475	0.5207	0.3485	0.3382	0.2966	0.3850

5.2.2.2 Daily-seasonal inter-comparisons

Figure 5.5 shows the results for the evaluations of IMERG and TRMM with respect to DOGs in the selected stations during the March–May period of 2016 and 2017 respectively.

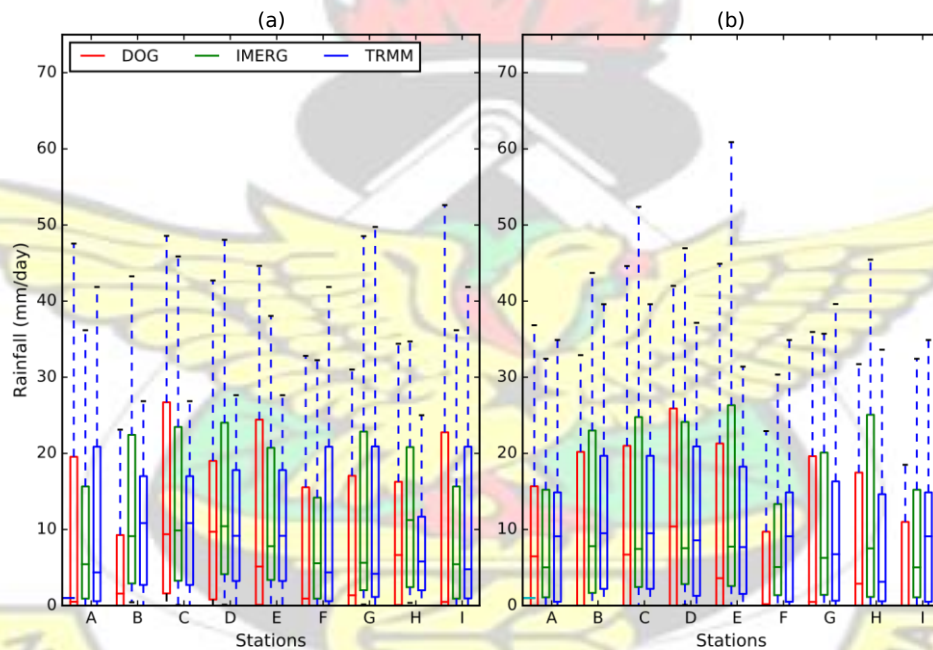


Figure 5.5: Rainfall distributions for IMERG (green) and TRMM (blue) rainfall products with respect to DOG (red) during March–May (MAM) season of (a) 2016 and (b) 2017 ; Mampong (A), Agromet (B), Bekwai (C), Akrokeri (D), Bompata (E), Ejura (F), Jamasi (G), Mankranso (H) and Nsuta (I).

The daily rainfall distributions in 2016 are considerably well captured by both products although IMERG showed a better skill than TRMM. For instance, it is observed for the Mampong, Agromet, Nsuta, Ejura and Bompata stations (Figure 5.5a) that the daily mean rainfall values were slightly overestimated by both products (>5 mm/day). For the Bekwai, Akrokeri and Ejura stations, IMERG

agrees well with gauge relative to TRMM. These findings are similar with results of Dezfuli et al. (2017) who revealed a better skill of IMERG than TRMM in Kumasi during 2016 and results of Tang et al. (2016), where rainfall estimates from IMERG agreed with the ground observations better than TMPA. This improvement of GPM over TRMM is attributed to the fact that the algorithm for rainfall inference for the former incorporates the unified and updated passive microwave techniques (Dezfuli et al., 2017).

During the short rain season (MAM) of 2017, the mean daily rainfall distributions were observed to be well represented by both TRMM and IMERG rainfall products particularly in Mampong and Mankranso stations (see Figure 5.5b). However, for Bekwai, Akrokeri and Bompata both products showed poor skill in capturing the rainfall distributions in the regions. Furthermore, the mean daily rainfall in Nsuta for TRMM and IMERG coincides however, both products overestimate the mean daily rainfall as captured by the DOGs. Rainfall patterns were observed to similar in most stations for TRMM and IMERG although the latter had a better agreement with gauge records which agrees with findings in Li et al.

(2017); Gaona et al. (2016); Dezfuli et al. (2017).

5.2.2.3 Monthly-seasonal anomalies inter-comparisons

The monthly evaluations of the IMERG and TRMM products with respect to DOGs revealed a considerably good skill by both products with correlation coefficients in the range of 0.60–0.88 and 0.60–0.90 respectively. TRMM is observed to show a better performance in the Bekwai station compared to IMERG with rmse values, 42 mm/month and 38 mm/month respectively for IMERG and TRMM (see Figure 5.6). Both products show almost no bias in the Bompata station while

revealing relatively high overestimation in Jamasi (bias > 35 mm/month). TRMM in Mampong station performed better than IMERG with bias values nearly zero for TRMM and 5 mm/month for IMERG. IMERG however reveals a better potency in the Ejura with bias values of about 12 mm/month and rmse approximately, 43 mm/month whereas TRMM had bias values of about 22 mm/month and rmse values approximately 48 mm/month.

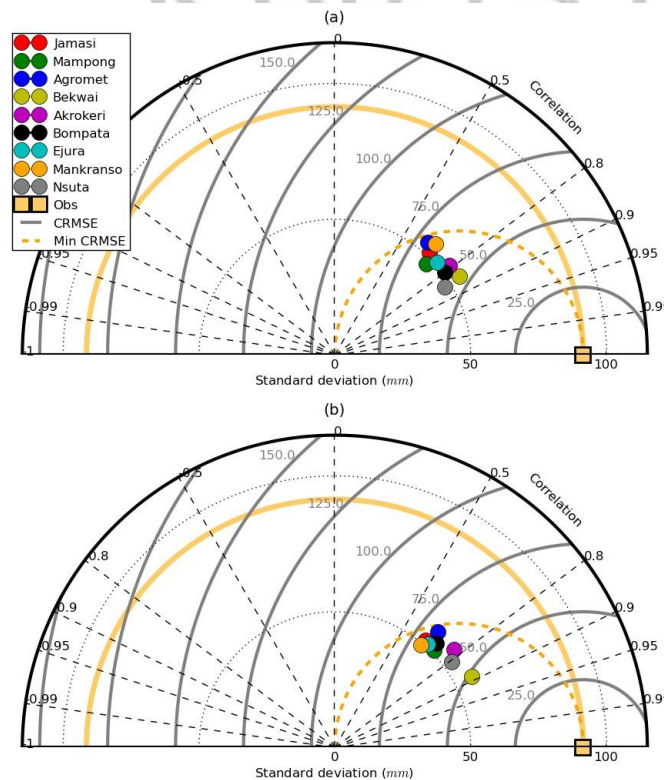


Figure 5.6: Taylor plots showing the skill of IMERG (a) and TRMM (b) products in capturing the seasonal rainfall with respect to gauge during March–November period of 2016–2017.

The Taylor diagrams shown in Figure 5.7a and 5.7b respectively depict the skill with which TRMM and IMERG capture the seasonal anomalies with respect to gauge during the March–November season of 2016–2017. This statistical evaluation measures the abilities of the two satellite rainfall products to capture the wet and dry spells in seasonal rainfall fields over select stations. Ideally, three

pertinent measures thus, the Pearson correlation (r), central root mean square error (CRMSE) and the standard deviations (std) are visualized in these figures.

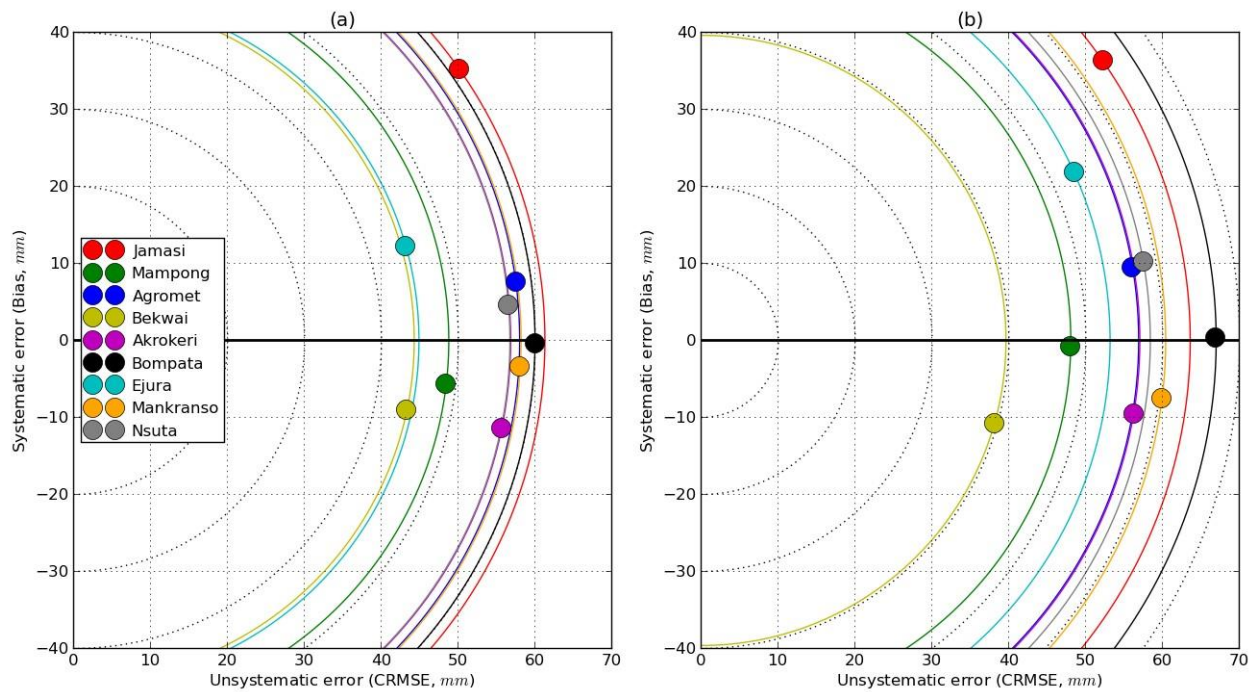


Figure 5.7: Error plots showing the skill of IMERG (a) and TRMM (b) products in capturing the seasonal rainfall with respect to gauge during March–November period of 2016–2017.

It is evident from the figures that, during the monsoonal season of 2016–2017, the IMERG and TRMM rainfall products showed nearly similar skill in capturing the seasonal rainfall anomalies as captured by gauge with correlation coefficients above 0.80 for all except the Jamasi station (see Figure 5.8).

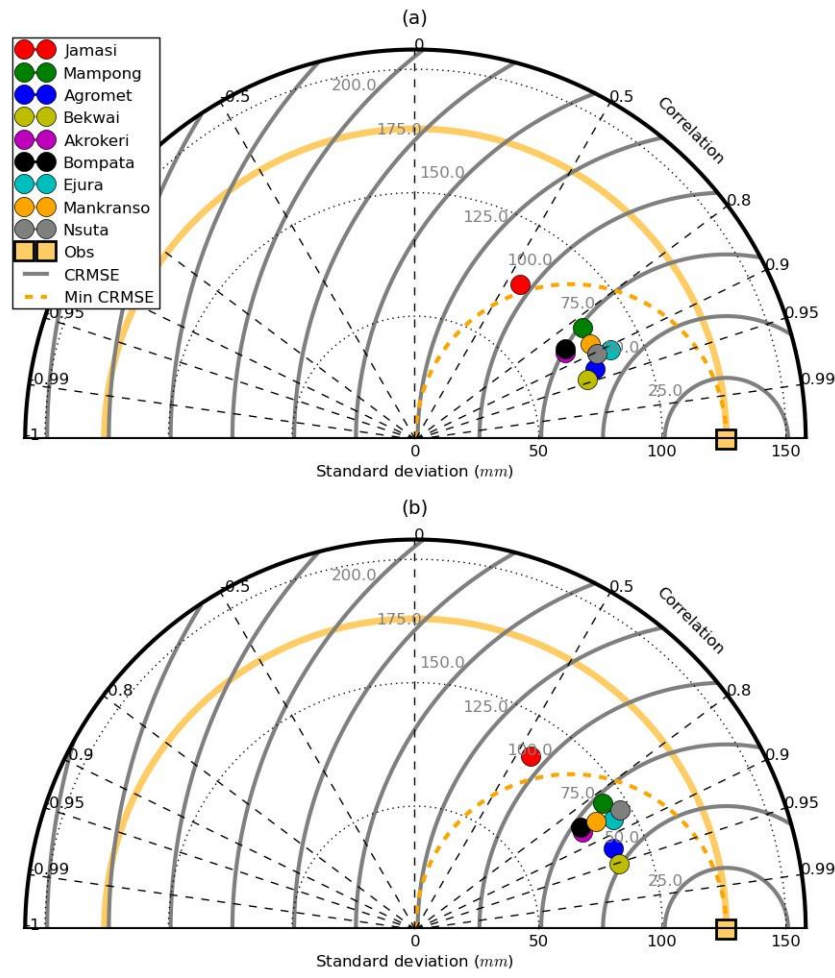


Figure 5.8: Taylor plots showing the skill of IMERG (a) and TRMM (b) products in capturing the seasonal rainfall anomalies with respect to gauge during March–November period of 2016–2017.

5.3 Summary

High spatio-temporal ground-based and satellite rainfall estimates are crucial for a proper assessment of small-large scale rainfall variability in sub-daily rainfall thus the essence of this study. As a follow-up to our recent validation study (Amekudzi et al., 2016), the current paper applies a minute resolution DACCWA optical rainfall data during the monsoonal seasons of 2016–2017 to assess the potencies and discrepancies of the new GPM (IMERG) and its predecessor, TRMM

subdaily rainfall estimates in selected stations over the Forest zones of Ghana. As a foremost step the DACCIWA optical rain gauges (DOG) for the first time were validated using daily rainfall data from the Ghana Meteorology Agency (GMet) for the period of 2016–2017 over nine co-located stations within the Ashanti region of Ghana. Thereafter, the DOGs were then applied to validate the IMERG and TRMM rainfall estimates on various temporal scales.

The results show the DOGs have a high potency in capturing the diurnal rainfall over all stations satisfactorily while revealing their abilities to capture lowintensity rainfall events considerably better than the traditional rain gauges. It was also found that the diurnal cycle has a uni peak which lies between 15:0021:00 GMT over the Forest zones of the country which is consistent with the findings of Dezfuli et al. (2017) over southern Ghana.

IMERG captures the diurnal to daily rainfall distributions relatively better than TRMM especially in the MAM and SON seasons but both IMERG and TRMM were observed to notably capture the daily rainfall intensities as captured by gauge. Overall, both IMERG and TRMM slightly overestimated (> 2 mm/day) in almost all stations during the 2016–2017 monsoonal season however showed similar strength particularly in the JJA season. In addition, both TRMM and IMERG showed excellent skill in capturing the wet and dry spells seasonal rainfall data with correlation coefficients above 0.80 for all except the Jamasi station.

On average IMERG from the results have shown to be better than the TRMM in most cases, however a clear superiority cannot not be necessarily claimed as this validation was only for the period of 2016–2017 coupled with the fact that each product's strength depends on the region, season, altitude and among other

factors. The future of the DACCIWA optical rain gauge network over the forest zones of Ghana would serve as valuable rainfall data for the extensive assessment of high impact rainfall events over southern Ghana.

KNUST



CHAPTER 6

Examination of the climatologies, trends and drivers of extreme rainfall events in Ghana.

This chapter is based on the analysis of the climatologies and trends of extreme rainfall in Ghana and their links to the SST anomalies over the oceanic basins.



6.1 Introduction

Rainfall variability has severe impacts on food production, water resource management and livelihood. Particularly, in West Africa where rain-fed agriculture is a predominant practice, rainfall impact studies are very crucial. In Ghana, the agricultural sector which is rain-fed has been reported to contribute over

70% of employment to citizens as well as 28% of the Gross Domestic Product (GDP) (Baidu et al., 2017; Ofori-Sarpong, 2001). In addition, rainfall controls the hydro-electric power generation, the main energy source in the country and other socio-economic activities (Kunstmann and Jung, 2005*b*).

Contemporary elevated hydrological cycles and weather extremes are understood to be consequences of climate change. In addition, the short- and long-term impacts of climate change on regional to global water resource management is highly significant as such, efforts are being made to understand the rainfall distribution, variability and trends over the region (e.g., Owusu and Waylen (2013*b*); Paeth and Hense (2004); Amekudzi et al. (2015)). Thus an adequate comprehension of the trends and variations in hydro-climatic extreme variables over an area proves very crucial for imminent development and sustainable water resource management (Machiwal and Jha, 2012).

Plethora of studies on the trends of extreme rainfall events have been conducted over various regions on varied spatio-temporal scales. For instance, over the Indochina Peninsula, trends of eleven extreme daily rainfall indices for a period of forty-seven years were analysed using highly resolved spatio-temporal rainfall fields from the Asian Precipitation–Highly-Resolved Observational Data

Integration Towards Evaluation of Water Resources (APHRODITE) (Yazid et al., 2015).

From their analysis, the eastern sectors of the Indochina Peninsula were mainly observed to show positive trends for a number of indices and further noted to correlate with the north-eastern monsoon. Conversely, over the western sectors of Indochina Peninsula, most extreme rainfall indices were dominated by negative trends. Dos Santos et al. (2011) in Utah analysed trends in some extreme rainfall indices using station rainfall data where they found very few significant trends over the area. Klein Tank et al. (2006) in their extreme rainfall trend analysis over Southern Asia revealed disproportionate changes in extreme precipitation over the years. Some studies over Ghana have revealed increased rainfall trends while others have noted negative trends depending on the period of investigation (Yengoh et al., 2010; Kemausuor et al., 2011).

Furthermore, various efforts have also been made over the West African continent to understand the link between SST anomalies over Ocean basins and rainfall over the region. Many of such studies were carried over the Sahel (Wolter, 1989; Hastenrath, 1990; Palmer, 1986; Nicholson and Webster, 2007; Lamb and Pepler, 1992*a*; Lough, 1986*a*; Janicot et al., 1996; Fontaine and Janicot, 1996*b*; Issa L'el'e and Lamb, 2010; Giannini et al., 2003; Bader and Latif, 2003*a*) whereas others where over sub-Saharan Africa (Lough, 1986*b*; Lamb and Pepler, 1992*b*; Lamb,

1978*a,b*), parts of West African region (Balas et al., 2007; Janicot et al., 1998; Fontaine and Bigot, 1993) and Eastern Africa (Tsidu, 2017; Bahaga et al., 2015). According to Fontaine and Bigot (1993), particularly, over the Sahel region, rainfall droughts are attributable to abnormally warm SSTs over south Atlantic,

south Pacific and the Indian Ocean whereas abundant rainfall over the region coincides with abnormally cold SST at the north Atlantic and Pacific. On the other hand, positive SSTs over the northern Atlantic were revealed to be associated with floods whereas positive SSTs over the eastern Pacific and Indian Oceans were linked to droughts over the West African region (Fontaine and Bigot, 1993; Fontaine and Janicot, 1996b; Janicot et al., 1998). Over the eastern Sahel, Palmer (1986) revealed that SSTs over the Indian ocean are accountable for rainfall deficits in the region.

However in Ghana, a handful of SST-rainfall links have been carried out (OpokuAnkomah and Cordery, 1994). SST-rainfall relationship in Ghana was revealed to oppose that of Sahel, which just lies a few degrees north of Ghana (OpokuAnkomah and Cordery, 1994). Opoku-Ankomah and Cordery (1994) highlighted a positive correlation between the equatorial Atlantic SSTs and the rainfall in Ghana.

The current study seeks to investigate the spatio-temporal trends of extreme rainfall indices over Ghana using high resolution and homogenized Climate Hazards Group Infra-red Precipitation with Station data (CHIRPS). Furthermore, the link between SST anomalies over different ocean basins and the spatio-temporal variability of rainfall extremes over Ghana are investigated.

6.2 Results and Discussions

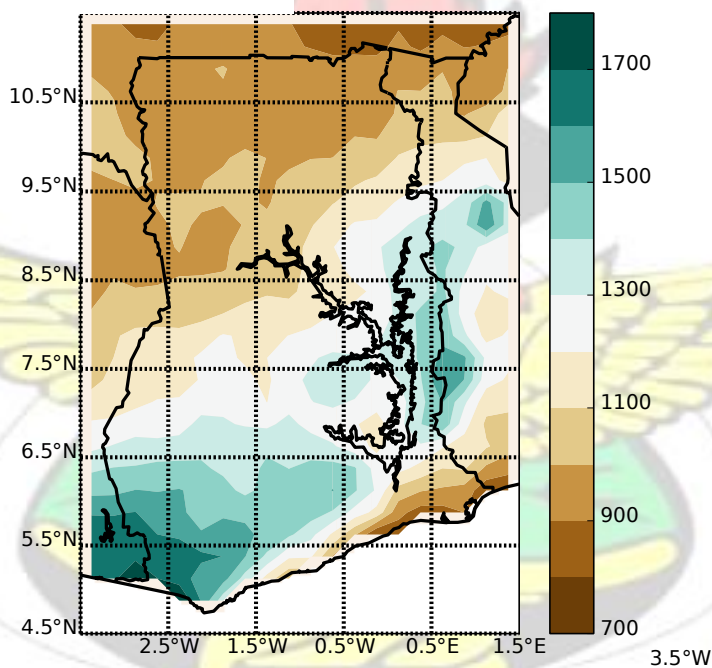
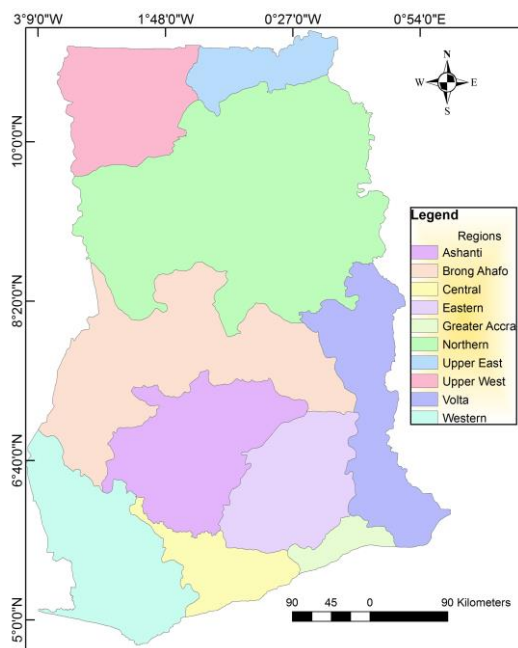
6.2.1 Mean climatology of rainfall indices

The spatio-temporal trends of ten extreme rainfall indices grouped into frequency indices: the CDD, CWD, R10mm and R20mm and intensity indices: PRCPTOT, R95p, R99p, SDII, RX1day and RX5day are analysed in this study.

Figure 6.2 represents the mean climatology of frequency indices over Ghana derived from data covering for the period of thirty-five years (1981–2015).

Figure 6.2a represents the spatial pattern of consecutive dry days (CDD) over Ghana which is between 5–140 days per annum on average. As rainfall over the country is relatively high in the south than north (see Figure 6.1b), it is expected that the CDD would be more pronounced over the northern compared to the southern sectors of the country. Consistent with this observation, maximum (approximately 80–140 days) CDD were observed in the northern part (between latitudes 8.5°N – 11.5°N) of the country where rainfall is generally low. In contrast, the number of CDD is minimum at locations in southern Ghana (see Figure 6.2a) while central Ghana (between latitudes 8°N – 9°N) is dominated by medium range CDD (about 45–60 days).

The heavy rainfall days (R10mm) and consecutive wet days (CWD) show opposing spatial pattern from that of the CDD (see Figure 6.2a).



(a)

(b)

Figure 6.1: The study area (a) and the mean annual rainfall climatology over Ghana for the period of 1981–2015 (b).

The heavy rainfall day (R10mm) index, which describes the annual counts of the days with rainfall exceeding 10 mm has an annual mean value in the range of 25–60 days over the entire country. The southwestern parts of Ghana, areas around the Volta lake of Ghana and the entire southern parts of the country (latitudes 5–8 °N and longitudes 0.5 °W–1.5 °E) enjoy relatively high number of

heavy rainfall days (40–60 days). The lowest heavy rainfall days (between 25–40 days per annum) are mostly found over most parts of Northern Ghana.

KNUST



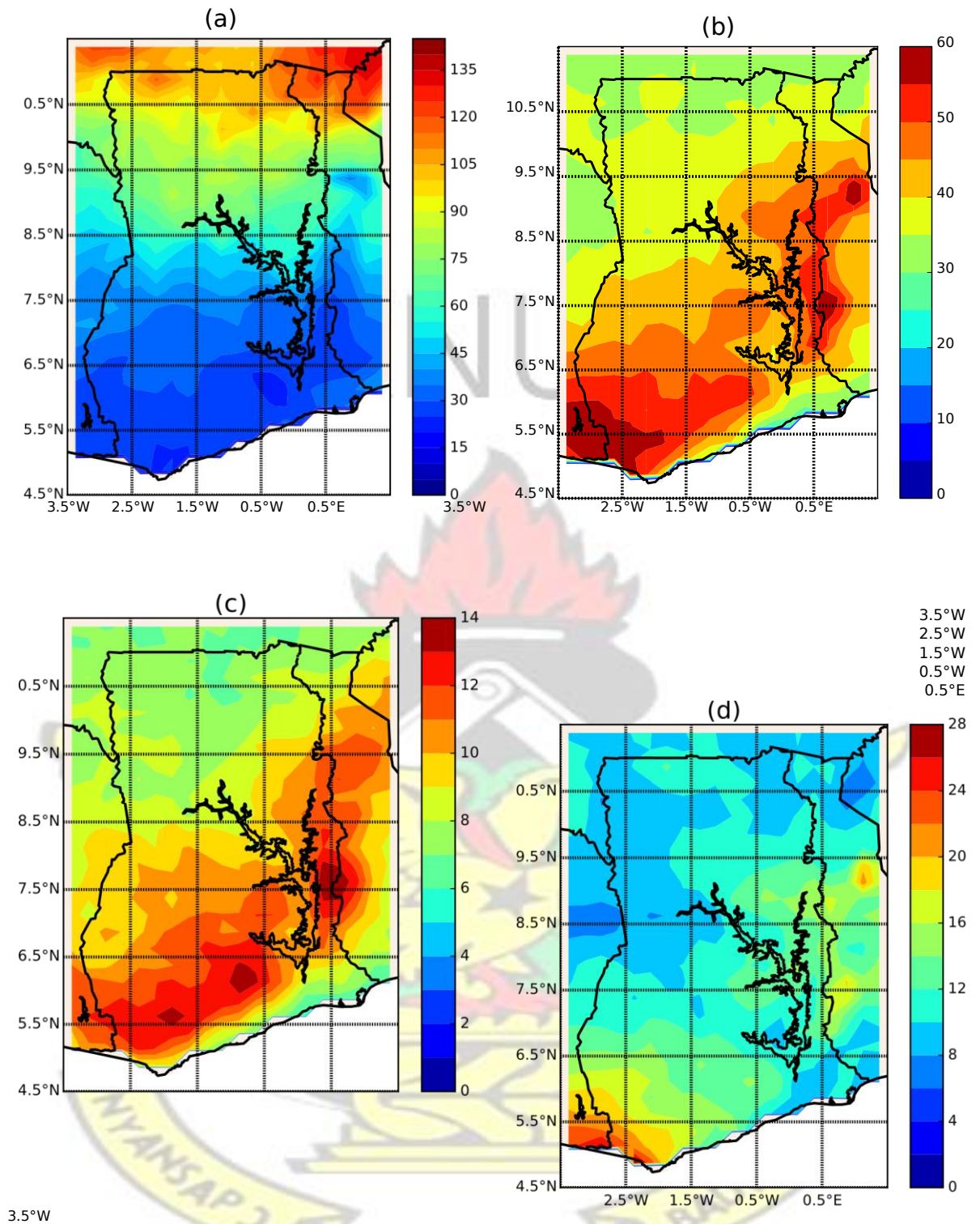


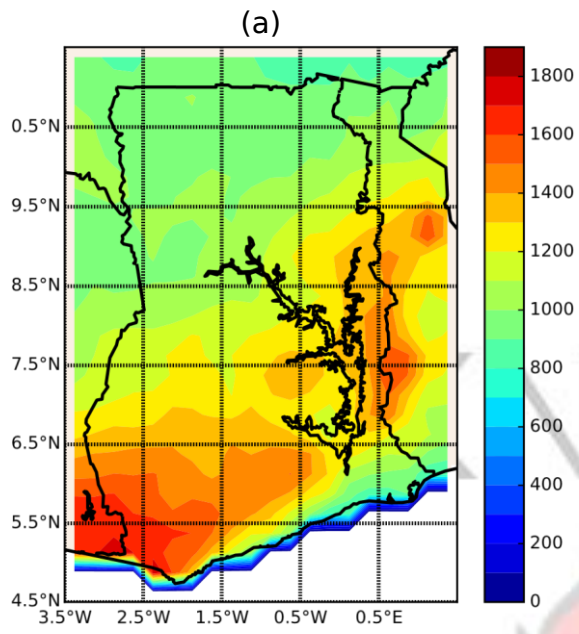
Figure 6.2: Mean climatology of frequency indices for the period of 1981–2015 over Ghana. (a) CDD; (b) R10mm; (c) CWD; (d) R20mm.

On the other hand, the consecutive wet days (CWD) index has a range of 5–14 days each year. The highest consecutive wet days is observed over areas around

the Volta lake stretching southwards to cover most parts of southern Ghana (at latitudes 5–8 N and longitudes 0.5 W–1.5 E of the country) with an average number of CWD of about 10 days. The lowest CWD on the other hand is observed over the northern and the eastern coastal sectors of Ghana with an average of about 6 CWD each year.

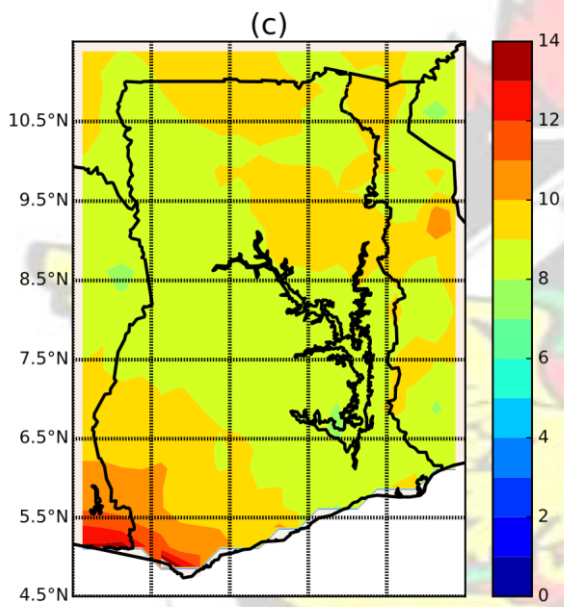
The annual frequency of very heavy rainfall days (R20mm) index has a range of 2–26 days each year over the entire country (see Figure 6.2d). Southern Ghana is observed to have more days (10–26 days) of very heavy rainfall compared to the northern sectors of the country (about 8–12 days). Southwestern Ghana experiences the greatest number of days with very heavy rainfall (>20 days) throughout the year.

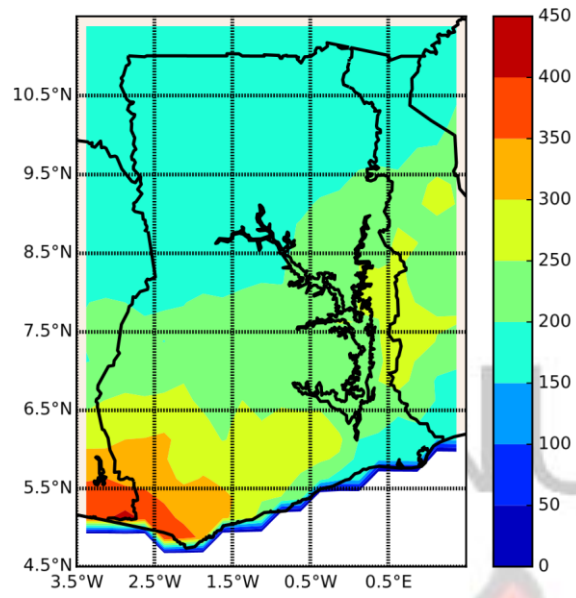
Figure 6.3 displays the mean climatology of the spatial patterns of the intensity indices over Ghana. These are annual mean of total rainfall (PRCPTOT) (Figure 6.3a), very wet day (R95p) (Figure 6.3b), the simple daily rainfall index (SDII) (Figure 6.3c), extremely wet day (R99p) (Figure 6.3d), daily maximum rainfall (RX1day) (Figure 6.3e) and the 5-day maximum rainfall (RX5day) (Figure 6.3f) over a period of thirty-five years.



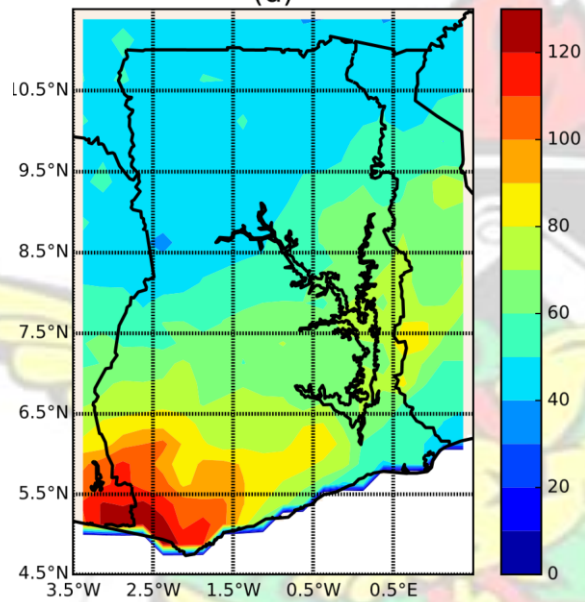
(b)

3.5°W
2.5°W
1.5°W
0.5°W

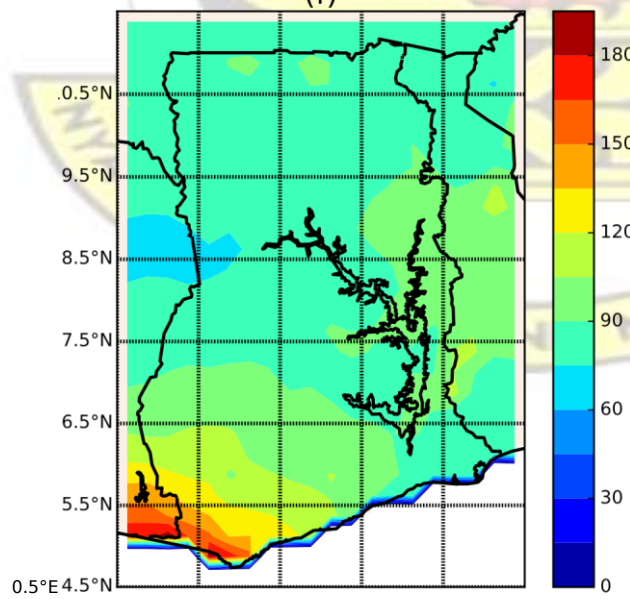




(d)



(f)



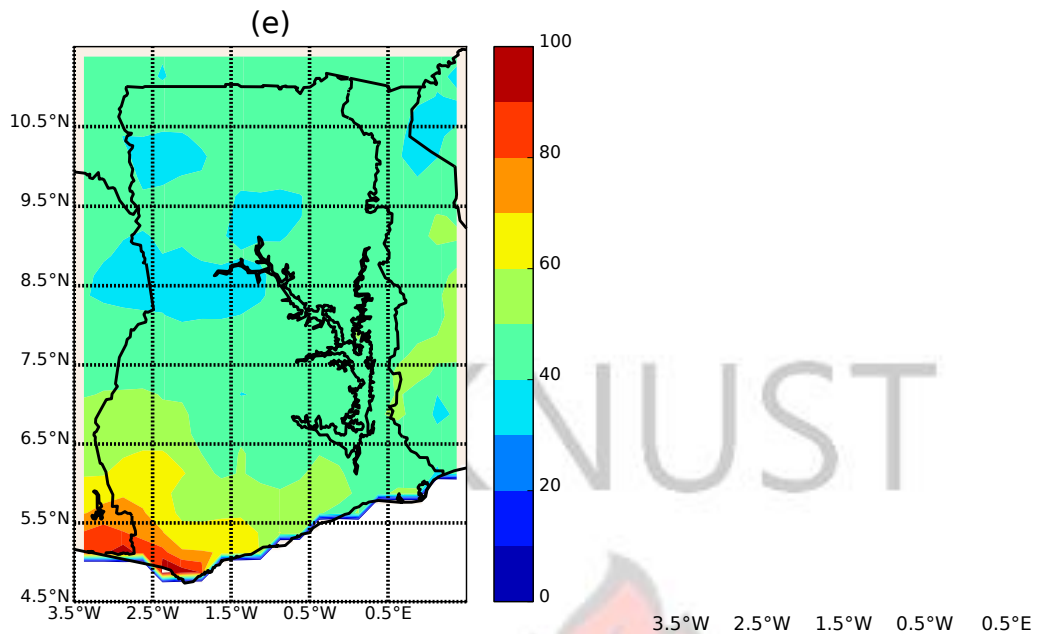


Figure 6.3: Mean climatology of intensity indices for the period of 1981–2015 over 107 Ghana. (a) PRCPTOT; (b) R95p; (c) SDII; (d) R99p; (e) RX1day; (f) RX5day.

The annual rainfall total (PRCPTOT) over the entire Ghana has a range between 800–1800 mm per year. The highest annual rainfall total in the range of 1200–1800 mm dominates over southwestern and eastern parts of the Volta lake while relatively low values, between 800–1050 mm are observed over the northwestern and eastern coasts of the country in agreement with findings in Baidu et al. (2017).

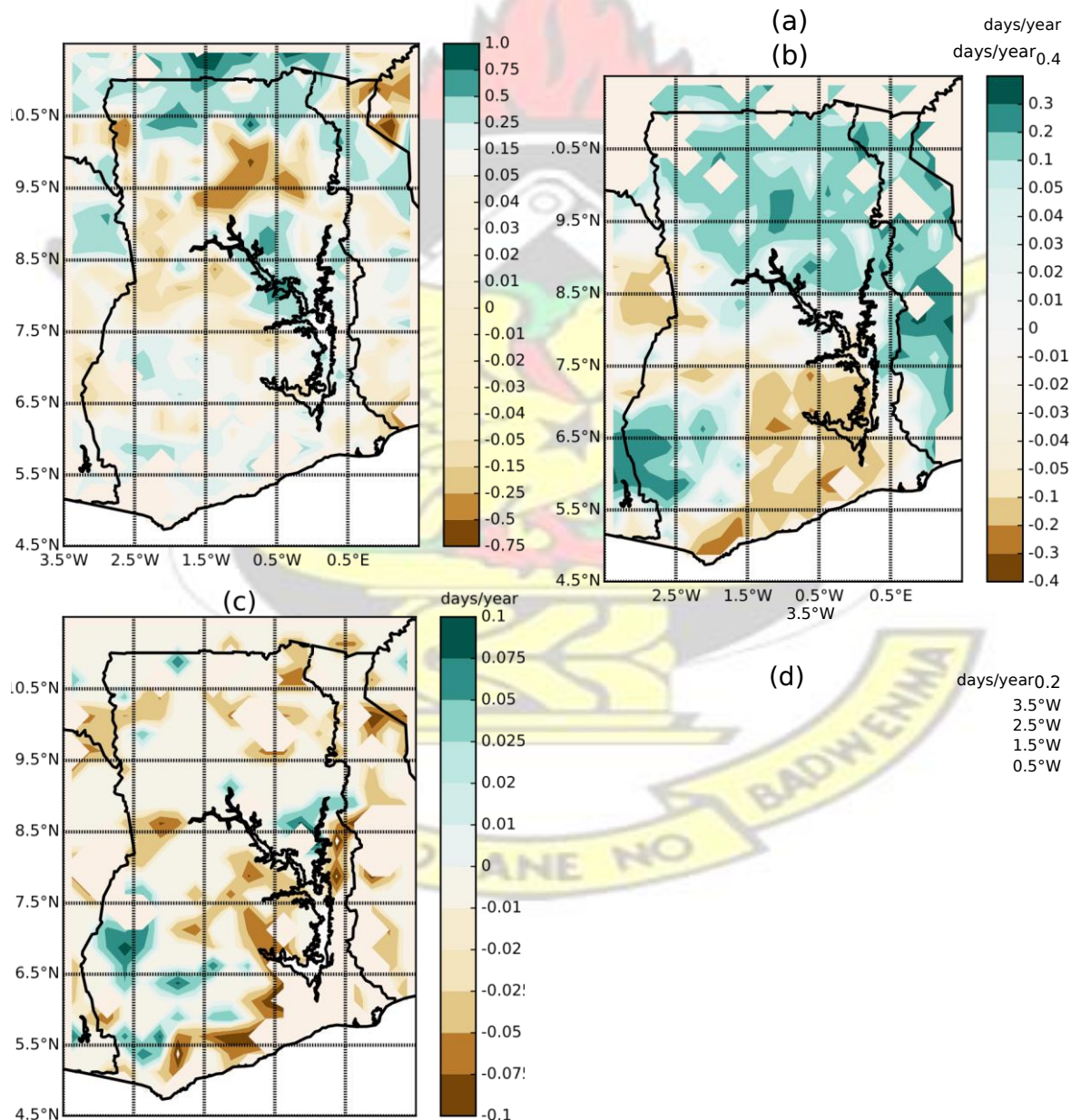
Very wet days (R95p) and extremely wet days (R99p) percentiles are highest over southwestern Ghana while lowest indices dominate most of the northern and parts of the eastern coasts of the country. The R95p index ranges between 150–450 mm per year while the R99p index on the other hand ranges between 30–130 mm per year over the entire country. Furthermore, the spatial patterns of the simple daily intensity index (SDII) ranges between 6–14 mm per year over the whole country. Relatively high daily intensities (9–14 mm) are seen to dominate over southwestern Ghana while lowest daily intensities (6–8 mm) stretches westward towards the north from the Volta lake region.

The annual RX1day and the annual RX5day indices range between 30–100 mm and 60–190 mm per year respectively over the entire country (see Figure 6.3e–f). The lowest intensities (averagely 25 mm) of the RX1day index mostly dominate over small portions of northern Ghana (8.2–9.0 °N), central Ghana (9–9.6 °N) and parts of northwestern Ghana (9.6–10.3 °N). Additionally, most of central Ghana extending to higher latitudes towards northern Ghana experience medium range (averagely 45 mm) RX1day while the highest is again observed over the southwestern Ghana (averagely 90 mm). Analogous to the RX1day index (see Figure 6.3e), the RX5day index (see Figure 6.3f) has high intensities over southwestern Ghana and low intensities over the eastern coasts and north western sectors of Ghana. A mean value of about 160 mm/year of RX5day index is dominant over most of southwestern Ghana while the lowest mean value (about 65 mm/year) is observed over western mid-Ghana within the latitude band 8.2– 9.00 °N. Most of central Ghana including northern sectors have a mean value of about 80 mm/year of the RX5day index.

6.2.2 Trends of rainfall indices

The spatial trends of the ten rainfall indices over Ghana for the period of 1981–2015 are as shown in Figs. 6.4 and 6.5. The CDD index (see Figure 6.4a) shows insignificant to negative trends over most of Ghana with the exceptions of northern Ghana and some isolated pocket along 0.5 W between 7.5 and 9 N that exhibit increasing trend in the number of annual continuous dry days (i.e., an increase of 3 to 10 days per decade in the last nearly four decades). Despite increase in CDD over these regions, the annual counts of days with rainfall

exceeding 10 mm has been increasing over northern half of the country and southwestern Ghana during the 1981–2015 period (see Figure 6.4b). The CWD index shows negative trends over most of the country with the exceptions of the isolated pocket over southwestern and central-eastern Ghana (see Figure 6.4c). The decrease in CDD did not lead to increase in CWD suggesting that these change in rainfall frequency indices are mainly reflected in increase in rainfall events with heavy and very heavy rainfalls as noted from the increase in R10mm (see Figure 6.4b) and R20mm (see Figure 6.4d) over most of Ghana.



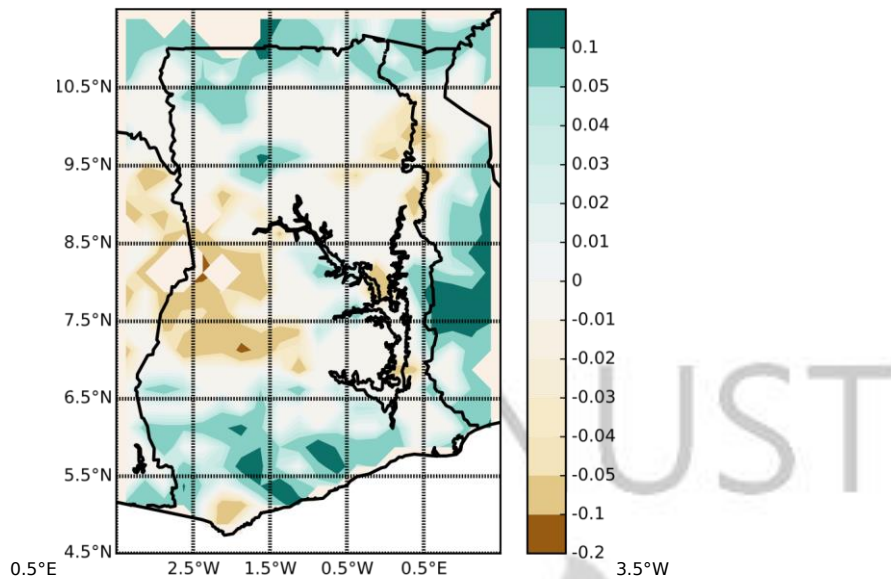


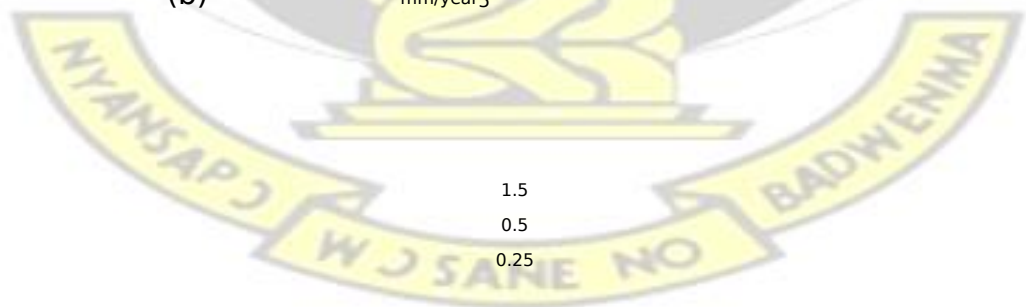
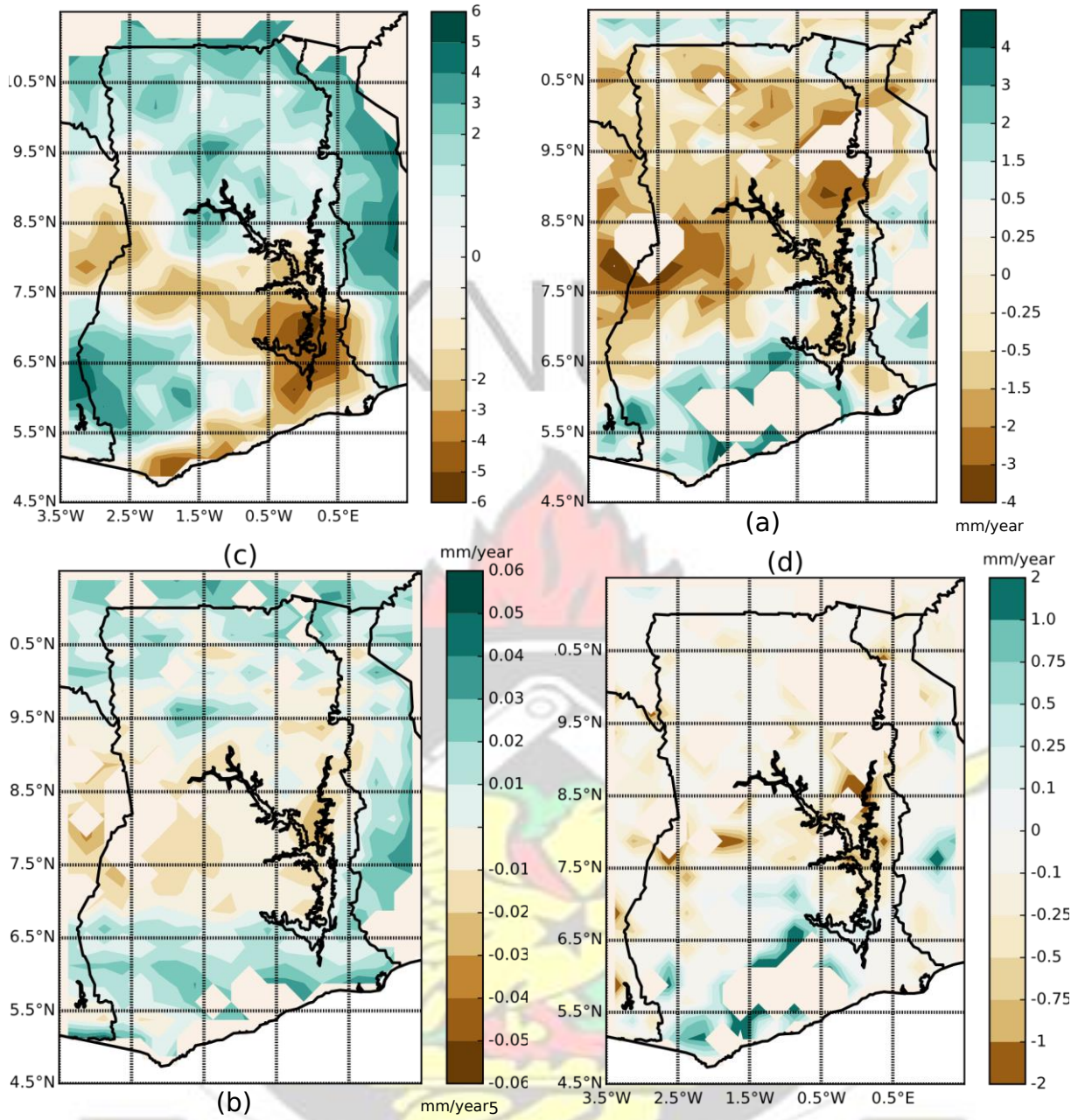
Figure 6.4: Trends of intensity indices for the period of 1981–2015 over Ghana. (a) CDD; (b) R10mm; (c) CWD; (d) R20mm.

Figure 6.5a displays the trends of the annual precipitation total over Ghana which shows drying trends over the entire Volta lake extending westwards to most parts of central, western (i.e., between latitudes 7–9° N) and eastern coasts of Ghana. Interestingly, southwestern Ghana with the highest annual rainfall total exhibits a positive trend. Positive trends similar to those over southwestern Ghana are observed over most parts of northern Ghana. The very wet (R95p) and extremely wet day (R99p) indices (see Fig 6.5b and 6.5f respectively) have similar spatial trends over the entire country. Negative trends dominates the entire country except for area lying south of 6.5 N which are dominated by normal to positive trends. In addition, the simple daily intensity over Ghana show negative trends over central Ghana between 7–9.3 N while positive trends dominates rest of the country. Figure 6.5e–f display the spatial patterns of trends in RX1day and RX5day indices over Ghana. Southeastern Ghana is dominated by positive trends in Rx1day whereas negative trends are found to cover almost all

other parts of the country. Similarly, positive trends in RX5day are observed in southern and northwestern Ghana whereas negative trends dominates the remaining parts of the country.

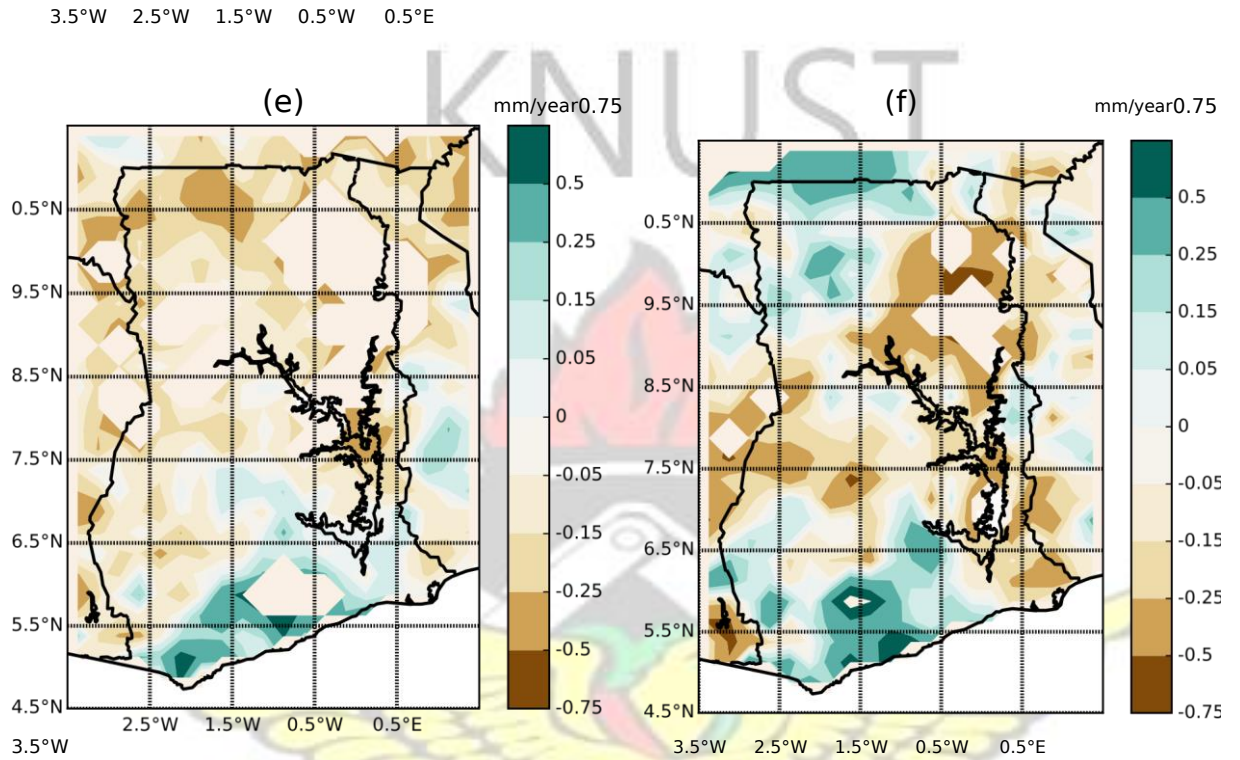
KNUST





1.5
0.5
0.25
-0.25
-0.5
-1.5

3.5°W 2.5°W 1.5°W 0.5°W 0.5°E



112

Figure 6.5: Trends of intensity indices for the period of 1981–2015 over Ghana. (a) PRCPTOT; (b) R95p; (c) SDII; (d) R99p; (e) RX1day; (f) RX5day.

6.2.3 Correlations of SST anomalies and the rainfall indices over

Ghana

6.2.3.1 Relation between sea surface temperature (SST) and rainfall indices

The correlation between the ten rainfall indices over Ghana and sea-surface temperatures (SSTs) have been analysed in this section. Specifically, the first three principal components (which contributed to more than 70% of the total variance) of the ten rainfall indices were computed and correlated (grid-wise)

with the SSTs (see Figs 6.6 and 6.7). Correlations that are statistically insignificant at 95% confidence level are masked in these figures. Generally, the results reveal some appreciably significant correlations between the the combined principal components of some rainfall indices and the SSTs over the Pacific, Atlantic and Indian oceans.

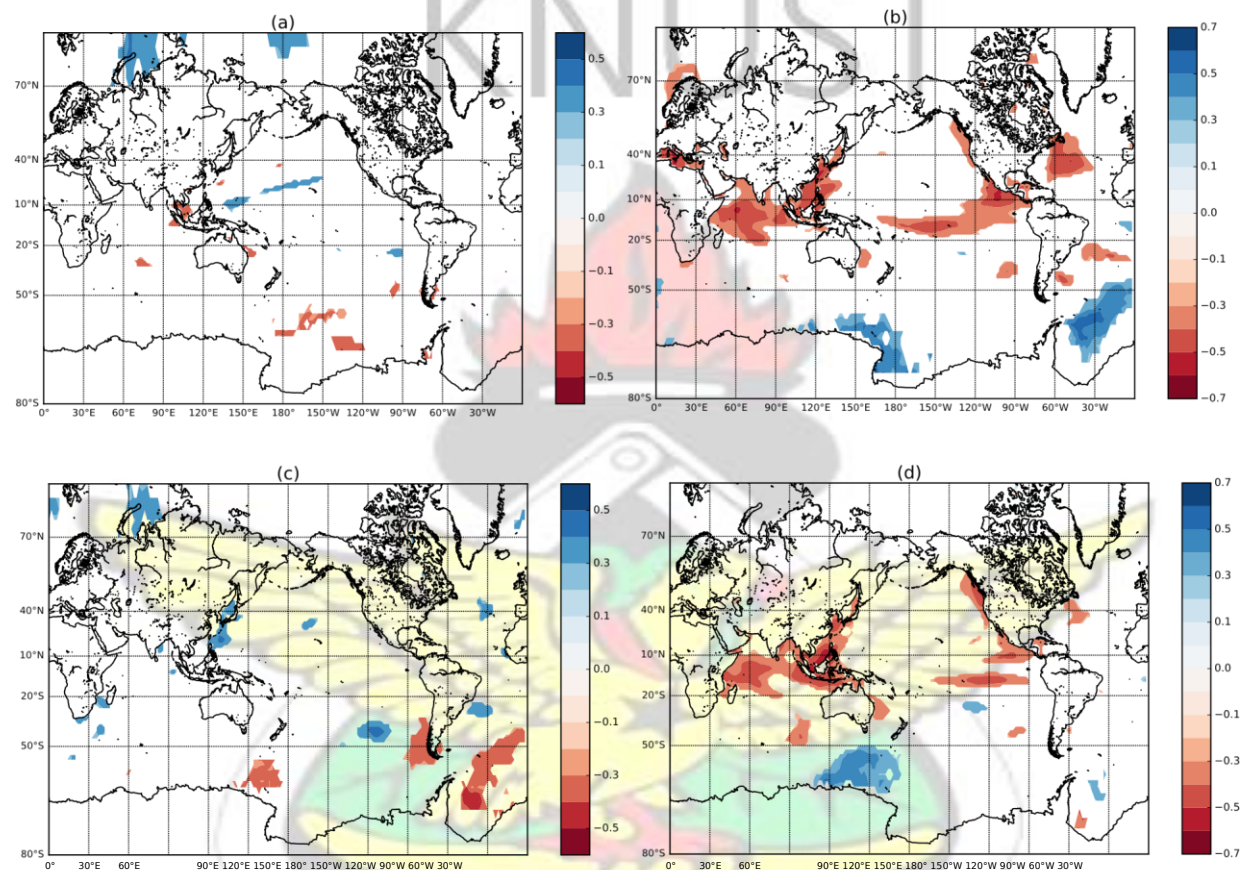


Figure 6.6: Spatial patterns of significant correlation between SST and rainfall indices; (a) CDD, (b) R10mm, (c) CWD, (d) R20mm for the period of 1981–2015.

No or few significant correlations were observed between SSTs anomalies and CDD and CWD rainfall indices thus indicating the frequency of these rainfall indices over the region are more driven by seasonal scale variability than interannual variability in SSTs over the ocean basins (Figure 6.6a and 6.6c). It

could also be that the variability in these indices are driven by local scale than large scale SST variability.

The number of heavy rainfall days (R10mm) over Ghana as shown in Figure 6.6b is observed to have negative correlation (-0.7 – -0.4) with SSTs over equatorial Pacific and northern and the Indian Oceans whereas positive correlation are observed over extreme southern of Atlantic ocean. Similarly, the number very heavy rainfall days (R20mm) have negative correlations with SSTs in the Pacific (equatorial and northern) and the Indian Oceans while southern Indian ocean is dominated by positive correlations (Fig 6.6d). These current findings are consistent with earlier finds which revealed similar interrelationship with rainfall over varied locations and the SSTs in oceanic basins (Diatta and Fink, 2014; Clark et al., 2003; Bader, 2005).

Figure 6.7a, on the other hand, reveals positive correlations over the Atlantic and southern Indian Oceans and negative correlations over the equatorial Indian and Pacific Oceans for the annual precipitation total (PRCPTOT) which is consistent with findings in Gadgil et al. (2004) who confirmed warm (cold) SSTs over equatorial Indian and Pacific are associated with negative (positive) rainfall anomalies over Ghana.

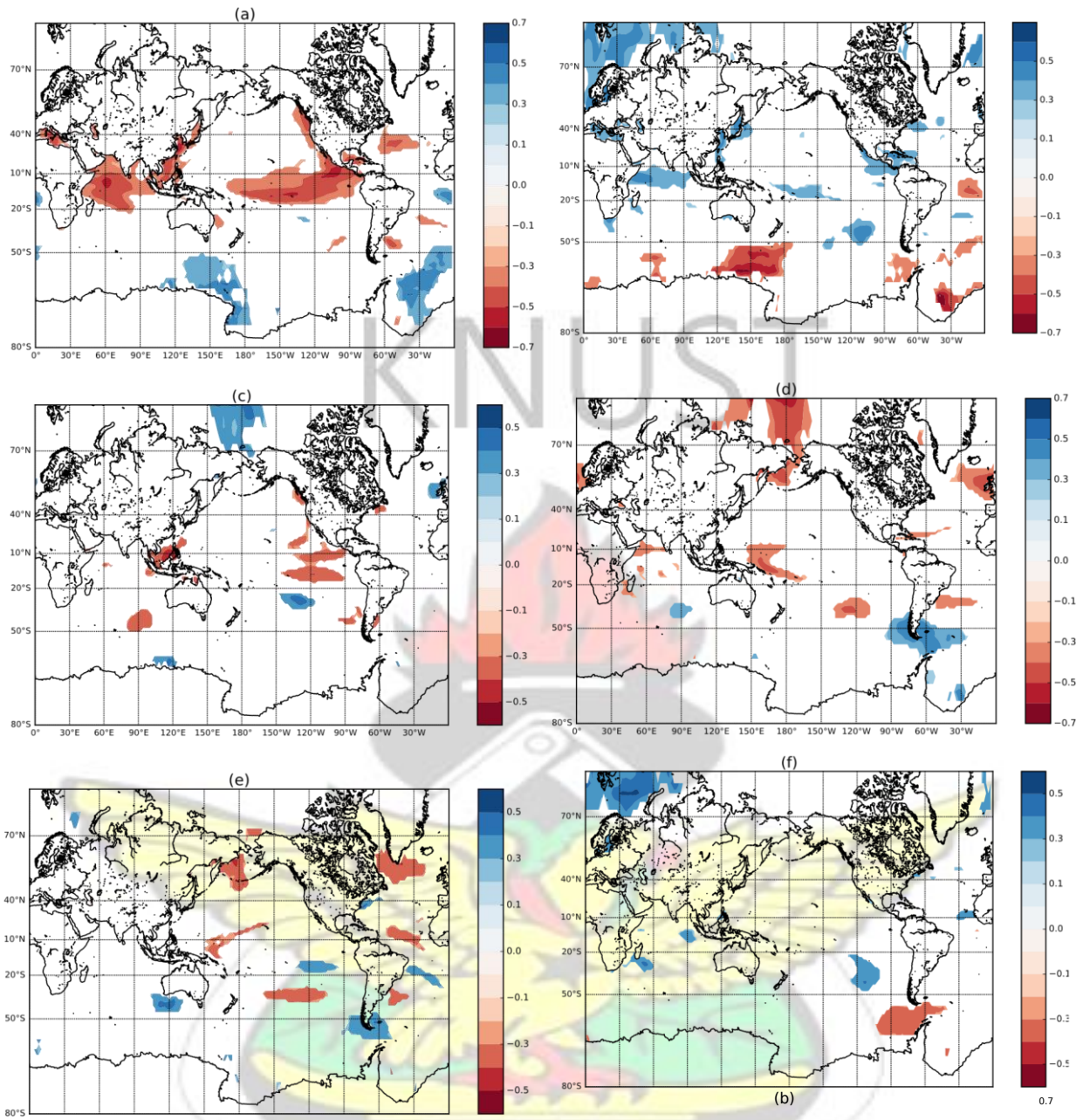


Figure 6.7: Spatial patterns of significant correlation between SST and rainfall indices; (a) PRCPTOT, (b) R95p, (c) SDII, (d) R99p, (e) RX1day and (f) RX5day rainfall indices for the period of 1981–2015.

The very wet day (R95p) index as shown in Figure 6.7b has positive correlation with SSTs northern Atlantic equatorial, Indian and some parts of the Pacific Oceans. In contrast, negative correlations are prevalent over parts of the Atlantic and southern Indian Oceans. These results do not deviate from observations in Lough (1986a) which revealed contrasting relationship between rainfall over Sahel and SST departures over the southeastern tropical Atlantic ocean. The SDII (see Figure 6.7c), on the other hand, exhibits negative and positive correlation with the SSTs over the parts of the Pacific Ocean. The R99p index have positive correlation with the SSTs in southern Atlantic and parts of southern Pacific whereas negative correlations dominate over far northern Pacific and Atlantic and the equatorial Indian Oceans (see Figure 6.7d).

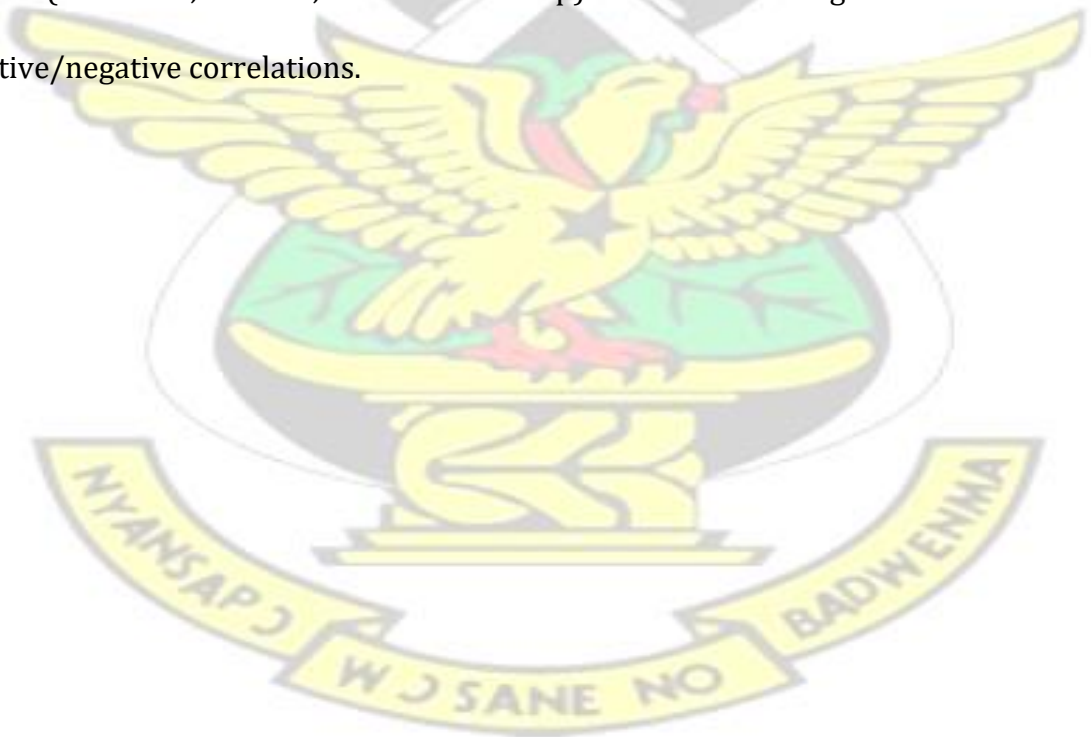
The RX1day is observed to have both positive and negative correlations with the SSTs over the parts of the Indian, Pacific and Atlantic oceans (see Figure 6.7e).

The RX5day (Figure 6.7f) index is observed to have positive correlations with the SSTs in northern Atlantic and parts of southern Pacific and negative correlations, over southern Pacific near southern south America.

These current findings show consistence with earlier finding by Balas et al. (2007) who found the rainfall variability over west central Africa to be linked to the SST fluctuations especially over Pacific nino regions and the western Indian Ocean and with the Atlantic Ocean particularly during the boreal summer season.

6.2.3.2 NINO3.4

In Section 6.2.3.1 it has been noted that the equatorial Indian Ocean and Pacific SST anomalies are closely correlated with indices such as total precipitation (PRCPTOT), R95p and R10mm and R20mm indices while equatorial Atlantic ocean SST anomalies correlate with the PRCPTOT and R95p indices. However, these correlations are the average of the whole country and does not indicate which parts of the country are influenced and the extent to which the various parts of the country are controlled by inter-annual SST variability. To answer this question, NINO3.4, IOD and AMO indices that represent equatorial Pacific, Indian and Atlantic Oceans are used for correlations with grid point extreme rainfall indices (PRCPTOT, R10mm, R20mm and R95p) that exhibit strong positive/negative correlations.



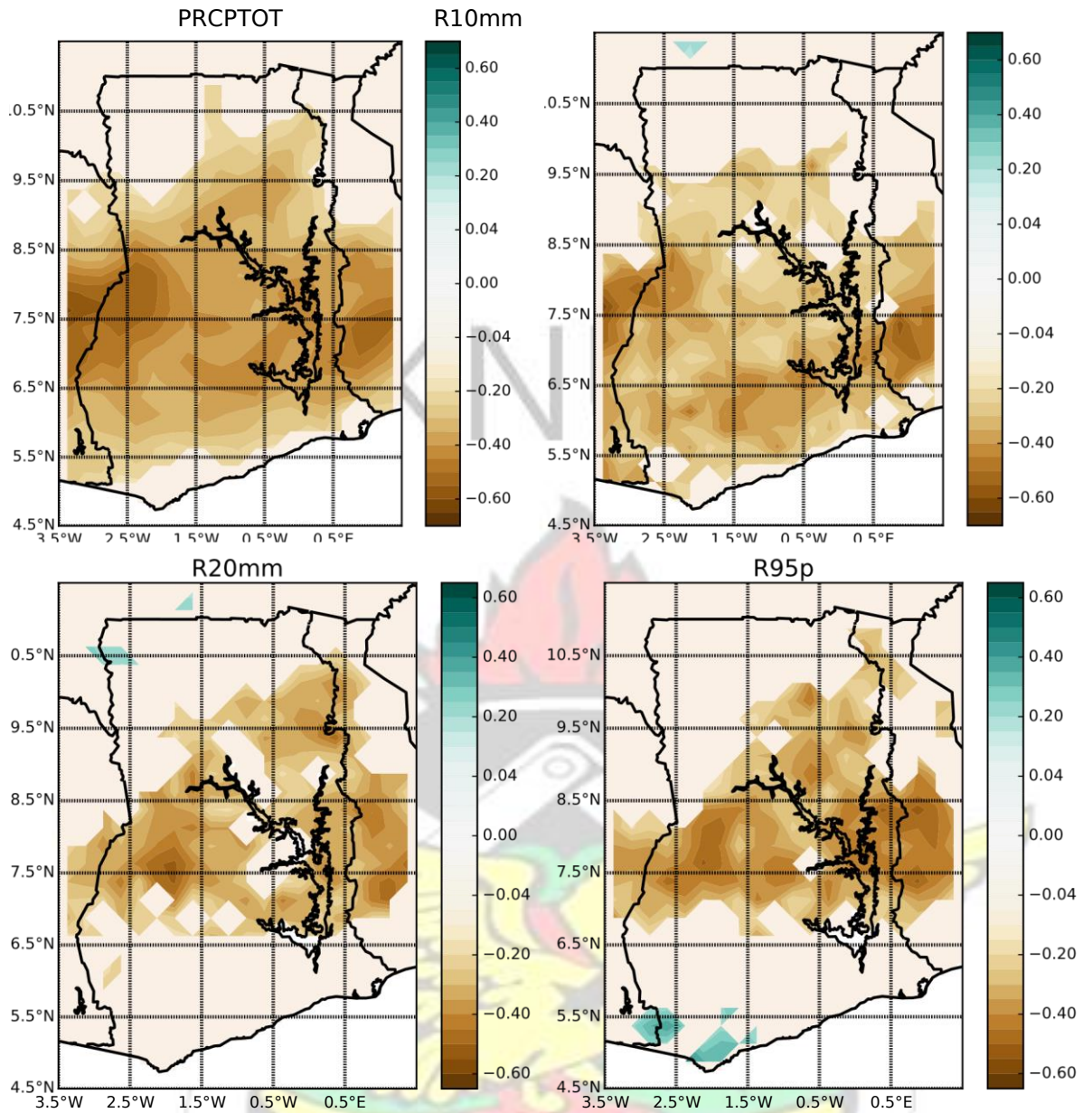


Figure 6.8: Correlation between NINO3.4 index and the PRCPTOT, R10mm and R20mm rainfall indices for the period of 1981–2015 over Ghana.

Figure 6.8 reveals association of low (high) PRCPTOT (Figure 6.8 top-left) and R10mm (Figure 6.8 top-right) indices with warm (cold) Nino3.4 SST indice over most of Ghana with exception of small latitude bands in the north of the country. However, these negative association shrinks to central Ghana in the western half and to 6.5–10.5N in the eastern half of the country in the cases of R20mm and R95p indices. The strongest influence of equatorial Pacific SST anomalies on rainfall indices is apparent over western-

central Ghana and Volta Lake region in the East as noted from negative correlation exceeding 0.7. These findings are inline with previous observations by Diatta and Fink (2014) and Clark et al. (2003) who have shown negative correlations between the Nino3.4 and parts of tropical West African rainfall. This negative correlation between parts of the

Ghanaian rainfall and the Nino3.4 is possibly attributable to the positive Pacific SSTs coinciding with subsistence within the tropics as highlighted in Janicot et al. (1998). Thus, a warm (cold) Pacific SST is tantamount to less (more) rainfall events within western-central and Volta Lake region of Ghana.

6.2.3.3 Indian Ocean Dipole (IOD)

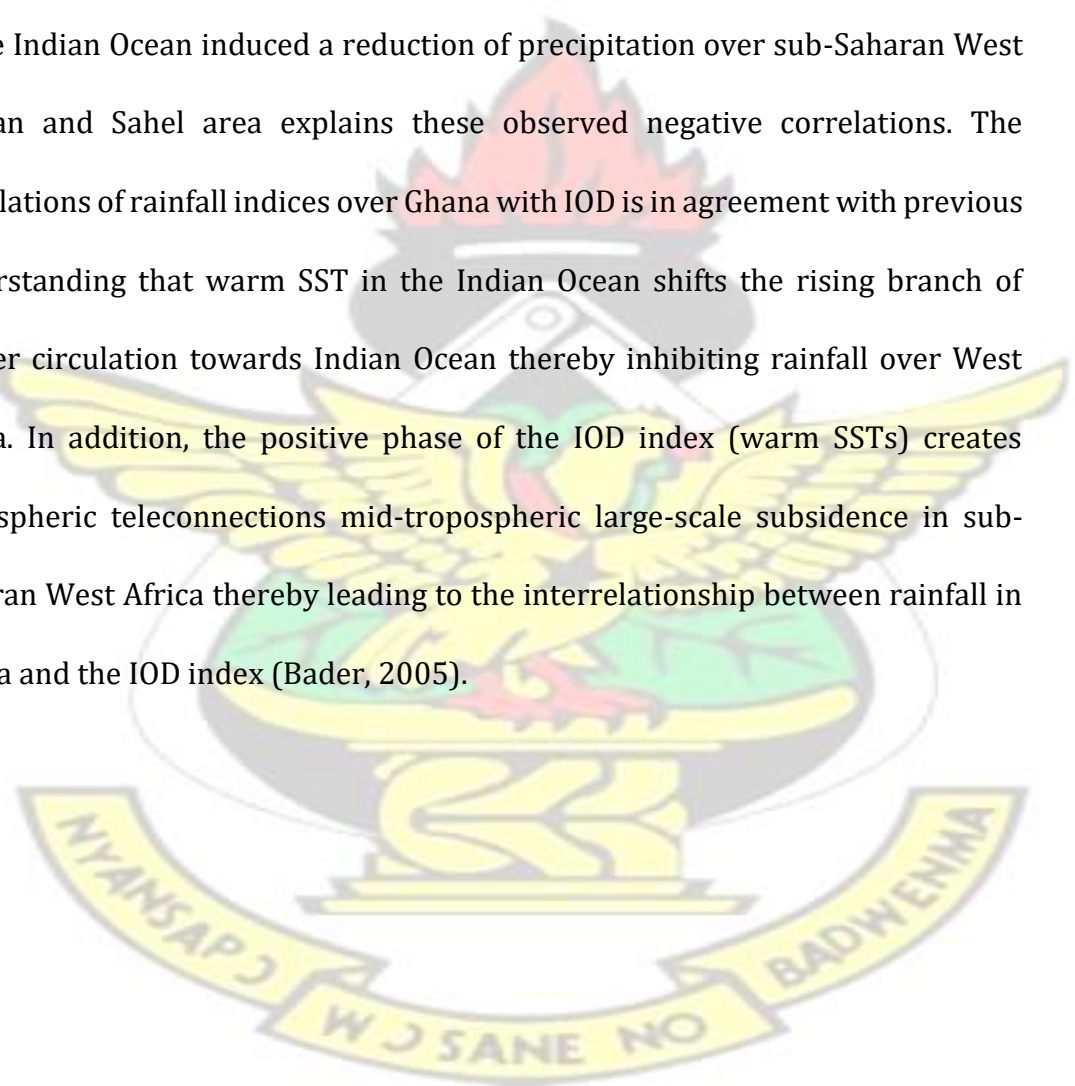
The IOD index generally has a sort of dipole effect on the rainfall indices over Ghana characterised by no or negative correlations over central Ghana and isolated pockets of positive correlations over the northern and southern boarder areas of the country as shown in Figure 6.9. For instance with the PRCPTOT, negative correlations are observed over the central western Ghana and some parts of the Volta lake. In contrast, positive correlations are observed far north of the country.

Similarly, for the R10mm, the northwestern portion of the country are dominated by positive correlations while central Ghana and southern Volta lake are dominated by negative correlation.

In addition, mid-northern and greater portions of central Ghana are marked by negative correlations while far northwestern and eastern coast of the country are

dominated by positive correlations of IOD and the R20mm index. Most of central and northwestern Ghana are mainly dominated by negative correlations whereas the coastal zones and far northeastern Ghana are influenced by positive correlations.

On average, throughout the entire country, negative correlations exist between wet indices and SSTs anomalies in the Indian Ocean. The argument of Fontaine and Janicot (1996a), Bader and Latif (2003b) and Lu (2009) that increasing SSTs in the Indian Ocean induced a reduction of precipitation over sub-Saharan West African and Sahel area explains these observed negative correlations. The correlations of rainfall indices over Ghana with IOD is in agreement with previous understanding that warm SST in the Indian Ocean shifts the rising branch of Walker circulation towards Indian Ocean thereby inhibiting rainfall over West Africa. In addition, the positive phase of the IOD index (warm SSTs) creates atmospheric teleconnections mid-tropospheric large-scale subsidence in sub-Saharan West Africa thereby leading to the interrelationship between rainfall in Ghana and the IOD index (Bader, 2005).



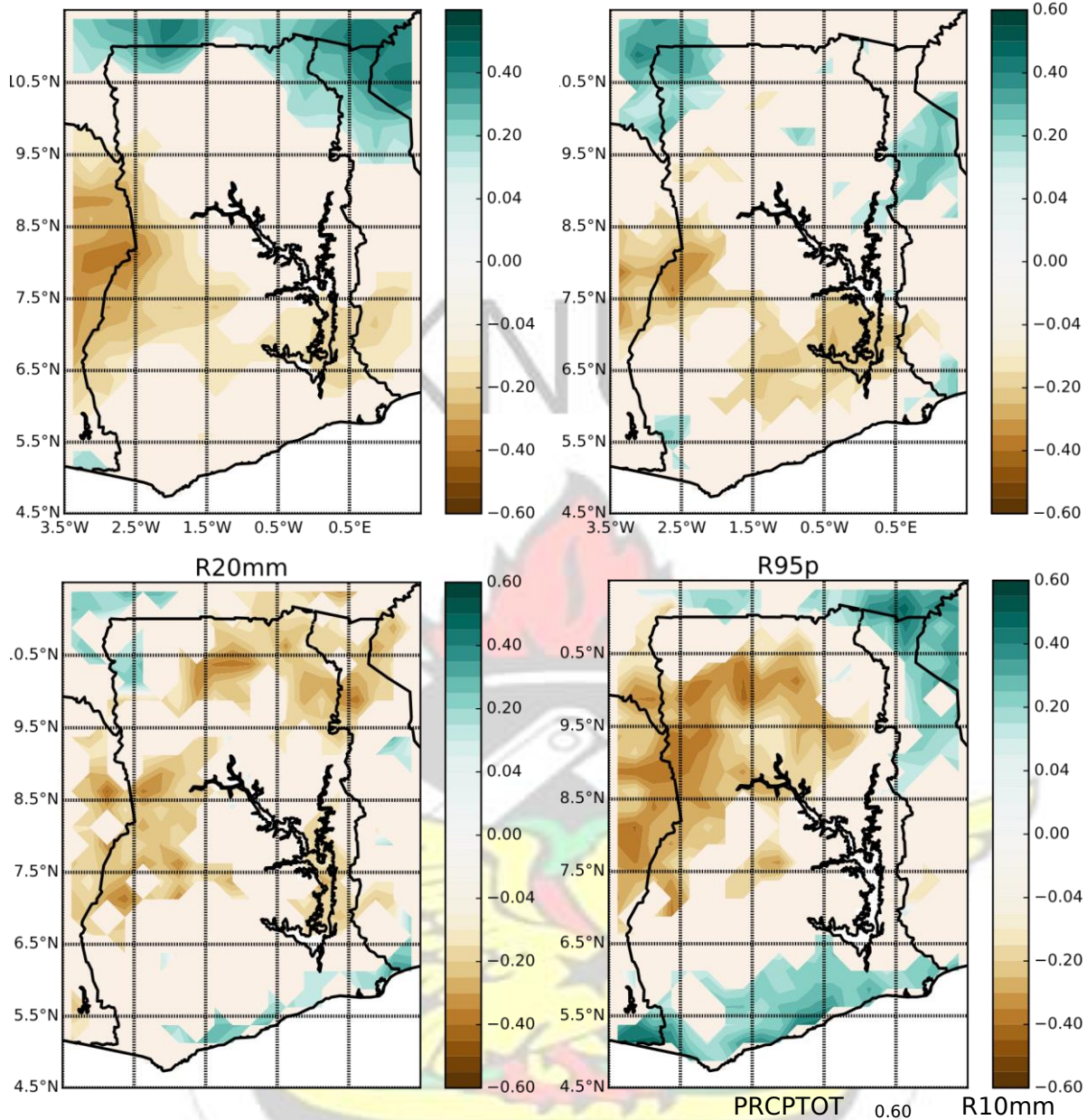


Figure 6.9: Correlation between IOD index and the PRCPTOT, R10mm and R20mm rainfall indices for the period of 1981–2015 over Ghana.

6.2.3.4 Atlantic Multidecadal Oscillation (AMO)

As established in Figs. 6.7a–b, SSTs anomalies over the Atlantic ocean averagely correlate positively (negatively) with the PRCPTOT (R95p) index in Ghana. Figure 6.10 depicts the grid-wise correlation between the PRCPTOT and R95p indices and the AMO index country-wide. For the PRCPTOT, it is observed that, far northern and further southwestern (5.5°N – 6.5°N) of the country is dominated by positive correlations (0.2–0.6) supporting the observations in Diatta and Fink (2014) who have determined positive correlations between the AMO index and rainfall over the Sahel within just a few degrees north of Ghana. In addition the results that are consistent with findings in Opoku-Ankomah and Cordery (1994) who found the SST anomalies over the equatorial Atlantic to correlate positively with the Ghanaian rainfall.

In contrast, negative correlations dominate some parts of central and southern Volta with correlation coefficients in the order of -0.4 – -0.1. This could possibly be due to abnormally warm SSTs persistent over the south Atlantic that can reduce meridional Atlantic SST gradients located south of the ITCZ.. This, in turn, weakens the intensity of the Hadley circulation (Opoku-Ankomah and Cordery, 1994; Palmer, 1986). This reduction in intensity of the Hadley circulation, responsible for rainfall/moisture over the West African would result in a reduction within the region.

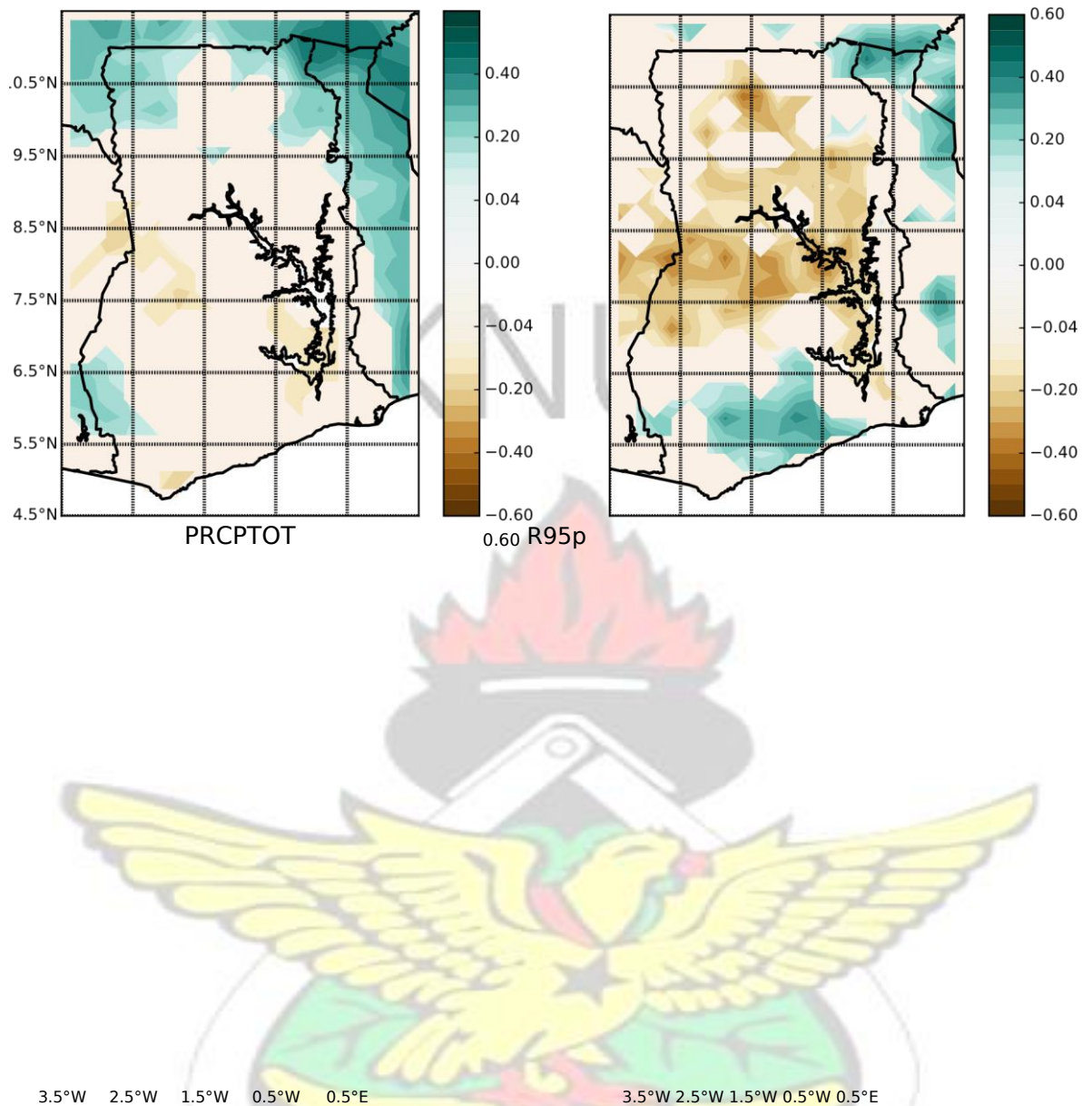


Figure 6.10: Correlation between AMO index and the PRCPTOT and R95p rainfall indices for the period of 1981–2015 over Ghana.

It is observed that most parts of central and northern Ghana are dominated by negative correlation (-0.6– -0.1) while far northeastern and mid-southern Ghana are influenced by positive correlation (0.1–0.6) of AMO and R95p index. These negative correlations observed in most parts of central and northern Ghana in essence is a result of the fact that, during the negative phase of the Atlantic SSTs, there is a southward shifting of the West African rain belt due to the strengthening the effect of the north Atlantic tropical high towards the equator.

This leads to a condition whereby regions south (north) of the rain belt would receive more (less) rainfall. More so, this southward position of the rain belt also inhibits the southwesterly monsoonal flow further north of the region.

6.3 Summary

The spatio-temporal variability of rainfall over West Africa continues to be a challenge to food security and other socio-economic activities. This study presents a comprehensive analysis of the rainfall climatology, trends and drivers of ten rainfall indices using the CHIRPS homogenized daily rainfall series for the period of 1981–2015 over Ghana.

The mean climatology of the CDD was found to range between 5–140 days/year with maximum (minimum) values over the northern (southwestern) parts of the country. Similar spatial patterns of mean climatologies were observed for the CWD and R10mm indices which range between 5–14 days/year and 25–60 days/year respectively whereas the R20mm was in the range of 2–26 mm/year with highest intensities dominating the southwestern Ghana and lowest intensities over northwestern Ghana. Furthermore, the PRCPTOT, R95p and R99p showed similar patterns with intensities ranging between 800–1800 mm, 150–450 mm and 30–130 mm per year respectively. The spatial patterns of the RX1day and RX5day indices were observed to be almost indistinguishable which range between 30–100 mm and 60–190 mm per year respectively with highest intensities over southwestern Ghana and lowest intensities over northeastern and eastern coasts of the country. The mean climatology of the SDII index ranges between 7–14 mm/year over the entire country with most parts of central Ghana

showing medium-range daily intensities and the southwestern sectors dominated by the highest daily intensities. In addition, trends of rainfall indices were significant over most parts of the country with negative trends dominating parts of the Volta lake and central Ghana whereas weak positive trends were observed over southwestern Ghana for wet indices.

More also, the results for the link between the rainfall indices and SST anomalies over Oceanic basins revealed very few significant correlation between the SST anomalies over oceanic basins and the CDD and CWD indices thus indicating the frequency of daily indices over the region are probably more driven by seasonal scale variability than inter-annual variability in SSTs over the ocean basins. Generally, the SSTs anomalies at the Pacific and Indian Oceans (Atlantic) had negative (positive) correlations with the most rainfall indices over Ghana. Specifically, the NINO3.4 had negative correlations with indices particularly over central and northern parts of the country. This is likely because, warm Pacific SSTs as highlighted by Janicot et al. (1998) coincides with subsistence within the tropics hence, the negative correlations between Pacific SSTs and wet indices over the country. IOD on the other hand had a dipole effect on rainfall indices where central and southern sectors generally revealed negative correlations whereas northern and coastal zones, positive correlations. More so, the negative correlation between Atlantic SSTs and parts of Ghana could be attributed to the fact that, during the negative phase of the Atlantic SSTs, the southward displacement of the West African rain belt becomes intensified thus, resulting to rainfall deficits such locations. Central portion of the country was influenced by negative correlations while positive correlations were dominant far northern Ghana for the

AMO index possibly attributed to the fact that, during the negative phase of the Atlantic SSTs, the southward displacement of the West African rain belt becomes intensified thus, resulting to rainfall deficits over those locations.

These results have implications on the improvement of seasonal-annual forecasts of the Ghanaian rainfall and its extremes, and also provides prior knowledge for better understanding of multidecadal modulations of global inter-annual teleconnections.



CHAPTER 7

Conclusions and Recommendations

7.1 Conclusions

Rainfall variability has significant implications on the key socio-economic activities such as, agriculture, water resource management, hydro-power generation and fresh water accessibility of any developing country. In Ghana for instance, rain-fed agriculture is reported to contribute more than 65% of employment to citizens and approximately 30% of GDP. For this reason, rainfall impact studies are very crucial towards enhancing the overall socio-economic development of the country. The study reported in this thesis assessed the performance of satellite and gauge rainfall products which further lead to the spatio-temporal analysis of climatologies, trends and drivers of extreme rainfall in Ghana during 1981–2015. On average, satellite-based rainfall products (SRPs) have shown good skills in presenting information on the rainfall variability in the entire country and at locations where rain gauge networks were limited (savannah zones). The performance of SRPs were observed to be a function of their temporal scale and the location. SRPs are liable to large errors ($rms > 0.50$) at coarse temporal aggregations and relatively poor in the coastal zones especially on annual scales. This comparatively poor performance of SRPs in the coastal zones could be partly attributed to some caveats that were observed at the western coasts of the country in the reference gridded gauge rainfall data. The

study observed that, a boundary station at the western coast in 1999 yielded some unrealistic values during the major rainfall peak (in June) which produced some extreme rainfall values. This extreme rainfall value presented by gauge at the western coast is suspected to have affected the performance of SRPs. However, the impact is confirmed to a large extent by the gauge-only (GPCC, CRU) rainfall products.

In addition, SRPs were observed to capture the rainfall patterns in the four agro-ecological zones of the country however, sometimes they either over/under estimated ground observations. TRMM showed a relatively better performance than the other SRPs on monthly scale which is possibly due to its monthly gauge correction technique. CHIRPS, CRU and TAMSAT would serve as good complements to gauge for annual rainfall studies in the country. The IMERG satellitebased and DOGs rainfall products were observed to effectively capture the diurnal, daily and monthly rainfall patterns in the Ashanti region of Ghana. Heavy rainfall was well captured by IMERG as such, it could be used for high impact rainfall studies.

Results from the trend analysis revealed the rainfall climatologies of frequency indices, CDD, CWD, R10mm and R20mm to be in a range of 5–140, 5–14, 25–60 and 2–26 days per year whilst intensity indices, PRCPTOT, R95p, R99p, SDII, RX1day and RX5day are in the range of 800–1800, 150–450, 30–130, 6–14, 30–100 and 60–190 mm per year respectively. The mean climatology of dry indices were maximum over the northern and minimum in southwestern parts of Ghana. The maximum of temporally averaged intensity indices covers southwestern

Ghana while the minimum of the indices lies over northwestern and eastern coasts of

Ghana. Trends of rainfall indices were significant (confidence value of 95%) over most parts of the country with negative rainfall trends dominating parts of the Volta lake and middle sectors of Ghana. Positive trends were observed over southwestern Ghana for wet indices. The observed decreasing rainfall trends in the Volta lake of the country would have serious implications on rain-fed agriculture, fishing and the hydroelectric power generation of the nation at large. SST anomalies over oceanic basins were observed to have a link with rainfall extremes in Ghana however, no significant correlations were observed for the CDD and CWD indices of the country. This implies that the frequency of daily indices over the country are probably more driven by seasonal scale variability than interannual variability. The SSTs anomalies at the Pacific and Indian Oceans had negative correlations whereas the Atlantic SSTs had positive correlations with most of rainfall indices over Ghana. NINO3.4 had negative correlations with indices particularly over central and northern parts of the country. This is most likely because, warm Pacific SSTs coincides with subsistence within the tropics. IOD had a dipole effect on rainfall indices where central and southern sectors generally revealed negative correlations whereas northern and coastal zones showed positive correlations. The negative correlation between Atlantic SSTs and parts of Ghana could be attributed to the intensification of the southward displacement of the West African rain belt during the negative phase of the Atlantic SSTs, thus resulting to rainfall deficits in the region.

The findings presented in this thesis would serve as benchmark on the validity of satellite and gauge-only rainfall products in Ghana which is valuable information

to safe guide users on the choice of rainfall data for climate impact studies to aid effective decision making process.

7.2 Recommendations

7.2.1 Recommendations For Further Studies

Satellite validation studies, SST forcing on extreme rainfall as well as extreme rainfall case studies are still not well documented in Ghana. This current study is distinctive because it presents for the first time the validities of the newly installed DOG rainfall data. The study also serves as a benchmark on the performance of various satellite rainfall products in Ghana. More also, the study also contributes to the limited knowledge on the drivers of rainfall extremes in the country. Further studies are still necessary in order to build upon the strength and lapses in this research.

Results from this study revealed some caveats of the gridded GMet data especially over the western coasts of the country. This study recommends an upgraded version where these bugs would be rectified for future validation and other climate impact studies in the country. Again, the present study did not explore the impacts of the gauge number distribution on the performance of SRPs in the country. It would be essential for future validation studies to consider investigating the impacts of the gauge number distribution on the performance of SRPs in the entire country and in the four ecological zones so as to better understand their abilities in the phase of gauge number variability. More sub-

daily validation studies would be crucial as this presents end-users with a variety of sub-daily SRPs to choose from for various applications.

The current study investigated the link between three remote climate indices, the AMO, Nino3.4 and IOD and rainfall extremes in Ghana. The study did not explore the inter-relationship between other remote climate indices and rainfall and that of its extremes in Ghana. This is however relevant to expand our knowledge on the SST forcing on rainfall variability in the region. Moreover, the insignificant correlations observed between the Nino3.4, IOD and AMO indices and the daily indices thus, CDD and CWD prompts future researches to explore inter-seasonal relationships between these indices to ascertain whether the daily rainfall indices are more driven by seasonal scale variability than the inter-annual variability investigated.

7.2.2 Recommendations For Policy Makers

Although satellite-based rainfall products revealed considerably good skill in capturing the seasonal and annual rainfall variability in Ghana, they showed a major challenge in the coastal zones. This study therefore recommends that, for climate impact studies over the coastal zone of Ghana on seasonal to annual scales, the gauge-only (GPCP and CRU) rainfall products should be explored as they performed very well on both time scales in this zone. TRMM and TAMSAT are recommended for seasonal rainfall studies whereas CHIRPS and CRU are recommended for annual climate impact studies in the region.

It is recommendable for satellite-based rainfall products to include information on the number of gauge stations that were available for the interpolation process as this would allow future validation studies to further investigate the impacts of the gauge number on the performance of these products in various locations. Furthermore, the dependence of the performance of satellite-based rainfall products on the scale and location revealed in this study implies that decisions on which satellite products to apply for climate impact studies should not be one taken in a hurry. It would be essential to assess the products over the region and time scale they are to be applied so as to understand their potencies before applications. For instance, the ability of the new IMERG GPM product to effectively capture the flood case investigated in this study partly infers its viability for use in flood monitoring studies in the region.

The decreasing trends in wet indices especially in the Volta lake of Ghana raises major concerns as this implies, if appropriate measures are not taken, the lake is liable to significantly dry out in the future. This situation would have severe implications on especially the hydro-electric power generation, fishing, irrigation and water supply. The study therefore recommends Government to consider investing into alternatives such as solar PVs and wind power generations in the future. Again, future researches on the hydro-climatic modelling in the Volta river basins is recommended to better understand the water level drop and its projections to help in decision making concerning this situation.

In addition, the results on the decreasing wet indices over the northern part of the country imply that farming, which is mainly dependent on rainfall and the major source of livelihood of these parts of the country would be highly impacted. It would be a wise decision to invest in rainfall harvesting to afford farmers

enough time for crop production and better crop yields. Increased flood case studies are recommended to facilitate better flood risk management strategies so as to improve drainage systems, proper land use practices among others in the country.

Bibliography

Adler, R. F., Gu, G., Sapiano, M., Wang, J.-J. and Huffman, G. J. (2017),

‘Global precipitation: Means, variations and trends during the satellite era (1979–2014)’, *Surveys in Geophysics* **38**(4), 679–699.

Adler, R. F., Huffman, G. J., Chang, A., Ferraro, R., Xie, P.-P., Janowiak, J., Rudolf, B., Schneider, U., Curtis, S., Bolvin, D. et al. (2003), ‘The version-2 global precipitation climatology project (gpcp) monthly precipitation analysis (1979-present)’, *Journal of hydrometeorology* **4**(6), 1147–1167.

Adu-Prah, S., Appiah-Opoku, S. and Aboagye, D. (2017), ‘Spatiotemporal evidence of recent climate variability in Ghana’, *African Geographical Review* pp. 1–19.

AghaKouchak, A., Behrangi, A., Sorooshian, S., Hsu, K. and Amitai, E. (2011), ‘Evaluation of satellite-retrieved extreme precipitation rates across the central United States’, *Journal of Geophysical Research: Atmospheres* **116**(D2).

Aguilar, E., Aziz Barry, A., Brunet, M., Ekan, L., Fernandes, A., Massoukina, M., Mbah, J., Mhanda, A., Do Nascimento, D., Peterson, T. et al. (2009),

'Changes in temperature and precipitation extremes in western central africa, guinea conakry, and zimbabwe, 1955–2006', *Journal of Geophysical Research: Atmospheres* **114**(D2).

Alexander, L., Zhang, X., Peterson, T., Caesar, J., Gleason, B., Klein Tank, A., Haylock, M., Collins, D., Trewin, B., Rahimzadeh, F. et al. (2006), 'Global observed changes in daily climate extremes of temperature and precipitation', *Journal of Geophysical Research: Atmospheres* **111**(D5).

Ali, A., Amani, A., Diedhiou, A. and Lebel, T. (2005), 'Rainfall estimation in the sahel. part ii: Evaluation of rain gauge networks in the cilss countries and objective intercomparison of rainfall products', *Journal of Applied Meteorology* **44**(11), 1707–1722.

Amekudzi, L. K., Osei, M. A., Atiah, W. A., Aryee, J. N., Ahiataku, M. A., Quansah, E., Preko, K., Danuor, S. K. and Fink, A. H. (2016), 'Validation of trmm and fews satellite rainfall estimates with rain gauge measurement over ashanti region, ghana'.

Amekudzi, L. K., Yamba, E. I., Preko, K., Asare, E. O., Aryee, J., Baidu, M. and Codjoe, S. N. (2015), 'Variabilities in rainfall onset, cessation and length of rainy season for the various agro-ecological zones of ghana', *Climate* **3**(2), 416– 434.

Armah, F. A., Yawson, D. O., Yengoh, G. T., Odoi, J. O. and Afrifa, E. K. (2010), 'Impact of flods on livelihoods and vulnerability of natural resource dependent communities in northern ghana', *Water* **2**(2), 120–139.

Aryee, J., Amekudzi, L., Atiah, W., Osei, M. and Agyapong, E. (2018), 'Overview of surface to near-surface atmospheric profiles over selected domain during the qweci project', *Meteorology and Atmospheric Physics* pp. 1–15.

Aryee, J., Amekudzi, L., Quansah, E., Klutse, N., Atiah, W. and Yorke, C. (2017), 'Development of high spatial resolution rainfall data for ghana', *International Journal of Climatology*.

Asadullah, A., McIntyre, N. and Kigobe, M. (2008), 'Evaluation of five satellite products for estimation of rainfall over uganda/evaluation de cinq produits satellitaires pour l'estimation des précipitations en ouganda', *Hydrological Sciences Journal* **53**(6), 1137–1150.

Asante, F. A. and Amuakwa-Mensah, F. (2014), 'Climate change and variability in ghana: Stocktaking', *Climate* **3**(1), 78–99.

Asumadu-Sarkodie, S., Owusu, P. A. and Rufangura, P. (2015), 'Impact analysis of flood in accra, ghana', *Advances in Applied Science Research*.

Bader, J. (2005), 'The role of the tropical indian ocean in global climate'.

Bader, J. and Latif, M. (2003a), 'The impact of decadal-scale indian ocean sea surface temperature anomalies on sahelian rainfall and the north atlantic oscillation', *Geophysical Research Letters* **30**(22).

Bader, J. and Latif, M. (2003b), 'The impact of decadal-scale indian ocean sea surface temperature anomalies on sahelian rainfall and the north atlantic oscillation', *Geophysical Research Letters* **30**(22).

- Bahaga, T., Mengistu Tsidu, G., Kucharski, F. and Diro, G. (2015), 'Potential predictability of the sea-surface temperature forced equatorial east african short rains interannual variability in the 20th century', *Quarterly Journal of the Royal Meteorological Society* **141**(686), 16–26.
- Baidu, M., Amekudzi, L. K., Aryee, J. N. and Annor, T. (2017), 'Assessment of long-term spatio-temporal rainfall variability over ghana using wavelet analysis', *Climate* **5**(2), 30.
- Balas, N., Nicholson, S. and Klotter, D. (2007), 'The relationship of rainfall variability in west central africa to sea-surface temperature fluctuations', *International journal of climatology* **27**(10), 1335–1349.
- Barnston, A. G. and Tippett, M. K. (2013), 'Predictions of nino3.4 sst in cfsv1 and cfsv2: a diagnostic comparison', *Climate dynamics* **41**(5-6), 1615–1633.
- Barrios, S., Bertinelli, L. and Strobl, E. (2010), 'Trends in rainfall and economic growth in africa: A neglected cause of the african growth tragedy', *The Review of Economics and Statistics* **92**(2), 350–366.
- Bartholomew, M. J. (2016), Impact disdrometers instrument handbook, Technical report, DOE Office of Science Atmospheric Radiation Measurement (ARM) Program (United States).
- Batisani, N. and Yarnal, B. (2010), 'Rainfall variability and trends in semi-arid botswana: implications for climate change adaptation policy', *Applied Geography* **30**(4), 483–489.

- Beer, T., Greenhut, G. K. and Tandoh, S. (1977), 'Relations between the z criterion for the subtropical high, hadley cell parameters and the rainfall in northern ghana', *Monthly Weather Review* **105**(7), 849–855.
- Berry, G. J. and Thorncroft, C. (2005), 'Case study of an intense african easterly wave', *Monthly Weather Review* **133**(4), 752–766.
- Blain, G. C. (2015), 'The influence of nonlinear trends on the power of the trendfree pre-whitening approach', *Acta Scientiarum. Agronomy* **37**(1), 21–28.
- Bryson, R. A. (1973), 'Drought in sahelia: Who or what is to blame', *Ecologist* **3**(10), 366–371.
- Camberlin, P., Janicot, S. and Pocard, I. (2001a), 'Seasonality and atmospheric dynamics of the teleconnection between african rainfall and tropical sea-surface temperature: Atlantic vs. enso', *International Journal of Climatology* **21**(8), 973–1005.
- Camberlin, P., Janicot, S. and Pocard, I. (2001b), 'Seasonality and atmospheric dynamics of the teleconnection between african rainfall and tropical sea-surface temperature: Atlantic vs. enso', *International Journal of Climatology* **21**(8), 973–1005.
- Cetrone, J. and Houze, R. A. (2009), 'Anvil clouds of tropical mesoscale convective systems in monsoon regions', *Quarterly Journal of the Royal Meteorological Society* **135**(639), 305–317.
- Change, I. C. (2007), 'The fourth assessment report of the intergovernmental panel on climate change', *Geneva, Switzerland* .

- Chen, H.-M., Arora, M. K. and Varshney, P. K. (2003), 'Mutual information based image registration for remote sensing data', *International Journal of Remote Sensing* **24**(18), 3701–3706.
- Clark, C. O., Webster, P. J. and Cole, J. E. (2003), 'Interdecadal variability of the relationship between the indian ocean zonal mode and east african coastal rainfall anomalies', *Journal of Climate* **16**(3), 548–554.
- Cotton, W., McAnelly, R. and Ashby, C. T. (n.d.), 'A modelling-based methodology for determining extreme precipitation potential at high elevations in colorado'.
- Dashkhuu, D., Kim, J. P., Chun, J. A. and Lee, W.-S. (2015), 'Long-term trends in daily temperature extremes over mongolia', *Weather and Climate Extremes* **8**, 26–33.
- DeLonge, M. S., Fuentes, J. D., Chan, S., Kucera, P. A., Joseph, E., Gaye, A. T. and Daouda, B. (2010), 'Attributes of mesoscale convective systems at the land-ocean transition in senegal during nasa african monsoon multidisciplinary analyses 2006', *Journal of Geophysical Research: Atmospheres* **115**(D10).
- Desbois, M., Kayiranga, T., Gnamien, B., Guessous, S. and Picon, L. (1988), 'Characterization of some elements of the sahelian climate and their interannual variations for july 1983, 1984 and 1985 from the analysis of meteosat isccp data', *Journal of Climate* **1**(9), 867–904.
- Desmet, P. (1997), 'Effects of interpolation errors on the analysis of DEMs', *Earth Surface Processes and Landforms: The Journal of the British Geomorphological Group* **22**(6), 563–580.

Dezfuli, A. K., Ichoku, C. M., Huffman, G. J., Selker, J. S. and Hochreutener, R.

(2016), Comparing imerg-v3 with gauge-based precipitation data in africa, *in* 'AGU Fall Meeting Abstracts'.

Dezfuli, A. K., Ichoku, C. M., Mohr, K. I. and Huffman, G. J. (2017), 'Precipitation characteristics in west and east africa from satellite and in situ observations', *Journal of Hydrometeorology* **18**(6), 1799–1805.

Diatta, S. and Fink, A. H. (2014), 'Statistical relationship between remote climate indices and west african monsoon variability', *International Journal of Climatology* **34**(12), 3348–3367.

Diedhiou, A., Janicot, S., Viltard, A., De Felice, P. and Laurent, H. (1999), 'Easterly wave regimes and associated convection over west africa and tropical atlantic: Results from the ncep/ncar and ecmwf reanalyses', *Climate Dynamics* **15**(11), 795–822.

Dinku, T., Ceccato, P., Grover-Kopec, E., Lemma, M., Connor, S. and Ropelewski, C. (2007), 'Validation of satellite rainfall products over east africa's complex topography', *International Journal of Remote Sensing* **28**(7), 1503–1526.

Dinku, T., Chidzambwa, S., Ceccato, P., Connor, S. and Ropelewski, C. (2008), 'Validation of high-resolution satellite rainfall products over complex terrain', *International Journal of Remote Sensing* **29**(14), 4097–4110.

dos Santos, C. A. C., de Brito, J. I., Ju'nior, C. H. d. S. and Dantas, L. G. (2012), 'Trends in precipitation extremes over the northern part of brazil from era40 dataset (tendências nos extremos de precipita,caõ sobre a parte norte do brasil

- através dos dados do era40)', *Revista Brasileira de Geografia Física* **5**(4), 836–851.
- Dos Santos, C. A., Neale, C. M., Rao, T. V. and da Silva, B. B. (2011), 'Trends in indices for extremes in daily temperature and precipitation over utah, usa', *International Journal of climatology* **31**(12), 1813–1822.
- Duvel, J. P. (1990), 'Convection over tropical africa and the atlantic ocean during northern summer. part ii: Modulation by easterly waves', *Monthly Weather Review* **118**(9), 1855–1868.
- Ebert, E. E. and Manton, M. J. (1998a), 'Performance of satellite rainfall estimation algorithms during toga coare', *Journal of the Atmospheric Sciences* **55**(9), 1537–1557.
- Ebert, E. E. and Manton, M. J. (1998b), 'Performance of satellite rainfall estimation algorithms during toga coare', *Journal of the Atmospheric Sciences* **55**(9), 1537–1557.
- Ebert, E. E., Manton, M. J., Arkin, P. A., Allam, R. J., Holpin, C. E. and Gruber, A. (1996), 'Results from the gpcp algorithm intercomparison programme', *Bulletin of the American Meteorological Society* **77**(12), 2875–2887.
- Eldridge, R. (1958), 'A synoptic study of west african disturbance lines', *Quarterly Journal of the Royal Meteorological Society* **84**(362), 468–469.
- Eltahir, E. A. and Gong, C. (1996), 'Dynamics of wet and dry years in west africa', *Journal of Climate* **9**(5), 1030–1042.

- Enfield, D. B., Mestas-Nun̄ez, A. M. and Trimble, P. J. (2001), 'The atlantic multidecadal oscillation and its relation to rainfall and river flows in the continental us', *Geophysical Research Letters* **28**(10), 2077–2080.
- Ermert, V., Fink, A. H., Morse, A. P., Jones, A. E., Paeth, H., Di Giuseppe, F. and Tompkins, A. M. (2012), 'Development of dynamical weather-disease models to project and forecast malaria in africa', *Malaria Journal* **11**(1), P133.
- Feidas, H. (2010), 'Validation of satellite rainfall products over greece', *Theoretical and Applied climatology* **99**(1-2), 193–216.
- Fensholt, R. and Rasmussen, K. (2011), 'Analysis of trends in the sahelian 'rainuse efficiency' using gimms ndvi, rfe and gpcp rainfall data', *Remote Sensing of Environment* **115**(2), 438–451.
- Fink, A. H., Engel, T., Ermert, V., van der Linden, R., Schneidewind, M., Redl, R., Afiesimama, E., Thiaw, W. M., Yorke, C., Evans, M. et al. (2017), 'Mean climate and seasonal cycle', *Meteorology of Tropical West Africa: The Forecasters' Handbook* pp. 1–39.
- Fink, A., Vincent, D. and Ermert, V. (2006), 'Rainfall types in the west african sudanian zone during the summer monsoon 2002', *Monthly weather review* **134**(8), 2143–2164.
- Fontaine, B. and Bigot, S. (1993), 'West african rainfall deficits and sea surface temperatures', *International Journal of Climatology* **13**(3), 271–285.
- Fontaine, B. and Janicot, S. (1996a), 'Sea surface temperature fields associated with west african rainfall anomaly types', *Journal of climate* **9**(11), 2935–2940.

- Fontaine, B. and Janicot, S. (1996b), 'Sea surface temperature fields associated with west african rainfall anomaly types', *Journal of climate* **9**(11), 2935–2940.
- Frank, W. M. (1978), 'The life cycles of gate convective systems', *Journal of the Atmospheric Sciences* **35**(7), 1256–1264.
- Fritsch, J. and Forbes, G. (2001), Mesoscale convective systems, in 'Severe convective storms', Springer, pp. 323–357.
- Funk, C., Peterson, P., Landsfeld, M., Pedreros, D., Verdin, J., Shukla, S., Husak, G., Rowland, J., Harrison, L., Hoell, A. et al. (2015), 'The climate hazards infrared precipitation with stations—a new environmental record for monitoring extremes', *Scientific data* **2**, 150066.
- Gadgil, S., Vinayachandran, P., Francis, P. and Gadgil, S. (2004), 'Extremes of the indian summer monsoon rainfall, enso and equatorial indian ocean oscillation', *Geophysical Research Letters* **31**(12).
- Gaona, M. R., Overeem, A., Leijnse, H. and Uijlenhoet, R. (2016), 'First-year evaluation of gpm rainfall over the netherlands: Imerg day 1 final run (v03d)', *Journal of Hydrometeorology* **17**(11), 2799–2814.
- Gebremichael, M., Krajewski, W. F., Morrissey, M. L., Huffman, G. J. and Adler, R. F. (2005), 'A detailed evaluation of gpcp 1 daily rainfall estimates over the mississippi river basin', *Journal of Applied Meteorology* **44**(5), 665–681.
- Giannini, A., Saravanan, R. and Chang, P. (2003), 'Oceanic forcing of sahel rainfall on interannual to interdecadal time scales', *Science* **302**(5647), 1027–1030.
- Greenhut, G. K. (1977), 'A new criterion for locating the subtropical high in west africa', *Journal of Applied Meteorology* **16**(7), 727–734.

- Harris, I., Jones, P., Osborn, T. and Lister, D. (2014), 'Updated high-resolution grids of monthly climatic observations—the cru ts3. 10 dataset', *International Journal of Climatology* **34**(3), 623–642.
- Hastenrath, S. (1990), 'Decadal-scale changes of the circulation in the tropical atlantic sector associated with sahel drought', *International Journal of Climatology* **10**(5), 459–472.
- Hodges, K. I. and Thorncroft, C. (1997), 'Distribution and statistics of african mesoscale convective weather systems based on the isccp meteosat imagery', *Monthly Weather Review* **125**(11), 2821–2837.
- Hou, A. Y., Kakar, R. K., Neeck, S., Azarbarzin, A. A., Kummerow, C. D., Kojima, M., Oki, R., Nakamura, K. and Iguchi, T. (2014), 'The global precipitation measurement mission', *Bulletin of the American Meteorological Society* **95**(5), 701–722.
- Houze, R. A. (1989), 'Observed structure of mesoscale convective systems and implications for large-scale heating', *Quarterly Journal of the Royal Meteorological Society* **115**(487), 425–461.
- Houze, R. A. (2004), 'Mesoscale convective systems', *Reviews of Geophysics* **42**(4).
- Huang, B., Thorne, P. W., Banzon, V. F., Boyer, T., Chepurin, G., Lawrimore, J. H., Menne, M. J., Smith, T. M., Vose, R. S. and Zhang, H.-M. (2017), 'Extended reconstructed sea surface temperature, version 5 (ersstv5): upgrades, validations, and intercomparisons', *Journal of Climate* **30**(20), 8179–8205.

- Huffman, G., Bolvin, D. and Adler, R. (2011), 'Gpcp version 2.2 combined precipitation data set', *WDC-A, NCDC, Asheville, NC*.
- Huffman, G. J., Adler, R. F., Arkin, P., Chang, A., Ferraro, R., Gruber, A., Janowiak, J., McNab, A., Rudolf, B. and Schneider, U. (1997), 'The global precipitation climatology project (gpcp) combined precipitation dataset'.
- Huffman, G. J., Bolvin, D. T., Nelkin, E. J., Wolff, D. B., Adler, R. F., Gu, G., Hong, Y., Bowman, K. P. and Stocker, E. F. (2007), 'The trmm multisatellite precipitation analysis (tmpa): Quasi-global, multiyear, combined-sensor precipitation estimates at fine scales', *Journal of Hydrometeorology* **8**(1), 38–55.
- Issa L'el'e, M. and Lamb, P. J. (2010), 'Variability of the intertropical front (itf) and rainfall over the west african sudan-sahel zone', *Journal of Climate* **23**(14), 3984–4004.
- Jamandre, C. and Narisma, G. (2013), 'Spatio-temporal validation of satellitebased rainfall estimates in the philippines', *Atmospheric research* **122**, 599–608.
- Janicot, S. (1992), 'Spatiotemporal variability of west african rainfall. part ii: Associated surface and airmass characteristics', *Journal of Climate* **5**(5), 499–511.
- Janicot, S., Harzallah, A., Fontaine, B. and Moron, V. (1998), 'West african monsoon dynamics and eastern equatorial atlantic and pacific sst anomalies (1970–88)', *Journal of Climate* **11**(8), 1874–1882.

- Janicot, S., Moron, V. and Fontaine, B. (1996), 'Sahel droughts and enso dynamics', *Geophysical Research Letters* **23**(5), 515–518.
- Jolliffe, I. T. (1986), Principal component analysis and factor analysis, in 'Principal component analysis', Springer, pp. 115–128.
- Joss, J., Waldvogel, A. and Collier, C. (1990), Precipitation measurement and hydrology, in 'Radar in meteorology', Springer, pp. 577–606.
- Joyce, R. J., Janowiak, J. E., Arkin, P. A. and Xie, P. (2004), 'Cmorph: A method that produces global precipitation estimates from passive microwave and infrared data at high spatial and temporal resolution', *Journal of Hydrometeorology* **5**(3), 487–503.
- Kemausuor, F., Dwamena, E., Bart-Plange, A. and Kyei-Baffour, N. (2011), 'Farmers' perception of climate change in the ejura-sekyedumase district of ghana', *ARPN Journal of Agricultural and Biological Science* **6**(19), 26–37.
- Kidd, C., Kniveton, D. R., Todd, M. C. and Bellerby, T. J. (2003), 'Satellite rainfall estimation using combined passive microwave and infrared algorithms', *Journal of Hydrometeorology* **4**(6), 1088–1104.
- Kidd, C. and Levizzani, V. (2011), 'Status of satellite precipitation retrievals', *Hydrology and Earth System Sciences* **15**(4), 1109–1116.
- Klein Tank, A., Peterson, T., Quadir, D., Dorji, S., Zou, X., Tang, H., Santhosh, K., Joshi, U., Jaswal, A., Kolli, R. et al. (2006), 'Changes in daily temperature and

- precipitation extremes in central and south asia', *Journal of Geophysical Research: Atmospheres* **111**(D16).
- Knippertz, P., Coe, H., Chiu, J. C., Evans, M. J., Fink, A. H., Kalthoff, N., Liousse, C., Mari, C., Allan, R. P., Brooks, B. et al. (2015a), 'The dacciya project: Dynamics–aerosol–chemistry–cloud interactions in west africa', *Bulletin of the American Meteorological Society* **96**(9), 1451–1460.
- Knippertz, P., Coe, H., Chiu, J. C., Evans, M. J., Fink, A. H., Kalthoff, N., Liousse, C., Mari, C., Allan, R. P., Brooks, B. et al. (2015b), 'The dacciya project: Dynamics–aerosol–chemistry–cloud interactions in west africa', *Bulletin of the American Meteorological Society* **96**(9), 1451–1460.
- Knippertz, P. and Fink, A. H. (2008), 'Dry-season precipitation in tropical west africa and its relation to forcing from the extratropics', *Monthly Weather Review* **136**(9), 3579–3596.
- Knippertz, P., Fink, A. H., Deroubaix, A., Morris, E., Tocquer, F., Evans, M. J., Flamant, C., Gaetani, M., Lavaysse, C., Mari, C. et al. (2017), 'A meteorological and chemical overview of the dacciya field campaign in west africa in june–july 2016', *Atmospheric Chemistry and Physics* **17**(17), 10893–10918.
- Kunstmann, H. and Jung, G. (2005a), 'Impact of regional climate change on water availability in the volta basin of west africa', *IAHS publication* (295), 75–85.
- Kunstmann, H. and Jung, G. (2005b), Impact of regional climate change on water availability in the volta basin of west africa. regional hydrological impacts of climate variability and change, in 'Proceedings of symposium S6 for the seventh IAHS scientific assembly. Foz de Iguacu, Brazil'.

- Lacombe, G., McCartney, M. and Forkuor, G. (2012), 'Drying climate in Ghana over the period 1960–2005: evidence from the resampling-based Mann-Kendall test at local and regional levels', *Hydrological Sciences Journal* **57**(8), 1594–1609.
- Laing, A. G. and Fritsch, J. M. (1993), 'Mesoscale convective complexes in Africa', *Monthly Weather Review* **121**(8), 2254–2263.
- Lamb, P. J. (1978a), 'Case studies of tropical Atlantic surface circulation patterns during recent sub-Saharan weather anomalies: 1967 and 1968', *Monthly Weather Review* **106**(4), 482–491.
- Lamb, P. J. (1978b), 'Large-scale tropical Atlantic surface circulation patterns associated with sub-Saharan weather anomalies', *Tellus* **30**(3), 240–251.
- Lamb, P. J. and Pepler, R. A. (1992a), 'Further case studies of tropical Atlantic surface atmospheric and oceanic patterns associated with sub-Saharan drought', *Journal of Climate* **5**(5), 476–488.
- Lamb, P. J. and Pepler, R. A. (1992b), 'Further case studies of tropical Atlantic surface atmospheric and oceanic patterns associated with sub-Saharan drought', *Journal of Climate* **5**(5), 476–488.
- Le Barbé, L., Lebel, T. and Tapsoba, D. (2002), 'Rainfall variability in West Africa during the years 1950–90', *Journal of Climate* **15**(2), 187–202.
- Lensky, I. M. and Rosenfeld, D. (2003), 'Satellite-based insights into precipitation formation processes in continental and maritime convective clouds at nighttime', *Journal of Applied Meteorology* **42**(9), 1227–1233.

- Li, N., Tang, G., Zhao, P., Hong, Y., Gou, Y. and Yang, K. (2017), 'Statistical assessment and hydrological utility of the latest multi-satellite precipitation analysis imerg in ganjiang river basin', *Atmospheric Research* **183**, 212–223.
- Losada, T., Rodriguez-Fonseca, B., Mohino, E., Bader, J., Janicot, S. and Mechoso, C. (n.d.), 'Impact of tropical sst anomalies on west african rainfall.'
- Lough, J. (1986a), 'Tropical atlantic sea surface temperatures and rainfall variations in subsaharan africa', *Monthly Weather Review* **114**(3), 561–570.
- Lough, J. (1986b), 'Tropical atlantic sea surface temperatures and rainfall variations in subsaharan africa', *Monthly Weather Review* **114**(3), 561–570.
- Love, T. B., Kumar, V., Xie, P. and Thiaw, W. (2004), P5. 4 a 20-year daily africa precipitation climatology using satellite and gauge data, in '14th Conference on Applied Climatology, Seattle, WA'.
- Lu, J. (2009), 'The dynamics of the indian ocean sea surface temperature forcing of sahel drought', *Climate dynamics* **33**(4), 445–460.
- Lund, R. and Reeves, J. (2002), 'Detection of undocumented changepoints: A revision of the two-phase regression model', *Journal of Climate* **15**(17), 2547–2554.
- Machiwal, D. and Jha, M. K. (2012), Analysis of trend and periodicity in longterm annual rainfall time series of nigeria, in 'Hydrologic Time Series Analysis: Theory and Practice', Springer, pp. 249–272.
- Maggioni, V., Meyers, P. C. and Robinson, M. D. (2016), 'A review of merged

- high-resolution satellite precipitation product accuracy during the tropical rainfall measuring mission (trmm) era', *Journal of Hydrometeorology* **17**(4), 1101– 1117.
- Maidment, R. I., Grimes, D., Black, E., Tarnavsky, E., Young, M., Greatrex, H., Allan, R. P., Stein, T., Nkonde, E., Senkunda, S. et al. (2017), 'A new, longterm daily satellite-based rainfall dataset for operational monitoring in africa', *Scientific data* **4**, 170063.
- Manzanas, R., Amekudzi, L., Preko, K., Herrera, S. and Gutierrez, J. (2014a), 'A comparison of methods to determine the onset of the growing season in nigeria', *Climate Change* **124**, 805–819.
- Manzanas, R., Amekudzi, L., Preko, K., Herrera, S. and Gutierrez, J. (2014b), 'Precipitation variability and trends in ghana: An intercomparison of observational and reanalysis products', *Climatic change* **124**(4), 805–819.
- Maranan, M., Fink, A. and Knippertz, P. (2018), 'Rainfall types over southern west africa: Objective identification, climatology and synoptic environment', *Quarterly Journal of the Royal Meteorological Society* . In Press.
- Mathon, V. and Laurent, H. (2001), 'Life cycle of sahelian mesoscale convective cloud systems', *Quarterly Journal of the Royal Meteorological Society* **127**(572), 377–406.
- Mathon, V., Laurent, H. and Lebel, T. (2002), 'Mesoscale convective system rainfall in the sahel', *Journal of applied meteorology* **41**(11), 1081–1092.

- McCollum, J. R., Krajewski, W. F., Ferraro, R. R. and Ba, M. B. (2002), 'Evaluation of biases of satellite rainfall estimation algorithms over the continental united states', *Journal of Applied Meteorology* **41**(11), 1065–1080.
- Morse, A., Caminade, C., Jones, A., MacLeod, D. and Heath, A. (2012), The qweci project: seamlessly linking climate science to society, in 'EGU General Assembly Conference Abstracts', Vol. 14, p. 1559.
- Nicholson, S. E. (1980), 'The nature of rainfall fluctuations in subtropical west africa', *Monthly Weather Review* **108**(4), 473–487.
- Nicholson, S. E. (1981), 'Rainfall and atmospheric circulation during drought periods and wetter years in west africa', *Monthly Weather Review* **109**(10), 2191– 2208.
- Nicholson, S. E. (1993), 'An overview of african rainfall fluctuations of the last decade', *Journal of climate* **6**(7), 1463–1466.
- Nicholson, S. E. (2000), 'The nature of rainfall variability over africa on time scales of decades to millenia', *Global and planetary change* **26**(1), 137–158.
- Nicholson, S. E., Some, B., McCollum, J., Nelkin, E., Klotter, D., Berte, Y., Diallo, B., Gaye, I., Kpabeba, G., Ndiaye, O. et al. (2003), 'Validation of trmm and other rainfall estimates with a high-density gauge dataset for west africa. part i: Validation of gpcc rainfall product and pre-trmm satellite and blended products', *Journal of Applied Meteorology* **42**(10), 1337–1354.

- Nicholson, S. E. and Webster, P. J. (2007), 'A physical basis for the interannual variability of rainfall in the sahel', *Quarterly Journal of the Royal Meteorological Society* **133**(629), 2065–2084.
- Ofori-Sarpong, E. (2001), 'Impact of climate change on agriculture and farmers coping strategies in the upper east region of ghana', *West African Journal of Applied Ecology* **2**, 21–35.
- Olivier, R. and Hanqiang, C. (2012), 'Nearest neighbor value interpolation', *arXiv preprint arXiv:1211.1768* .
- Opoku-Ankomah, Y. and Cordery, I. (1994), 'Atlantic sea surface temperatures and rainfall variability in ghana', *Journal of Climate* **7**(4), 551–558.
- Owusu, K. and Waylen, P. (2009), 'Trends in spatio-temporal variability in annual rainfall in ghana (1951-2000)', *Weather* **64**(5), 115–120.
- Owusu, K., Waylen, P. and Qiu, Y. (2008), 'Changing rainfall inputs in the volta basin: implications for water sharing in ghana', *GeoJournal* **71**(4), 201–210.
- Owusu, K. and Waylen, P. R. (2013a), 'The changing rainy season climatology of mid-ghana', *Theoretical and Applied Climatology* **112**(3-4), 419–430.
- Owusu, K. and Waylen, P. R. (2013b), 'The changing rainy season climatology of mid-ghana', *Theoretical and applied climatology* **112**(3-4), 419–430.
- Paeth, H. and Hense, A. (2004), 'Sst versus climate change signals in west african rainfall: 20th-century variations and future projections', *Climatic Change* **65**(1), 179–208.

- Palmer, T. (1986), 'Influence of the atlantic, pacific and indian oceans on sahel rainfall', *Nature* **322**(6076), 251.
- Payne, S. W. and McGarry, M. M. (1977), 'The relationship of satellite inferred convective activity to easterly waves over west africa and the adjacent ocean during phase iii of gate', *Monthly Weather Review* **105**(4), 413–420.
- Pfeifroth, U., Trentmann, J., Fink, A. H. and Ahrens, B. (2016), 'Evaluating satellite-based diurnal cycles of precipitation in the african tropics', *Journal of Applied Meteorology and Climatology* **55**(1), 23–39.
- Pohlert, T. (2016), 'Non-parametric trend tests and change-point detection', *CC BY-ND 4*.
- Polcher, J. (1995), 'Sensitivity of tropical convection to land surface processes', *Journal of the atmospheric sciences* **52**(17), 3143–3161.
- Rauber, R. M., Olthoff, L. S., Ramamurthy, M. K. and Kunkel, K. E. (2000), 'The relative importance of warm rain and melting processes in freezing precipitation events', *Journal of Applied Meteorology* **39**(7), 1185–1195.
- Richardson, M. (2009), 'Principal component analysis', **6**, 16.
- Roca, R., Chambon, P., Jobard, I., Kirstetter, P.-E., Gosset, M. and Berg`es, J. C. (2010), 'Comparing satellite and surface rainfall products over west africa at meteorologically relevant scales during the amma campaign using error estimates', *Journal of Applied Meteorology and Climatology* **49**(4), 715–731.
- Rowell, D. P., Folland, C. K., Maskell, K. and Ward, M. N. (1995), 'Variability of summer rainfall over tropical north africa (1906–92): Observations and

- modelling', *Quarterly Journal of the Royal Meteorological Society* **121**(523), 669– 704.
- Rowell, D. P. and Milford, J. R. (1993), 'On the generation of african squall lines', *Journal of Climate* **6**(6), 1181–1193.
- Sanogo, S., Fink, A. H., Omotosho, J. A., Ba, A., Redl, R. and Ermert, V. (2015), 'Spatio-temporal characteristics of the recent rainfall recovery in west africa', *International Journal of Climatology* **35**(15), 4589–4605.
- Schneider, U., Becker, A., Finger, P., Meyer-Christoffer, A., Ziese, M. and Rudolf, B. (2014), 'Gpcc's new land surface precipitation climatology based on qualitycontrolled in situ data and its role in quantifying the global water cycle', *Theoretical and Applied Climatology* **115**(1-2), 15–40.
- Schneider, U., Fuchs, T., Meyer-Christoffer, A. and Rudolf, B. (2008), 'Global precipitation analysis products of the gpcc', *Global Precipitation Climatology Centre (GPCC), DWD, Internet Publikation* **112**.
- Seleshi, Y. and Camberlin, P. (2006), 'Recent changes in dry spell and extreme rainfall events in ethiopia', *Theoretical and Applied Climatology* **83**(1-4), 181–191.
- Seleshi, Y. and Zanke, U. (2004), 'Recent changes in rainfall and rainy days in ethiopia', *International journal of climatology* **24**(8), 973–983.
- Shongwe, M. E., Van Oldenborgh, G., Van Den Hurk, B., De Boer, B., Coelho, C. and Van Aalst, M. (2009), 'Projected changes in mean and extreme precipitation in

africa under global warming. part i: Southern africa', *Journal of climate* **22**(13), 3819–3837.

Smith, W. and Wessel, P. (1990), 'Gridding with continuous curvature splines in tension', *Geophysics* **55**(3), 293–305.

Snyder, A. D., Pu, Z. and Zhu, Y. (2010), 'Tracking and verification of east atlantic tropical cyclone genesis in the ncep global ensemble: Case studies during the nasa african monsoon multidisciplinary analyses', *Weather and Forecasting* **25**(5), 1397–1411.

Sohn, B., Han, H.-J. and Seo, E.-K. (2010), 'Validation of satellite-based highresolution rainfall products over the korean peninsula using data from a dense rain gauge network', *Journal of Applied Meteorology and Climatology* **49**(4), 701–714.

Strangeways, I. (2006), *Precipitation: theory, measurement and distribution*, Cambridge University Press.

Strangeways, I. (2010), 'A history of rain gauges', *Weather* **65**(5), 133–138.

Tang, G., Zeng, Z., Long, D., Guo, X., Yong, B., Zhang, W. and Hong, Y. (2016), 'Statistical and hydrological comparisons between trmm and gpm level-3 products over a midlatitude basin: Is day-1 imerg a good successor for tmpa 3b42v7?', *Journal of Hydrometeorology* **17**(1), 121–137.

Tapiador, F., Checa, R. and De Castro, M. (2010), 'An experiment to measure the spatial variability of rain drop size distribution using sixteen laser disdrometers', *Geophysical Research Letters* **37**(16).

- Tapiador, F. J., Turk, F. J., Petersen, W., Hou, A. Y., Garc'ia-Ortega, E., Machado, L. A., Angelis, C. F., Salio, P., Kidd, C., Huffman, G. J. et al. (2012), 'Global precipitation measurement: Methods, datasets and applications', *Atmospheric Research* **104**, 70–97.
- Tarhule, A. and Woo, M.-K. (1998), 'Changes in rainfall characteristics in northern nigeria', *International Journal of Climatology* **18**(11), 1261–1271.
- Tarnavsky, E., Grimes, D., Maidment, R., Black, E., Allan, R. P., Stringer, M., Chadwick, R. and Kayitakire, F. (2014), 'Extension of the tamsat satellitebased rainfall monitoring over africa and from 1983 to present', *Journal of Applied Meteorology and Climatology* **53**(12), 2805–2822.
- Taylor, C. M. and Lebel, T. (1998), 'Observational evidence of persistent convective-scale rainfall patterns', *Monthly Weather Review* **126**(6), 1597–1607.
- Thiemig, V., Rojas, R., Zambrano-Bigiarini, M., Levizzani, V. and De Roo, A. (2012), 'Validation of satellite-based precipitation products over sparsely gauged african river basins', *Journal of Hydrometeorology* **13**(6), 1760–1783.
- Thorncroft, C. and Hodges, K. (2001), 'African easterly wave variability and its relationship to atlantic tropical cyclone activity', *Journal of Climate* **14**(6), 1166–1179.
- Thorne, V., Coakeley, P., Grimes, D. and Dugdale, G. (2001), 'Comparison of tamsat and cpc rainfall estimates with raingauges, for southern africa', *International Journal of Remote Sensing* **22**(10), 1951–1974.

- Tokay, A., Petersen, W. A., Gatlin, P. and Wingo, M. (2013), 'Comparison of raindrop size distribution measurements by collocated disdrometers', *Journal of Atmospheric and Oceanic Technology* **30**(8), 1672–1690.
- Trenberth, K. E. (2011), 'Changes in precipitation with climate change', *Climate Research* **47**(1/2), 123–138.
- Trenberth, K. E., Caron, J. M. and Stepaniak, D. P. (2001), 'The atmospheric energy budget and implications for surface fluxes and ocean heat transports', *Climate dynamics* **17**(4), 259–276.
- Trenberth, K. E., Dai, A., van der Schrier, G., Jones, P. D., Barichivich, J., Briffa, K. R. and Sheffield, J. (2014), 'Global warming and changes in drought', *Nature Climate Change* **4**(1), 17–22.
- Trenberth, K. E. and Stepaniak, D. P. (2001), 'Indices of el ninõ evolution', *Journal of Climate* **14**(8), 1697–1701.
- Tsidu, G. M. (2017), 'Secular spring rainfall variability at local scale over ethiopia: trend and associated dynamics', *Theoretical and Applied Climatology* **130**(12), 91–106.
- Turk, F. J., Arkin, P., Sapiano, M. R. and Ebert, E. E. (2008), 'Evaluating high-resolution precipitation products', *Bulletin of the American Meteorological Society* **89**(12), 1911–1916.
- Van De Giesen, N., Hut, R., Andreini, M. and Selker, J. (2013), Trans-african hydro-meteorological observatory (tahmo): A network to monitor weather, water, and climate in africa, in 'AGU Fall Meeting Abstracts'.

- Vinayachandran, P., Iizuka, S. and Yamagata, T. (2002), 'Indian ocean dipole mode events in an ocean general circulation model', *Deep Sea Research Part II: Topical Studies in Oceanography* **49**(7-8), 1573–1596.
- Wang, X. L. (2008a), 'Accounting for autocorrelation in detecting mean shifts in climate data series using the penalized maximal t or f test', *Journal of Applied Meteorology and Climatology* **47**(9), 2423–2444.
- Wang, X. L. (2008b), 'Penalized maximal f test for detecting undocumented mean shift without trend change', *Journal of Atmospheric and Oceanic Technology* **25**(3), 368–384.
- Wang, X. L. and Feng, Y. (2010), 'Rhtestsv3 user manual', *Climate Research Division. Atmospheric Science and Technology Directorate. Science and Technology Branch, Environment Canada* **24**.
- Wang, X. L. and Lin, A. (2015), 'An algorithm for integrating satellite precipitation estimates with in situ precipitation data on a pentad time scale', *Journal of Geophysical Research: Atmospheres* **120**(9), 3728–3744.
- Wang, X. L., Wen, Q. H. and Wu, Y. (2007), 'Penalized maximal t test for detecting undocumented mean change in climate data series', *Journal of Applied Meteorology and Climatology* **46**(6), 916–931.
- Wigley, T. M., Ingram, M. J. and Farmer, G. (1985), *Climate and history: studies in past climates and their impact on man*, CUP Archive.

- Wolter, K. (1989), 'Modes of tropical circulation, southern oscillation, and sahel rainfall anomalies', *Journal of Climate* **2**(2), 149–172.
- Wu, L. (2009), 'Comparison of atmospheric infrared sounder temperature and relative humidity profiles with nasa african monsoon multidisciplinary analyses (namma) dropsonde observations', *Journal of Geophysical Research: Atmospheres* **114**(D19).
- Xie, P. and Arkin, P. A. (1997), 'Global precipitation: A 17-year monthly analysis based on gauge observations, satellite estimates, and numerical model outputs', *Bulletin of the American Meteorological Society* **78**(11), 2539.
- Xie, P., Rudolf, B., Schneider, U. and Arkin, P. A. (1996), 'Gauge-based monthly analysis of global land precipitation from 1971 to 1994', *Journal of Geophysical Research: Atmospheres* **101**(D14), 19023–19034.
- Yazid, M. et al. (2015), 'Regional observed trends in daily rainfall indices of extremes over the indochina peninsula from 1960 to 2007', *Climate* **3**(1), 168–192.
- Yengoh, G. T., Armah, F. A., Onumah, E. E. and Odoi, J. O. (2010), 'Trends in agriculturally-relevant rainfall characteristics for small-scale agriculture in northern ghana', *Journal of Agricultural Science* **2**(3), 3.
- Zeweldi, D. A. and Gebremichael, M. (2009a), 'Evaluation of cmorph precipitation products at fine space–time scales', *Journal of Hydrometeorology* **10**(1), 300–307.

Zeweldi, D. A. and Gebremichael, M. (2009b), 'Sub-daily scale validation of satellite-based high-resolution rainfall products', *Atmospheric Research* **92**(4), 427–433.

Zhang, X., Hogg, W. and Mekis, E. (2001), 'Spatial and temporal characteristics' of heavy precipitation events over canada', *Journal of Climate* **14**(9), 1923– 1936.

Zheng, X. and Eltahir, E. A. (1998), 'The role of vegetation in the dynamics of west african monsoons', *Journal of Climate* **11**(8), 2078–2096.

